
SAPIENZA
UNIVERSITÀ DI ROMA

# *"Exploring defective Golgi N-glycosylation: interplay between cell stress response and calcium signaling in Kluyveromyces lactis."*

*PhD course in Developmental and Cell Biology*

*XXV cycle*

Supervisor
Prof. Daniela Uccelletti

PhD student
Elena Zanni

Tutor
Dr. Paola Ballario

# INDEX

# INTRODUCTION

## *1. CALCIUM HOMEOSTASIS*

In the course of evolution a number of agents have emerged as carriers of signals that are essential for the correct functioning of cell life. Among the second messengers, calcium ion ($Ca^{2+}$) may be the most universal as it can be spatially and temporally controlled with remarkable finesse, interacting with a dizzying array of proteins to execute its many regulatory functions. Secretion, motility, proliferation, cell survival, some forms of programmed cell death (e.g., apoptosis), gene expression, muscle contraction, neurotransmission, hormone secretion, and mitosis are among the several cellular functions that depend on $Ca^{2+}$ homeostasis (Santella & Carafoli, 1997).

If $Ca^{2+}$ functions to deliver signals to targets that govern essential processes, its intracellular concentration ($[Ca^{2+}]_i$) must be precisely controlled independently of the external environment; impaired regulation of $[Ca^{2+}]_i$ often results in altered cellular physiology. The $Ca^{2+}$ concentration is normally maintained at 100–200 nM in the cytosol of cells at rest but this level rises up to 1 mM when cells become activated. Once it happened, the calcium elevation is capable of regulating so different processes. At the synaptic junction, for instance, $Ca^{2+}$ induces exocytosis within microseconds, whereas at the other end of the scale $Ca^{2+}$ has to operate over minutes to hours to drive events such as gene transcription and cell proliferation. This versatility, in terms of speed, amplitude and spatio-temporal patterning, emerges from the use of an extensive molecular repertoire of signaling components, which comprise a $Ca^{2+}$ signaling toolkit that can be assembled in combinations to create signals with widely different spatial and temporal profiles (Berridge, 2000).

At any moment in time, the level of intracellular $Ca^{2+}$ is finely regulated by means of a balance between the 'ON' reactions that enter $Ca^{2+}$ into the cytoplasm and the 'OFF' reactions responsible for calcium removal by the

combined action of pumps and exchangers (Fig. 1). The $Ca^{2+}$ signaling orchestra can be divided into four functional units. Initially, (i) signaling is triggered by a stimulus that, in turn provokes, various $Ca^{2+}$-mobilizing signals. Once generated, (ii) activate the 'on' reactions that feed $Ca^{2+}$ into the cytoplasm so that (iii) $Ca^{2+}$ works as a messenger to modulate numerous $Ca^{2+}$-sensitive processes. Finally, (iv) during the OFF mechanisms pumps and exchangers together remove $Ca^{2+}$ from the cytoplasm to reestablish the resting state (Berridge *et al.*, 2003).

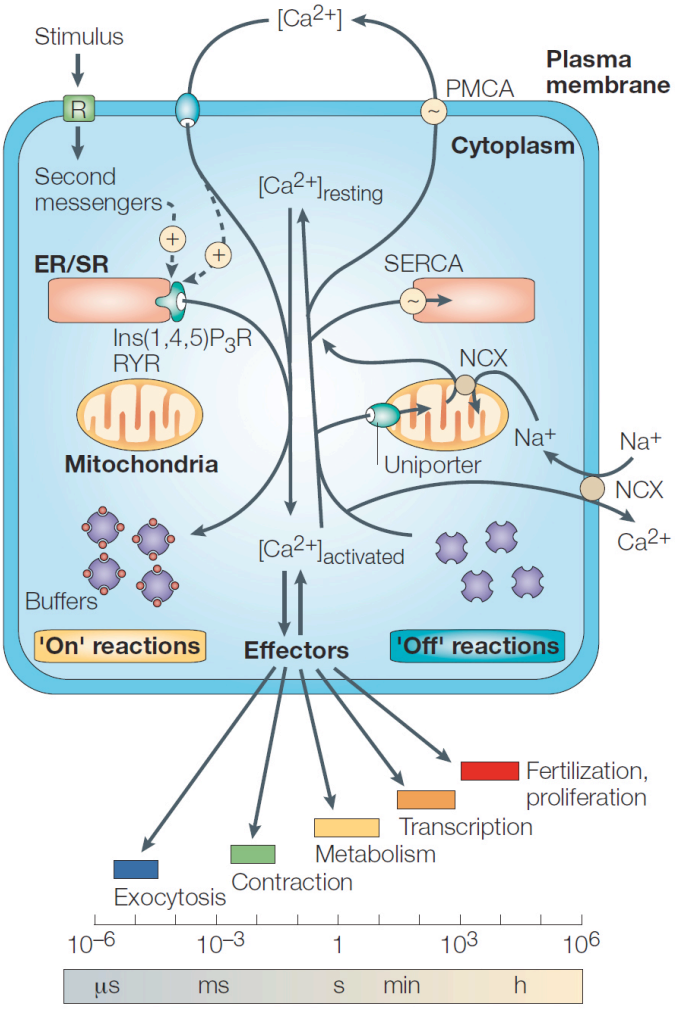


**Figure 1: Calcium-signaling dynamics and homeostasis. During the 'ON' reactions, stimuli induce both the entry of external $Ca^{2+}$ and the formation of second messengers that release internal $Ca^{2+}$ that is stored within the endoplasmic/sarcoplasmic reticulum (ER/SR). Most of this $Ca^{2+}$ is bound to buffers, whereas a small proportion binds to the effectors that activate various cellular processes that operate over a wide temporal spectrum. During the 'OFF' reactions, $Ca^{2+}$ leaves the effectors and buffers and is removed from the cell by various exchangers and pumps (Berridge *et al.*, 2003).**

To regulate this cytosolic $Ca^{2+}$ level, numerous proteins are capable of binding $Ca^{2+}$ and/or to transport it out of the cell. These proteins are members of two distinct classes: those that are intrinsic to membranes and move $Ca^{2+}$ across them, thus acting substantially as $Ca^{2+}$ buffers, and those that are not membrane-bound. Soluble $Ca^{2+}$-binding proteins, residing in the cytosol or in the organelles, store large amounts of $Ca^{2+}$ but also are capable of decoding its signal. These proteins are thus appropriately called $Ca^{2+}$ sensors (Brini & Carafoli, 2009).

## *1.1 $Ca^{2+}$-signals*

$Ca^{2+}$ signals are generated by exploiting both internal and external cellular sources. In human the internal stores are believed to represent the endoplasmic reticulum (ER) or the corresponding organelle in muscle cells, namely the sarcoplasmic reticulum (SR). Release from these internal stores is controlled by various channels, such as the inositol-1,4,5-trisphosphate receptor ($InsP_3R$) and ryanodine receptor (RYR) families, which are the most well-characterized (Berridge, 1993; Clapham, 1995).

The master activator of these channels is held to be $Ca^{2+}$ itself and this process of $Ca^{2+}$ release triggered by calcium is crucial for $Ca^{2+}$ signaling. $Ca^{2+}$-mobilizing second messengers, originated once stimuli are sensed by cell surface receptors, determine whether $Ca^{2+}$ can activate these channels. The most studied is $Ins(1,4,5)P_3$ (Berridge, 1993), which is responsible for contacting the $InsP_3Rs$ and, in turn, promoting $Ca^{2+}$ release from the ER. The ability of $Ca^{2+}$ to stimulate the RYRs depends on the cyclic ADP ribose (cADPR) (Bootman, 2002). Sphingosine 1-phosphate (S1P) releases $Ca^{2+}$ from the ER possibly by binding to a sphingolipid $Ca^{2+}$ release-mediating protein of the ER (SCaMPER) (Saunders, 2002).

## *1.2 ON reactions*

The 'ON' reactions are accomplished by $Ca^{2+}$ channels which mediate the entry of external $Ca^{2+}$ into the cell or its exit from the ER, the principal internal store in higher eukaryotes. In the plasma membrane, $Ca^{2+}$ channels are gated (i) by voltage changes namely voltage-operated channels (VOCs), (ii) by ligand interactions called receptor-operated channels (ROCs), or (iii) by a not well-characterized mechanism that is linked to the emptying of intracellular $Ca^{2+}$ stores, namely the capacitative $Ca^{2+}$ entry (Fig. 2).

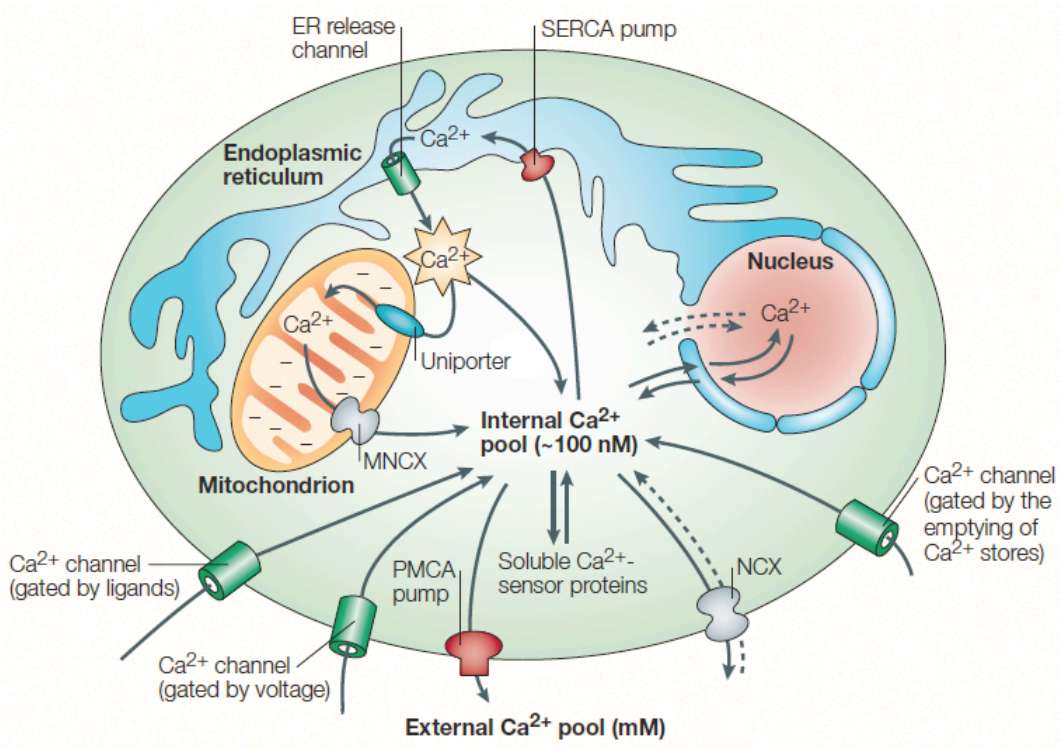


**Figure 2: Three types of gated channel (ligand, $Ca^{2+}$ and voltage) mediate $Ca^{2+}$ entry into cells. The intracellular $Ca^{2+}$ pool is regulated by binding to $Ca^{2+}$ sensors and by transport into organelles (Carafoli, 2003).**

The voltage-gated channels have distinct sub-types, of which the L-type is the target of widely-used $Ca^{2+}$ antagonists (Carafoli, 2003).

$Ca^{2+}$ is pumped in the endoplasmic reticulum through the sarco(endo)plasmic reticulum $Ca^{2+}$ ATPase (SERCA) pump and is released through channels that are

controlled by $Ca^{2+}$ itself; however it is believed that effectors like Ins(1,4,5)$P_3$ are involved in such process. The release route from the sarco(endo)plasmic reticulum creates $Ca^{2+}$ hotspots, which induce the low affinity electrophoretic uniporter of adjoining mitochondria. In such way, $Ca^{2+}$ can leave mitochondria through a $Na^+/Ca^{2+}$ exchanger (MNCX). $Ca^{2+}$ is instead expelled from the cell by a high-affinity/low-capacity plasma-membrane $Ca^{2+}$ ATPase (PMCA) pump and a low-affinity/high-capacity $Na^+/Ca^{2+}$ exchanger (NCX).

As introduced above, $Ca^{2+}$ signal originates also from the internal stores. Channels opened by Ins$P_3$Rs and the RYRs are regulated by several factors, the most important of which is $Ca^{2+}$ itself, which regulates $Ca^{2+}$ release by acting from either the lumenal either cytoplasmic side of the channel. In general, low concentrations of $Ca^{2+}$ (100–300 nM) are stimulatory for Ins$P_3$Rs but above 300 nM, $Ca^{2+}$ becomes inhibitory and switches the channel off (Bootman & Lipp, 1999). The autocatalytic process of $Ca^{2+}$-induced $Ca^{2+}$ release enables the Ins$P_3$Rs and RYRs to interact in order to orchestrate $Ca^{2+}$ signals, often organized into propagating waves (Berridge, 1993; Clapham 1995). The main function of the $Ca^{2+}$-mobilizing messengers, therefore, is to change the sensitivity of the Ins$P_3$Rs and RYRs to this stimulatory action of $Ca^{2+}$.

As a result of these 'ON' mechanisms, $Ca^{2+}$ that enters the cytoplasm is rapidly bound to various cytosolic buffers such as parvalbumin, calbindin-D28K and calretinin. Cytosolic buffers function to model both the amplitude and duration of $Ca^{2+}$ signals. Troponin C (TnC) and calmodulin (CAM) represent the principal protein sensors, which have four EF hands that bind $Ca^{2+}$ and undergo a conformational change to activate the downstream effectors. CAM is usually involved in the contraction of smooth muscle as well as crosstalk between signaling pathways, gene transcription, ion channel modulation and metabolism. The same cell can use different sensors to regulate separate processes.

## *1.3 OFF reactions*

Once $Ca^{2+}$ has accomplished its signaling functions, it is rapidly removed from the cytoplasm by various pumps (Pozzan *et al.*, 1994) and exchangers (Blaustein & Lederer, 1999). The plasma membrane Ca2+-ATPase (PMCA) pumps and Na+/Ca2+ exchangers control calcium exit outside the cells whereas the SERCA pumps are involved in the replenishment of calcium internal stores. The mitochondrion is another important component of the OFF mechanism since it rapidly entrap $Ca^{2+}$ during the development of the $Ca^{2+}$ signal and then releases it back slowly during the recovery phase. This mitochondrial uptake of $Ca^{2+}$ is important in shaping both the amplitude and the spatio-temporal patterns of $Ca^{2+}$ signals (Berridge *et al.*, 2000). Mitochondria extrude protons to create the electrochemical gradient that allows ATP synthesis. The same gradient is used to drive $Ca^{2+}$ uptake through a uniporter that has a low sensitivity to $Ca^{2+}$. This low sensitivity means that mitochondria accumulate $Ca^{2+}$ more efficiently when they are close to $Ca^{2+}$-releasing channels (Rizzuto, *et al.*, 1993). Here, they may form a 'quasi-synapse', allowing them to directly sense the high local $Ca^{2+}$ concentration that builds up in the vicinity of open $Ca^{2+}$ channels, such as the $InsP_3Rs$ and RYRs. There seem to be reciprocal interactions between the two organelles in that the ER/SR provides the $Ca^{2+}$ that enters the mitochondria, which in turn modifies the $Ca^{2+}$ feedback mechanisms that regulate $Ca^{2+}$ release from the ER/SR.

## *2. YEAST AS VERSATILY MODEL SYSTEM*

Yeast is a eukaryotic unicellular organism belonging to the kingdom of Fungi. Its size typically varies in the range of 3–4 μm in diameter although some yeasts such as *Blastomyces dermatitidis* can reach over 40 μm (Walker *et al.*, 2002). Some of the properties that make yeast particularly suitable for biological research include rapid growth, dispersed cells, the ease of mutant isolation, a well-characterized genetic system, and most importantly a highly versatile DNA transformation system. Cells reproduce asexually by mitosis principally through the budding of the daughter from the mother cell. The useful physiological properties of yeasts have led to their use in the field of biotechnology; fermentation of sugars by yeast is the oldest and largest application of this technology. Nowadays yeast represents one of the most widely used model organisms for genetics and cell biology (Fig. 3).

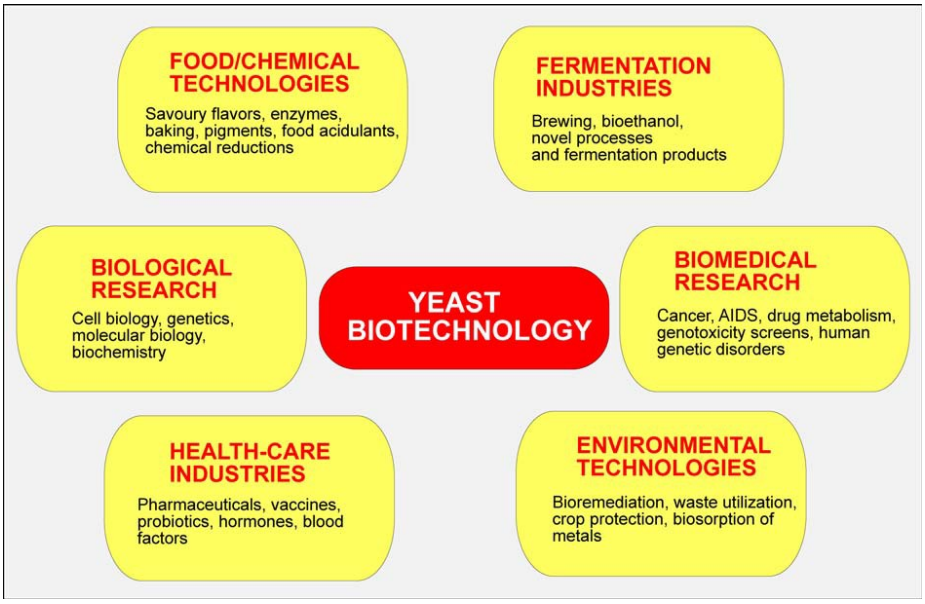


**Figure 3: Biotechnology fields involving yeast. (Tenreiro & Outeiro, 2010)**

*Saccharomyces cerevisiae,* also knows as baker's or budding yeast, is the most extensively characterized eukaryotic organism. It is well established that yeast

is an ideal system in which cell architecture and fundamental cellular mechanisms can be successfully investigated. Among all eukaryotic model organisms, *S. cerevisiae* combines several advantages such as a short generation time (1.5–3 hours) and its genetic manipulability; its DNA is easily transformed, and homologous recombination is efficient. It is a microorganism that, unlike more complex eukaryotes, can be grown on defined media and in a highly reproducible and genetically stable way. It is also a scalable system and therefore exploited in high-throughput genetic and small-molecule screens. Its cell cycle that involves haploid and diploid forms allows the study of lethal mutations in heterozygous diploids and recessive mutations in haploids is extremely simplified in yeast (Tenreiro & Outeiro, 2010). In addition, genetic manipulations are easy to perform by mating the haploid strains and then make the diploid strains sporulating. Molecular genetics take advantage from the high transformation efficiency of yeast cells also considering the extremely efficient homologous recombination pathway, which renders relatively easy to insert, delete or mutate any genomic sequence up to the chromosome level (Sugiyama *et al.*, 2009).

Starting from 1960, *S. cerevisiae* was introduced as an experimental system for molecular biology. As early as in 1980, yeast was used to produce Hepatitis B vaccine. In 1996, *S. cerevisiae* became the first eukaryote to have its 1,3 $\times 10^7$ base pair-long genome sequenced. By comparison, the human genome has 3,08 $\times$ $10^9$ base pairs but only 3 to 5 times as many genes. So the yeast genome is about 200 times smaller than the human genome but less than four times bigger than that of *E. coli.* Sixteen chromosomes ranging in size between 250 kb and >2500 kb compose the *S. cerevisiae* genome.

To date, approximately 6,600 open reading frames (ORF) have been annotated, with more than 80% functionally characterized. At least 60% of yeast genes have human homologues or at least one conserved domain with human genes. In addition, more than 25% of known human disease genes have a yeast homologue. Genomic homology explains the conservation of fundamental cell biological processes between yeast and mammalian cells. Yeast cells summarize

the key aspects of eukaryotic biology, such as a distinctive process of cell division and genetic transmission, transcriptional regulation, biogenesis and function of cellular organelles, protein targeting and secretion, cytoskeletal dynamics and regulation, and cellular metabolism. The conservation of homologous genes fulfilling similar functions has been a recurrent research field in eukaryotic cell biology, often with interchangeability of yeast and mammalian homologues (genetic complementation). Homology to a yeast gene has often provided the first clue to the function of many higher eukaryotic genes. A few conserved aspects of cellular biology, which have benefited from rigorous molecular dissection in yeast, include for example mitochondrial dysfunction and oxidative stress. In yeast, as in mammalian cells, the central organelle for the production of reactive oxygen species (ROS) is the mitochondrion. The ability of yeast to grow in fermentative states allows to analyze mitochondrial defects that would be lethal in mammalian cells. However, the results obtained in yeast might be confirmed in other *in vivo* models, such as mice, worms or flies, validating novel putative targets for therapeutic intervention.

The yeast models are also being used for drug discovery efforts. Together with the genetic tools available, these approaches are expected to lead to the identification of novel drug targets for therapeutic intervention. Resembling other model organisms, yeast system has obvious limitations. Nevertheless, the use of this simple model organism has been become widespread, especially in combination with other model systems, leading to new insights both in the basic knowledge and in the development of novel possibilities for therapeutic interventions in human diseases (Tenreiro *et al.*, 2010).

## *2.1 Kluyveromyces lactis*

*Kluyveromyces lactis* is both scientifically and biotechnologically one of the most relevant non-*Saccharomyces* yeasts. Its biotechnological significance builds on its history of safe use in the food industry and its well-known ability to produce enzymes like lactase and bovine chymosin on industrial scale (Faraco *et al.*, 2008; van Ooyen *et al.*, 2006).

This microorganism grows in optimal temperature at 25°C to 40°C. *K. lactis* cells have oval form and typically measure 3–4 μm in diameter (Fig. 4).

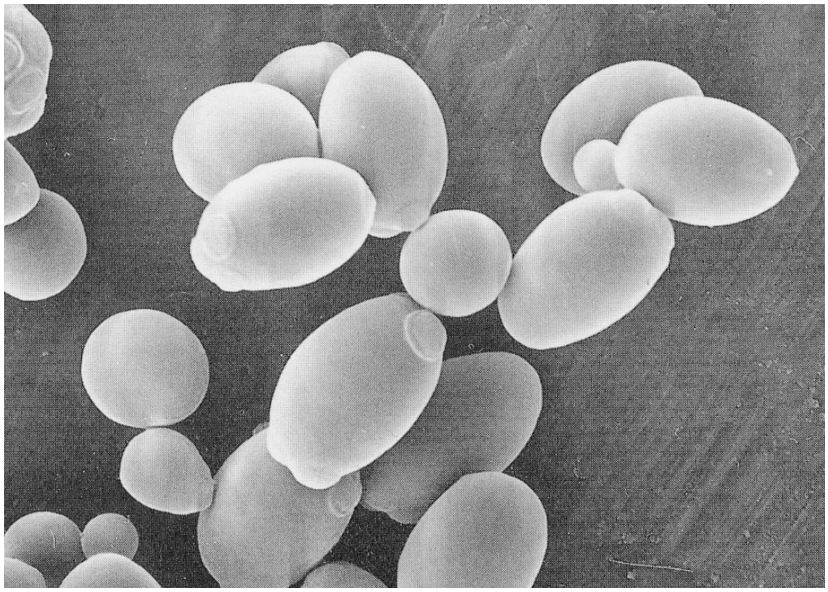

**Figure 4*: Kluyveromyces lactis* cells.**

Its genome is divided up into 6 chromosomes ranging in size between 1 Mbp and >3 Mbp. As discussed above, the yeast *Kluyveromyces lactis* has been studied for decades and has a well-established track record of safe use in various food industry applications (Swinkels *et al.*, 1994). Since the 1950s, *K. lactis* has been used as a source of lactase (β-galactosidase), an enzyme that degrades milk sugar (lactose) and is necessary for production of lactose-free dairy products. Dried and inactivated *K. lactis* was also used as a protein

supplement in food in the 1960s. In the 1980s, *K. lactis* was one of the first yeasts for which a transformation system was established (Das et al, 1984), leading to its development as an efficient host for heterologous protein expression. As a 'cell factory', *K. lactis* is best known for its use in commercial production of the milk clotting enzyme bovine chymosin (Van den Berg, 1990). This protein was the first heterologous enzyme originating from a higher eukaryote that was produced at low cost in a microorganism, and the process developed for its industrial-scale production was widely recognized as a major biotechnological achievement. In 1993, Swinkels first reviewed the use of *K. lactis* as a host for heterologous protein expression. At that time, eight proteins had been successfully secreted from *K. lactis*. Today, over 40 proteins have been produced with *K. lactis*, illustrating its utility as an alternative yeast expression system. These proteins originate from bacteria, fungi, viruses, plants, and mammals, emphasizing the ability of *K. lactis* to efficiently produce a diverse range of heterologous proteins. An example is the efficient expression and proper localization of murine Acetylcholinesterase (Uccelletti *et al*., 2002).

As a host for heterologous protein production, *K. lactis* has a number of advantages over other yeast expression systems, including easy genetic manipulation, the ability to use both integrative and episomal expression vectors, and the availablility of a fully sequenced genome (Dujon, 2004). Growth of *K. lactis* cells can be performed in standard yeast medium and does not require the explosion-proof fermentation equipment necessary for large-scale growth of methylotrophic yeasts such as *Pichia pastoris*. In addition, enzymes from *K. lactis* have GRAS (generally regarded as safe) FDA status, permitting their use in various food and feed applications (van Ooyen *et al*., 2006).

## *2.2 Yeast as a model for eukaryotic calcium homeostasis*

Calcium homeostasis mechanisms are highly regulated metabolic pathways used by cells to maintain $Ca^{2+}$ within optimal concentration ranges in the cytosol and other organelles. Several studies have shown that $Ca^{2+}$ homeostasis and signaling systems are basically conserved from yeast to higher eukaryotes (Ton & Rao, 2004). In yeast, distinct environmental insults including osmotic shock, alkaline pH, cell wall damage, ER stress and exposure to high levels of mating factor can trigger $Ca^{2+}$ influx and the activation of a calcium stress response (Iida *et al.*, 1990; Bonilla *et al.*, 2002).

For instance, in the bakery's yeast, cytosolic $Ca^{2+}$ is maintained in a range of 50–200nM, that is essentially similar to human cells, in face of environmental $Ca^{2+}$ concentrations ranging from 1 μM to 100 mM. The resting calcium concentrations in Golgi and ER (internal calcium stores) are about 300 μM (Pinton et al. 1998) and 10 μM (Strayle et al. 1999), respectively. The calcium in ER and Golgi will be secreted along with the canonical secretory pathways. Cytosolic calcium levels are originated by the net resulting from an elaborate calcium homeostasis system (Bonilla *et al.*, 2002). Among the $Ca^{2+}$ signaling cascades, those that have been well characterized in yeast are the response to mating pheromone (Iida *et al.*, 1990), salt and environmental stresses (Matsumoto *et al.*, 2002), nutrient sensing, and the cell integrity response (Garrett-Engele *et al.*, 1995).

Nowadays, in the *–omics* era, it results not so weird that the building blocks of the $Ca^{2+}$ signaling machinery are named as 'calciome' (Ton & Rao, 2004). This class includes, as in higher eukaryotes, two classes of proteins. On one hand, $Ca^{2+}$ channels and transporters are members of membrane-bound proteins. On the other hand, calcium machinery is also composed by soluble $Ca^{2+}$-binding proteins as well as $Ca^{2+}$ sensors, and signal transducers.

Basically the intracellular calcium concentration is the net resulting from components belonging to the first class of the calciome elements. Among them,

the channel localized at the plasma membrane (Mid1p, Cch1p) increases calcium content (Bonilla, 2003) in face of the pumps or transporters distributed instead along the Golgi (Pmr1p) or vacuolar (Pmc1p, Vcx1p) membranes, that work to sequester $Ca^{2+}$ into stores or transport it out of the cell (Fig. 5).

Among calcium sensors, calmodulin and calcineurin proteins control the functioning of channels and pumps (Courchesne & Ozturk 2003).

Yeast cells allow calcium entry from the outside via Mid1p-Cch1p, and possibly other unidentified transporters. Once a stimulus has been sensed, the subsequent rise of cytosolic calcium binds calmodulin which in turn activates the serine/threonine phosphatase calcineurin (Fig. 5).

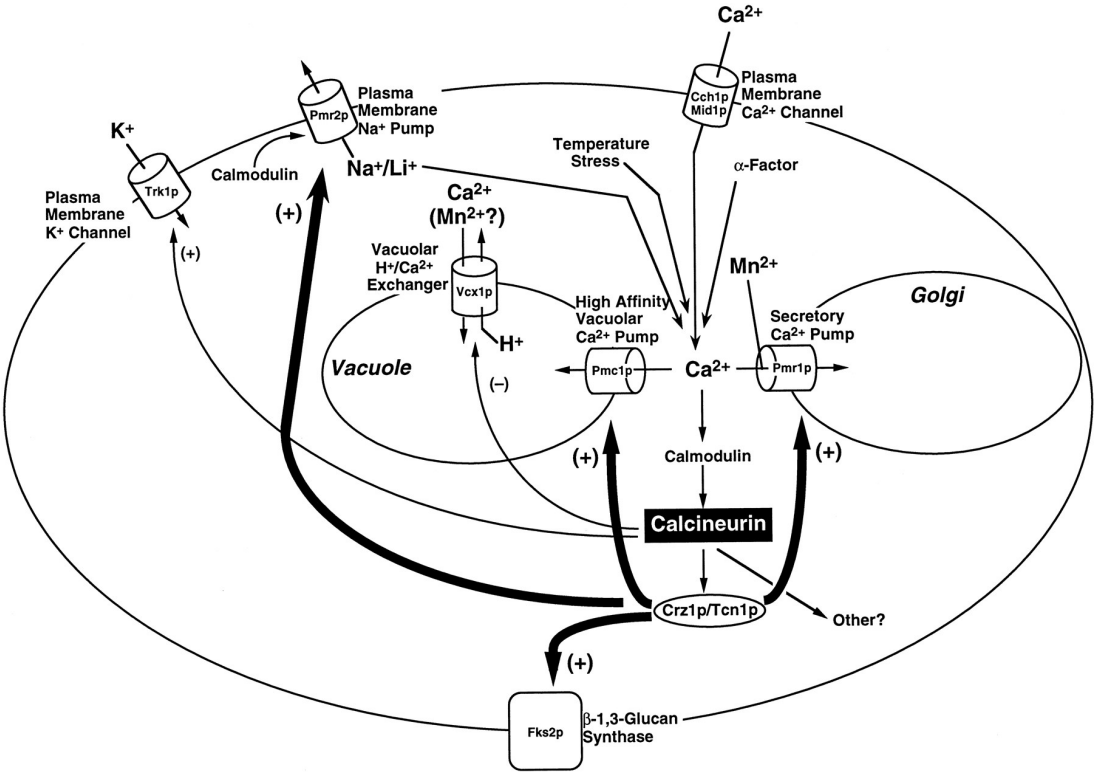


**Figure 5: Physiological roles of calcineurin in *Saccharomyces cerevisiae*. Crz1p/Tcn1p, a calcineurin-dependent transcription factor is necessary for the transcriptional induction of Pmc1p, Pmr1p, Pmr2p, and Fks2. In addition, calcineurin inhibits the activity of the vacuolar $H^+/Ca^{2+}$ exchanger (Vcx1p) and causes conversion of the $K^+$ channel, Trk1p, to the high-affinity state. (Ton & Rao, 2004).**

Calcineurin dephosphorylates the transcriptional factor Crz1p that is free of migrating into the nucleus. Herein is capable of suppressing or enhancing the transcription of distinct genes evoking the calcium response.

### 2.2.1 Yeast $Ca^{2+}$ channels

In *S. cerevisiae*, at least two different carrier systems have been identified: a high-affinity calcium influx system (HACS) and a low-affinity calcium influx system (LACS) that still remains poorly characterized. The HACS consists of at least two known subunits, Cch1p and Mid1p, which act as the master calcium entry route when calcium availability is low. Cch1p is a homolog to the catalytic α-subunits in mammals whereas Mid1p is probably a putative stretch-activated $Ca^{2+}$ channel (Cunningham, 2011). It has been reported that Cch1 and Mid1 form a stable complex (Locke *et al.*, 2000), and both proteins are required for $Ca^{2+}$ influx, elevation of cytosolic free $Ca^{2+}$, and activation of calcineurin in response to different stimuli. These channels have been implicated in $Ca^{2+}$ entry during exposure to mating pheromone, ER stress, and depletion of $Ca^{2+}$ stores in the ER/secretory pathway.

In addition it has been noted that MAP kinase activation leads to phosphorylation of Cch1 at unknown sites in the absence of calcineurin, and subsequent calcineurin activation leads to dephosphorylation of Cch1, thus in turn inhibiting the channel activity (Locke 2000). Whether these stimuli-dependent modifications of Cch1 can occur in the absence of Mid1 remains still unclear.

In yeast, the vacuole serves as the principal store of $Ca^{2+}$, for both detoxification and signaling reactions. A homolog of the mammalian transient receptor potential (TRP)-like channel, Yvc1, has been shown to release $Ca^{2+}$ from the vacuole into the cytosol in response to hyperosmotic shock and the antiarrhythmic drug amiodarone (Courchesne & Ozturk, 2003).

Both mechanical activation of Yvc1 and $Ca^{2+}$-induced $Ca^{2+}$ release have been demonstrated under osmotic shock (Denis *et al.*, 2002). Notably, yeast inositol 1,4,5-trisphosphate receptor channels have not been identified, correlating with low levels of $InsP_3$ in yeast and it is not known how $Ca^{2+}$ is released, if at all, from the ER/Golgi stores.

### 2.2.2 $Ca^{2+}$ pumps and transporters

In yeast like in other eukaryotes, $Ca^{2+}$ transfer from the cytosol to intracellular stores or extracellular enviroment is carried out by ATP-driven pumps and cation-coupled exchangers.

Although there are no SERCA homologs in *S. cerevisiae*, the ER concentrates $Ca^{2+}$ approximately 100-fold more than the cytoplasm, largely through the $Ca^{2+}$ transport activity of Pmr1p (Strayle *et al.*, 1999). Yeast Pmr1p (Plasma Membrane ATPase Related") was the first member of the family of the secretory pathway $Ca^{2+}$-ATPases (SPCA) to be identified. Pmr1p localizes primarily in the Golgi complex and therefore supplies $Ca^{2+}$ and Mn2+ to the lumen for protein sorting, processing, and glycosylation and to the endoplasmic reticulum during its early biogenesis or through vesicle-mediated trafficking in the retrograde direction from the Golgi complex.

Plasma membrane $Ca^{2+}$-ATPases (PMCA) constitute a third branch of this superfamily of related pumps, represented in yeast by Pmc1. This pump acts together with the low-affinity $Ca^{2+}$ /H+ exchanger Vcx1p to sequester calcium in the main $Ca^{2+}$ store of a yeast cell, namely the vacuole. Although clearly related in sequence to the PMCA family, yeast Pmc1 lacks domains involved in regulation by calmodulin and acidic phospholipids typical of the mammalian members. Moreover calcineurin activation by calmodulin and elevated cytosolic $Ca^{2+}$ leads to increased expression of PMC1 (Cunningham, 2011).

Another key player in the vacuolar $Ca^{2+}$ sequestration is Vcx1p, a $Ca^{2+}$ /$H^{+}$ exchanger driven by the proton electrochemical gradient set up by the vacuolar $H^{+}$-ATPase (Cagnac *et al.*, 2010). At the beginning it was thought that Vcx1 was responsible for most $Ca^{2+}$ transport into the vacuole under normal growth conditions. However, Vcx1 knockout mutants exhibited wild type-like levels of vacuolar $Ca^{2+}$. Besides, the contributions of Vcx1 to vacuolar $Ca^{2+}$ uptake and to $Ca^{2+}$ tolerance are markedly increased when calcineurin is inactivated.

### 2.2.3 Calmodulin as the calcium sensor

Many downstream transcriptional and translational events in yeast are controlled by the $Ca^{2+}$-mediated activation of calmodulin. The unique gene encoding calmodulin in *S. cerevisiae* is *CMD1* and it is essential for life as in all organisms. This protein acts in yeast cells in both its $Ca^{2+}$-bound and $Ca^{2+}$-free form. On one hand performs essential roles in mitosis, through its regulation of Nuf1p, a component of the spindle pole body, and in bud growth, by binding Myo2p, an unconventional class V myosin required for polarized secretion. Specifically these are the roles for which it is not required calcium binding. On the other hand, calmodulin plays a pivotal role for endocytosis and is involved in $Ca^{2+}$-dependent stress response pathways through regulation of calcineurin and the protein kinases, Cmk1p and Cmk2p (Cyert, 2001).

Concerning its calcium-dependent function, calmodulin serves as the key intracellular $Ca^{2+}$ receptor and regulate many of the effects of this ion.

In absence of a stimulus, calmodulin exists in the $Ca^{2+}$ -free, or apo-calmodulin form. Once the $Ca^{2+}$ signal is sensed, calmodulin binds calcium ions and undergoes a consequently conformational change allowing it to interact with target enzymes such as the phosphatase calcineurin.

Dephosphorylation by calcineurin results in nuclear translocation of Crz1p/Tcn1p, analogous to mammalian NFATc, and transcriptional activation of more than 160 target genes involved in cell wall and lipid synthesis, ion and small molecule transport, vesicle trafficking, and other signaling proteins (Ton & Rao, 2004).

Calmodulin contains four copies of a $Ca^{2+}$ -binding motif known as an EF-hand, each of which binds one $Ca^{2+}$ ion. An EF-hand is made up of a 12-residue $Ca^{2+}$-binding loop flanked by two α-helices (Falke *et al.*, 1991). Within the loop, $Ca^{2+}$ is coordinated by oxygens on six different amino acid residues.

In the absence of $Ca^{2+}$, the EF-hands are in a 'closed' conformation. This $Ca^{2+}$-free form of calmodulin is able to bind to a subset of target proteins. $Ca^{2+}$ binding causes a change to an 'open' conformation, which also results in

exposure of two hydrophobic surfaces that allow calmodulin to bind to its $Ca^{2+}$ -dependent target proteins (Cyert, 2001).

### 2.2.4 Calcineurin signaling pathway

Calcineurin is a highly conserved, $Ca^{2+}$ calmodulin-dependent phosphoserine/phosphothreonine-specific phosphatase. Purified calcineurin is a heterodimer consisting of a catalytic subunit, calcineurin A, and a "regulatory" subunit, calcineurin B. In *S. cerevisiae*, calcineurin is encoded by two genes: *CNA1* encodes the catalytic subunit whereas *CNB1* codes for the regulatory subunit.

Highly specific inhibitors of calcineurin, FK506 and cyclosporin A, bind to an intracellular binding protein (FKBP or cyclophilin, respectively), and form a drug-protein complex, which then binds to and inhibits calcineurin.

The active site of calcineurin is located on the A subunit which, in mammals, is 57–59 kDa depending on the isoform. The size of the catalytic subunit can be up to ~20% larger in lower eukaryotic species (e.g., *Saccharomyces cerevisiae*, 63 and 69 kDa; *Schizosaccharomyces pombe*, 64 kDa; *Drosophila melanogaster*, 62 and 65 kDa; *Cryptococcus neoformans* and *Dictyostelium discoideum*, 71 kDa). Besides that, calcineurin A gene of all eukaryotic organisms encode for a protein consisting of a catalytic domain homologous to other serine/threonine protein phosphatases and three regulatory domains at the C-terminus. These domains have been identified as the calcineurin B binding domain, the calmodulin-binding domain, and the "autoinhibitory" domain. (Rusnak & Mertz, 2000). Upon elevation of $[Ca^{2+}]$, $Ca^{2+}$-bound calmodulin contacts the A subunit and displaces the autoinhibitory domain, thus activating phosphatase activity (Nakajima-Shimada *et al.*, 2000).

Yeast calcineurin carries out at least three different functions in yeast, regulating (i) a stress-activated transcriptional pathway, (ii) $Ca^{2+}$ homeostasis, and (iii) the G2 to M transition of the cell cycle. These different functions reflect the activities of distinct calcineurin substrates.

Calcineurin regulates the signal transduction pathway in *S. cerevisiae* that is activated by intracellular $Ca^{2+}$ and results in increased expression of a specific set of calcineurin-dependent genes. Under specific environmental conditions, including exposure to high concentrations of ions ($Ca^{2+}$, $OH^{-}$, $Mn^{2+}$, $Na^{+}/Li^{+}$), mating pheromone (α-factor) and high temperature, and in mutants in which cell wall structure is compromised, calcineurin-mediated gene expression is activated (Cyert, 2001). $Ca^{2+}$/calcineurin-dependent transcription is mediated by a zinc-finger transcription factor, encoded by *CRZ1*/*TCN1* that activates the expression of the structural genes for several P-type ATPases (*PMC1*, *ENA1*, *PMR1*), cell wall biosynthetic enzymes (*FKS2*), and many other genes. Dissection of the *FKS2* promoter defined the CDRE (calcineurin dependent response element), a 24-bp DNA element that is necessary and sufficient to mediate $Ca^{2+}$-induced, calcineurin-dependent activation of gene expression.

The generation of $Ca^{2+}$ signals requires a sufficient concentration of $Ca^{2+}$ in the extracellular medium, and in media lacking $Ca^{2+}$, yeast cells exposed to pheromone die (Iida *et al*, 1990). Thus, activation of calcineurin and other $Ca^{2+}$-regulated processes is dependent on $Ca^{2+}$ entry (Withee *et al.*, 1997), which is mediated by the plasma membrane $Ca^{2+}$ channel Mid1p/Cch1p as discussed above.

As yet mentioned, more than 95% of $Ca^{2+}$ in yeast cells is stored in the vacuole, and this organelle plays a critical role in regulating $Ca^{2+}$ homeostasis in yeast. Once the response is triggered, cell achieves the resting status by calcineurin functioning. Specifically, calcineurin activates *PMC1* expression through the Crz1p transcription factor leading thus to the vacuolar $Ca^{2+}$ sequestration.

To date, it is believed that calcineurin's effects on $Ca^{2+}$ homeostasis cannot be explained by regulation of Vcx1p.

### 2.2.5 Calmodulin-stimulated protein kinases

In *S. cerevisiae*, there are only two protein kinases, encoded by *CMK1* and *CMK2* genes, which are regulated by calmodulin. In the presence of $Ca^{2+}$ and calmodulin they phosphorylate a number of different substrates *in vitro* and

also become autophosphorylated. Cmk2p activity becomes $Ca^{2+}$/calmodulin independent after autophosphorylation; however, this is not observed for Cmk1p (Ohya *et al.*, 1991). Unlike mammalian Cam kinase II, the yeast kinases do not appear to form large oligomers, although the active form of Cmk1p may be a dimer.

The physiological role(s) of Cmk1p and Cmk2p are not well understood. However, like calcineurin, these enzymes seem to participate in a multitude of stress responses. The specific role of calmodulin-stimulated kinases in maintaining viability during pheromone treatment is not understood. However, the expression of *CMK2* is induced in a $Ca^{2+}$/calcineurin/*CRZ1*-dependent manner, suggesting that conditions that lead to calcineurin activation also may stimulate calmodulin-dependent kinase activity (Cyert, 2001).

# *3. CELLULAR STRESS*

Biological structures as well as their building blocks are the basis for roles and their efficiency in adaptation to metabolic and environmental changes. Once the insult is perceived, cell homeostasis results from the balance between cell capability to adapt or succumb to environmental stress. When challenged by stressful conditions, cells displayed a molecular response which allows them to survive or, alternatively, cause cell death. The existence of molecular mechanisms involved in response, repair and adaptation, many of which are greatly conserved across nature, endows the cell with the plasticity it requires to adjust to its ever-changing environment, a homeostatic event that is termed the stress response.

A common need for microbial cells is the ability to respond to potentially toxic environmental insults. Organisms are constantly faced with ever-changing variables in their environment, including nutrient levels, osmotic stress, exposure to toxic molecules, and non-optimal temperatures. Multicellular organisms can usually modify these conditions by varying location or physiology. By contrast, single-cell organisms such as yeast are at the mercy of their situation, and must adapt or perish. The study of these environmental stress responses in *S. cerevisiae* has highlighted many of the features now considered as central to our understanding of eukaryotic cell biology. (Morano *et al.*, 2011). The yeast *S. cerevisiae* displays an elaborate program of gene expression when exposed to different environmental cues. Yeast cell homeostasis is achieved through a highly coordinated mechanism of transcription regulation, involving several transcription factors, each one acting singly or in combination to perform specific functions. Thus, a genetic reprogramming occurs leading to a transient arrest of normal cellular processes, such as a decrease in protein synthesis. On the other hand, the transciption of genes encoding stress proteins is induced. Among them, molecular chaperones are responsible for protein folding whereas transcription

factors further modulate the expression of different genes, including membrane transporters and proteins involved in repair, degradation and detoxification pathways, nutrient metabolism and osmolyte production.

Yeast cells are often challenged by two strictly-related stresses: oxidative stress and endoplasmic reticulum stress. (Zdralević *et al.*, 2012). Mantenaince of an optimal redox environment is fundamental for a proper functioning of cellular processes and cell survival. Despite the importance of maintaining redox homeostasis, it is not clear how the optimal redox potential is sensed and set, and the processes that impact redox on a cellular level are poorly understood. The majority of intracellular functions require a strongly reducing environment, which maintains key sulfhydryl groups in a reduced and active form and other key elements of proteins and enzymes to remain functional. In eukaryotic cells, highly reducing environments are found in compartments including the cytosol, mitochondrial matrix and peroxisome. Conversely, optimal oxidative protein folding and maturation requires disulfide bond formation and a more oxidative redox environment, found in the endoplasmic reticulum (Tu *et al.*, 2004) and mitochondrial inter-membrane space (Riemer *et al.*, 2009). Maintenance of appropriate cellular and sub-cellular redox environments is crucial since alterations in redox can adversely affect biological processes such as signal transduction, protein structure an function, DNA and RNA synthesis, enzyme activation and regulation of the cell cycle (Ayer *et al.*, 2012). Moreover, altered cellular redox homeostasis has been associated with neurodegenerative disorders including Alzheimer's and Parkinson's diseases and metabolic syndromes such as diabetes (Barnham *et al.*, 2004).

## *3.1 Oxidative stress*

The generation of reactive oxygen species (ROS) is an unavoidable consequence of life under aerobic conditions. Over 90% of oxygen consumed by living organisms is used to produce ATP in cell mitochondria through a series of oxidative phosphorylation processes that lead a four-electron reduction of $O_2$ to water. However, during this process, one- or two-electron reductions of $O_2$ can occur, causing the generation of ROS. Such molecules have higher reactivity than molecular oxygen ($O_2$). Among them, unstable oxygen radicals such as superoxide radical ($O_2\bullet^-$) and hydroxyl radical (HO•), and non-radical molecules like hydrogen peroxide ($H_2O_2$) are recurrently generated as byproducts of normal aerobic metabolism. Under stress and pathological conditions, ROS can also be produced to a greater extent. Thus, all organisms living in an aerobic environment are constantly exposed to ROS. However, organisms also have evolved a multitude of antioxidant defenses to protect their cells from toxic properties of oxygen (Willcox *et al.*, 2004). ROS are degraded via several mechanisms, both, specific and non-specific. Formation and degradation of ROS usually are finely regulated and very low ($< 10^{-8}$ M) steady-state ROS concentrations are maintained inside the cell (Murphy *et al.*, 2011). However, when the antioxidant defenses become insufficient, cell fails in ROS detoxifying leading to oxidative stress as a means of a marked imbalance between the production and removal ROS in favor of the prooxidant balance (Fig. 6).

Under such conditions cell biomolecules such as nucleic acids, proteins, and lipids undergo severe oxidative damage, thus affecting the functioning of cells (Halliwell, 2012), that in turn can lead to different severe human pathologies ranging from diabetes (Giugliano *et al*., 2000) to neurodegenerative diseases such as Parkinson's disease (Facecchia *et al.*, 2011), Alzheimer's disease (Jimenez del Rio *et al.*, 2012), or amyotrophic lateral sclerosis (Barber *et al.*, 2006). ROS have also been implicated in the aging process (Rizzetto *et al.*, 2012)

and are known to play a pivotal role in the development of cancer (Jimenez del Rio *et al.*, 2012).

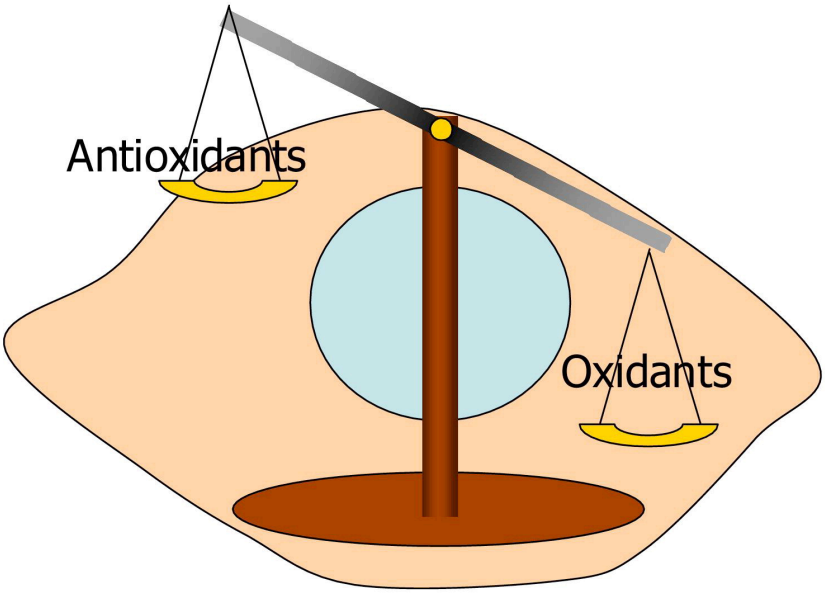


**Figure 6: Oxidative stress represents a condition in which the cellular balance of oxidants and antioxidants is altered in favor of the latter (Harrison *et al.*, 2007).**

On the other hand, reactive oxygen species are not considered only as cell damagers. Accordingly, numerous findings reported that ROS can evoke cellular signaling that induces metabolic health and longevity. It has been proposed that they act as key signaling molecules delivering messages from the mitochondria to other cellular compartments in response to physiological or pathophysiological changes (Veal *et al.*, 2011). Oxidative stress can thus trigger distinct signaling pathways via ROS-mediated modulation of various enzymes and critical transcription factors. The balance between ROS production, cellular antioxidant defenses, activation of stress-related signaling pathways, and the expression of various genes will determine whether a cell exposed to an increase in ROS will be destined for survival or death. In fact, ROS production has long been found to govern programmed cell death (PCD), or even – at very high concentrations – necrosis, in various cell types (Kregel & Zhang, 2007).

### 3.1.1 Antioxidant systems.

Different sophisticated antioxidant systems exist in aerobic organisms, and they function to balance the cellular production of ROS. Endogenous antioxidant defenses include a network of compartmentalized antioxidant enzymes, such as superoxide dismutase (SOD), catalase responsible for the conversion of hydrogen peroxide to water and molecular oxygen, and different forms of peroxidases. These antioxidant enzymes cooperate to convert ROS to more stable molecules, such as water and $O_2$ (Fig. 7).

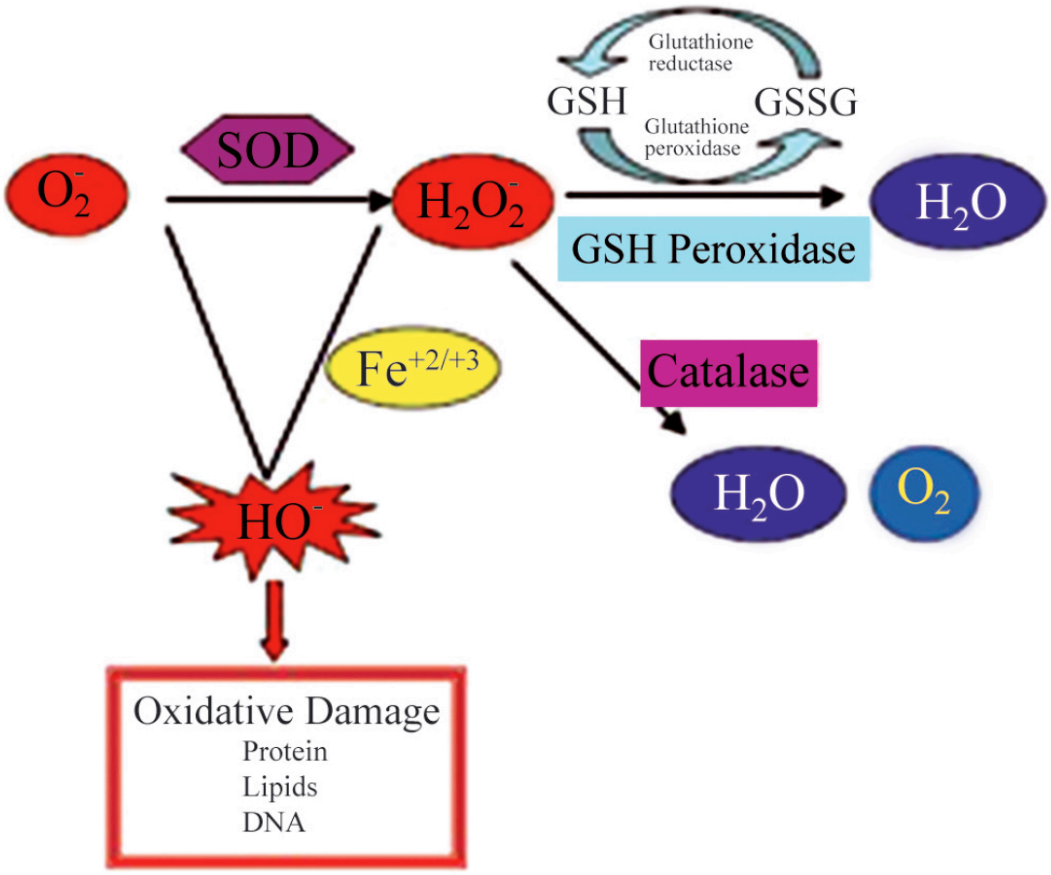


**Figure 7: The toxic effect of ROS can be eliminated by enzymes such as superoxide dismutase (SOD) which eliminates $O_2^-$ to produce $H_2O_2$. Hydrogen peroxide is then eliminated by glutathione peroxidase or by catalase.**

Sod1p is one of the main antioxidant systems and in yeast is made up of two components: Cu-Zn-Sod1p exists in the cytosol and Mn-Sod2p in the mitochondrial matrix. Because the superoxide anion radical substrate poorly

penetrates membranes, the SOD isoenzymes primarily exert their protective functions in their respective compartments.

Besides the primary antioxidant enzymes, different secondary enzymes work together with small molecular-weight antioxidants to form redox cycles that provide necessary cofactors for primary antioxidant enzyme functions. Small molecular-weight antioxidants (e.g., GSH, NADPH, thioredoxin) can also function as direct scavengers of ROS. These enzymatic and non-enzymatic antioxidant systems are necessary for sustaining life by their ability to both maintain a delicate intracellular redox balance and reduce or prevent cellular damage caused by ROS (Willcox *et al.*, 2004).

Although superoxide can directly inactivate certain proteins such as catalases and dehydratases, it is a relatively selective and unreactive ROS (Halliwell, 2012). Nevertheless, the prompt and successful removal of $O_2\bullet^-$ from living cells is of great biological importance, given its tendency to generate $H_2O_2$ and subsequent, more harmful ROS. In fact, studies have shown that $O_2\bullet^-$ detoxification mechanisms such as the superoxide dismutase enzymes (SODs), are essential for survival of *S. cerevisiae* against hyperoxia (Liochev & Fridovich, 2007). Superoxide radical dismutation, which mainly occurs via enzymatic Sod1 activity, is a major source of $H_2O_2$ (Liochev & Fridovich, 2007). In yeast, $H_2O_2$ is also generated by aminoacid oxidases, peroxisomal acyl-coenzyme A oxidases, and protein folding events in the ER (Herrero *et al.*, 2008). Like $O_2\bullet^-$, $H_2O_2$ is relatively unreactive (Halliwell, 2012) and is also a signaling molecule in mammals, plants and yeast. In fact, $H_2O_2$ signaling activates transcription factors that regulate antioxidant gene expression in yeast. Furthermore, pre-treatment with low concentration of $H_2O_2$ enhances the sensitivity of budding yeast cells to heat stress, suggesting that ROS (presumably $H_2O_2$) relay signals induced by heat stress to transcription factors that initiate the heat shock response (Moraitis & Curran, 2004). Both $O_2\bullet^-$ and $H_2O_2$ can combine to form the hydroxyl radical OH•, via the Fenton and Haber–Weiss reactions catalyzed by free metal cations such as those of iron. Ferrous $Fe^{2+}$ ions are oxidized to ferric $Fe^{3+}$ ions by $H_2O_2$ to produce OH•. These

$Fe^{3+}$ ions can be reduced again by $O_2\bullet^-$ resulting in a reaction cycle capable of generating a never-ending supply of OH•. The OH• radical is an exceedingly powerful oxidant that indiscriminately oxidizes cell biomolecules at a diffusion-limited rate (Fridovich, 1998). Biomolecules oxidized by OH• can become radicals themselves, which propagate even further non-specific cell oxidative damage. In fact, most oxidative damage in cells is mediated by OH•, which is far more toxic than its precursors $O_2\bullet^-$ and $H_2O_2$, the impact of which mainly lies in their propensity to form OH• (Halliwell & Cross, 1994). The nitric oxide radical NO• is another important free radical species associated with oxidative damage in organisms (Farrugia & Balzan, 2012). Under normoxic conditions, cells can very efficiently prevent ROS accumulation. However, it has been reported that progressive depletion of nutrients or temperature increase cause stress that is frequently associated with ROS leading to depletion of antioxidants or enhancement of ROS accumulation, or both (Avery, 2011). The accumulation of cellular ROS inevitably results in oxidative damage to important cell biomolecules such as proteins, DNA, and lipids (Fig. 8).

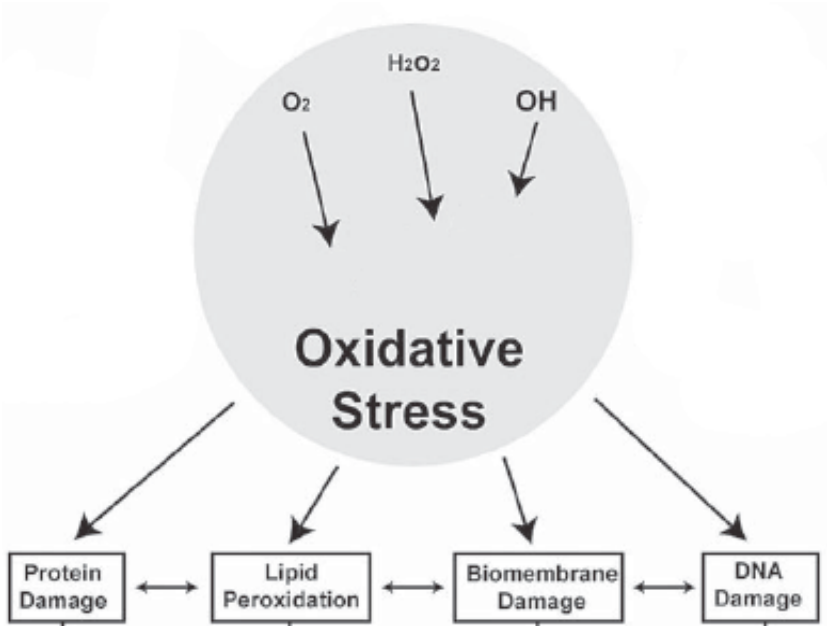


**Figure 8: Oxidative stress leads to cell damage of different biomolecules.**

Failure to prevent such damage influences cell homeostatic functions and rapidly compromises cell viability. In fact, accumulation of oxidized proteins has

been associated with aging and several ROS-related diseases such as ALS and Alzheimer's disease. All ROS, including lipid peroxides, can oxidize proteins via several different pathways, provoking the generation of protein carbonyls. Prompt removal of protein carbonyls is important, given their tendency to form large protein aggregates which cannot then be degraded by cells via normal proteolytic pathways, disrupting cell homeostasis and triggering also endoplasmic reticulum stress (Cecarini *et al.*, 2007).

### 3.1.4 Oxidative Stress Response in yeast

*S. cerevisiae* counteract oxidative stress by evoking responses that ensure the survival of the cell following exposure to oxidants. Such defense systems provide ROS detoxification, reduce their rate of production, and repair the damage caused by them.

The intracellular concentration of $H_2O_2$ in yeast is strongly maintained at very low levels despite of permanent endogenous production by cellular metabolism and large extracellular variations. Oxidant-specific sensors regulate this level by detecting cellular peroxide and controlling the expression of oxidant-scavenger genes in proportion to this concentration. These sensors are thought to detect very low non-toxic levels of $H_2O_2$ that are otherwise not perceived by the cell. Studies of microbial $H_2O_2$ sensing have shown that the underlying mechanisms involve direct protein oxidation by $H_2O_2$ at unique cysteine residues (Toledano *et al.*, 2004).

Specifically the redox relay system includes the $H_2O_2$ sensor Orp1 and the downstream transcriptional regulator Yap1, which is activated by Orp1-mediated oxidation. Basically, one of Orp1 cysteine residues is oxidized and thus interacts and activates Yap1p (Isoyama *et al.*, 2001). This activation occurs rapidly (within 1 min) and transiently (lasting ~30–45 min), with half-maximal oxidation at a concentration of 100 μM $H_2O_2$(Toledano *et al.*, 2004).

## *3.2 ER stress*

The endoplasmic reticulum is the organelle that hosts protein synthesis and folding, calcium storage and calcium signaling. It also serves as a site of biosynthesis for steroids, cholesterol and other lipids. The ER relies on numerous resident chaperone proteins, a high level of calcium and an oxidative environment to carry out these functions efficiently. Given that protein function depends on its three-dimensional structure, its folding must be efficient and successful. In the ER, a complex orchestra of chaperones helps proteins acquire their final form (Trombetta & Parodi, 2003; Anelli & Sitia, 2008). Besides that, proteins that are translocated into the ER lumen experience post-translational modifications, such as glycosylation. Once properly folded, proteins can thus exit from the ER and progress down the secretory pathway. By contrast unfolded and misfolded proteins are exported from the ER and degraded by cytoplasmic proteasome.

The ER is highly sensitive to changes in its environment leading to disruption of its normal homeostasis. A multitude of environmental insults affecting $Ca^{2+}$ homeostasis or glycosylation, such as chemical toxicants but also oxidative stress and/or accumulation of misfolded proteins can all disturb ER function, resulting in what has been referred as ER stress. Such condition occurs when protein folding and secretion overburden the redox capacity of the ER, resulting in ROS accumulation and misfolded or unfolded proteins in this compartment. That is one of the reasons because ER stress and oxidative stress are intimately associated (Walter *et al.*, 2011). The consequent damage and compromised ER activities originate from aggregates of misfolded or unfolded proteins. Processes such as protein synthesis, protein folding and cell viability are notably reduced due to a decrease in essential proteins (Moreno & Orellana, 2011). To overcome this situation, cells react mostly with the activation of the unfolded protein response (UPR) synthesizing more chaperones to rescue misfolded proteins. Proteins remain unfolded or misfolded even after assistance

by ER chaperones and are therefore retrotranslocated back to the cytosol. In this cellular compartment misfolded proteins are ubiquitinated and degraded by the proteasome through a process termed ER-associated degradation (ERAD) *pathway*. If this proves impossible, the apoptosis pathway is activated and the cell eventually dies (Ron & Walter, 2007). ER stress as a reaction to protein misfolding has been associated with various human diseases, such as Alzheimer, Parkinson, diabetes mellitus, atherosclerosis, and ischemia, as well as liver and heart diseases (Yoshida, 2007).

The oxidizing environment of the ER is well suited to the formation of disulfide bonds in proteins entering the secretory pathway. This highly organized cellular compartment contains a high number of chaperones and oxidoreductases assisting in the correct folding of proteins. The redox-active enzyme protein disulfide isomerase (Pdip) plays a crucial role in formation, isomerization, and reduction of disulfide bonds. During disulfide bond formation, Pdi1p accepts electrons from cysteine residues in nascent proteins, leading to the reduction of Pdi1p. Ero1p (ER oxidoreductin) interacts with Pdi1p during this process and passes the electrons to molecular oxygen (or other electron acceptors) to restore the oxidized form of Pdi1p (Tu *et al.*, 2000). This electron transfer cascade potentially leads to generation of ROS, a frequent source of oxidative stress and damage in the cell. Glutathione, the principal low-molecular-weight redox buffer, is a tripeptide with a critical role in bioreduction, protection against oxidative damage, detoxification from xenobiotics, and endogenous toxic metabolites (Penninckx, 2002). In this respect, glutathione peroxidase (Gpx1p) acts as a preventive antioxidant enzyme that is involved in the detoxification of ROS at the expense of reduced glutathione, whereas glutathione reductase (Glr1p) is involved in the recycling of the redox buffer. Glutathione is found in both the reduced (GSH) and the oxidized form (GSSG) in different concentrations and ratios, depending on the cellular compartment. The GSH/GSSG ratio of the ER can range from 3/1 to 1/1 in mammalian and yeast cells (Hwang *et al.*, 1992; Delic *et al.*, 2010).

Yeast has been successfully exploited as a model for protein folding and secretion, considering the differences from higher eukaryotic cells (Khono, 2010). Notably, the secretion pathway of *S. cerevisiae* differs considerably from that of higher eukaryotes and other yeasts. From this point of view *K. lactis* better resembles mammalian cells (Papanikou & Glick, 2009). As *K. lactis* well proven as a host for recombinant protein production, it is an ideal model for both eukaryotic cell physiology and biotechnological process development.

### 3.2.1 Unfolded Protein Response

Proteins must be correctly folded and assembled to fulfill their functions as assigned by genetic code. All living cells have developed systems to avoid unfolding or misfolding of proteins. Productive folding and ERAD together ensure the quality of proteins that pass through the ER, allowing the entry in the secretory pathway for only well-folded molecules.

However, in some cases the ER quality control system fails and ER stress is triggered inside the cell, resulting in the accumulation of unfolded proteins in the secretory apparatus. Basically, all eukaryotic cells counteract ER stress and maintain the homoeostasis of the ER by activating the unfolded protein response (UPR). Nevertheless, under severe ER stress the defensive mechanisms activated by the UPR are not sufficient to restore normal ER function and cells die by apoptosis.

ER stress signals originated from the lumen of the ER are perceived and transmitted across the membrane by an ER transmembrane protein. The number of functional UPR transducers, has increased during evolution. In yeast has been found a unique component, namely Ire1p, in face of two response elements displayed by *Caenorhabditis elegans* and *Drosophila melanogaster* such as (ire-1 and pek-1). Concerning mammals ER homeostasis, UPR *pathways* are regulated by three sensors (Fig. 9), known as IRE1, PERK and ATF6. Thanks to these three *pathways*, mammalian cells are able to cope with ER stress by (i) causing attenuation of translation process to decrease the burden on the folding machinery (via the PERK pathway) (ii) inducing the transcription of ER

chaperones to augment folding capacity and (iii) inducing the transcription of ERAD components to enhance degradation capacity (via IRE1 and ATF6 pathways). The combined effect of these responses aims to ensure the maintenance of the ER (Mori *et al*., 2009).

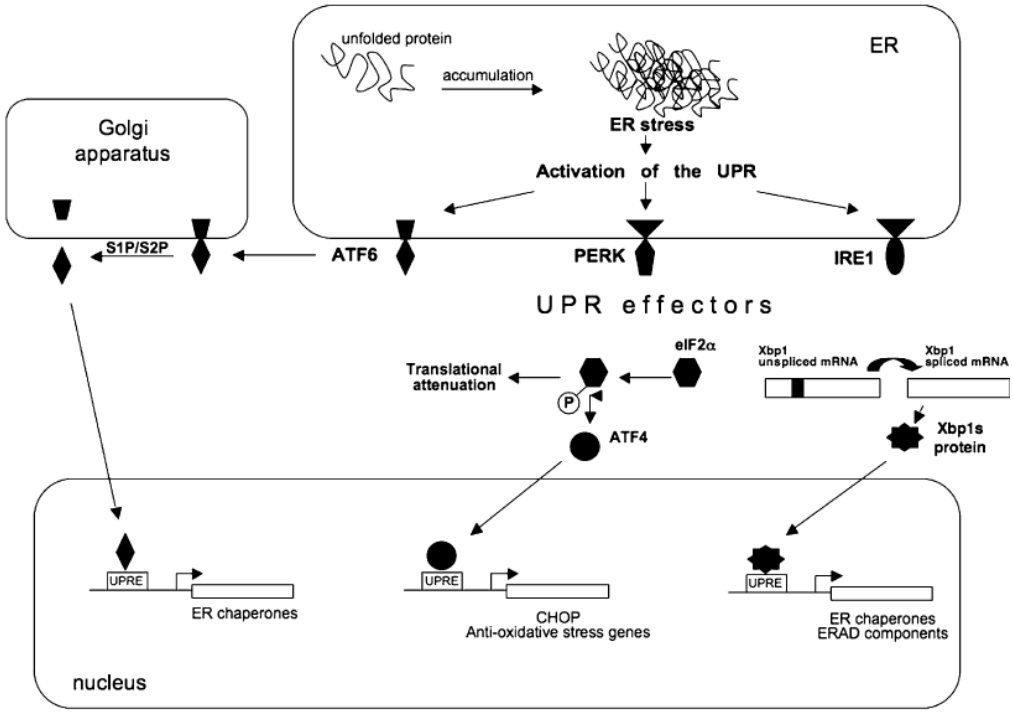


**Figure 9: The response to ER stress includes three distinct pathways that are activated by different ER stress sensors: ATF6, PERK and IRE1. Under ER stress, ATF6 is transported to the Golgi and after being cleaved by S1P/S2P proteases, its cytoplasmic domain activates transcription of chaperones in nucleus. PERK phosphorylates eIF2a, which leads to attenuation of protein translation and activation of ATF4. IRE1 splices Xbp1 mRNA and the translated Xbp1spliced activates the transcription of chaperones and ERAD components (Rasheva *et al*., 2009).**

## 3.2.2 UPR mechanism in mammals

Nowadays it's well known that UPR mechanisms have been conserved during evolution (Mori *et al*., 2009) although ER homeostasis orchestra of mammalian cells results wider than yeast (Fig. 10).

Two homologues of Ire1, Ire1α and Ire1β, have been identified (Tirasophon *et al.,* 1998; Iwawaki *et al.,* 2001). IRE1 functions to promote splicing of a mRNA encoding the transcription factor XBP1. This Ire1-XBP1 signaling pathway is

reported to act synergistically with another signaling *pathway* regulated by the ER-located transmembrane protein ATF6. Together, such pathways trigger the mammalian UPR (Yoshida *et al.,* 2001). A third mechanism interplays to maintain ER homeostasis by attenuating bulk protein synthesis to avoid accumulation of unfolded proteins in the ER. Such condition occurs when the eukaryotic translation initiation factor 2 is phosphorylated by PERK (PKR-like ER kinase), a transmembrane kinase containing an Ire1-like lumenal domain (Harding *et al.,* 1999), and the 28S rRNA is processed by Ire1β (Iwawaki *et al.,* 2001).

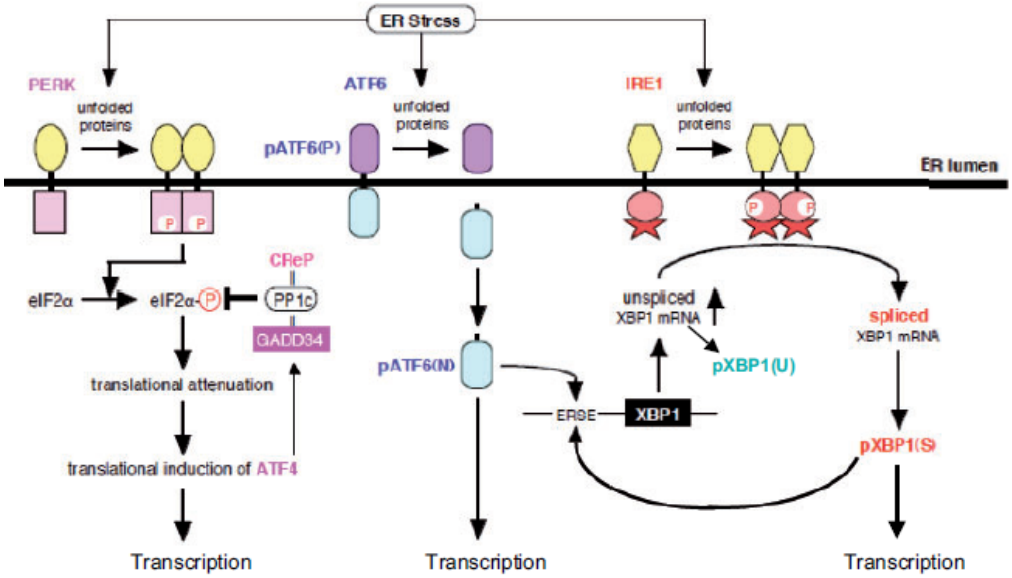


**Figure 10: UPR mechanism in mammals (Mori *et al.*, 2009).**

### 3.2.3 UPR mechanism in yeast

The UPR effectors characterization started by exploiting *S. cerevisiae* as model system. Notably, genetic screens showed that three proteins are necessary for signal transduction from the ER to the nucleus. These are (i) Ire1p, which senses abnormally high levels of unfolded protein in the ER lumen and communicates it across the ER membrane; (ii) Hac1p, which directly activates transcription of UPR target genes; (iii) Rlg1p (tRNA ligase), which plays a critical role in Ire1 activation and Hac1p production (Patil & Walter, 2011).

Specifically, Ire1p is a transmembrane serine/threonine kinase with three functional domains. The amino-terminal domain localizes in the ER lumen and is able to sense the ER unfolded protein accumulation. Once this happened, Ire1p tend to oligomerize (Fig. 11) and trans-autophosphorylation is achieved thanks to its cytosolic kinase domain (Shamu & Walter, 1996). The activated kinase then stimulates the activity of Ire1p's most carboxy-terminal domain, which is a site-specific endoribonuclease.

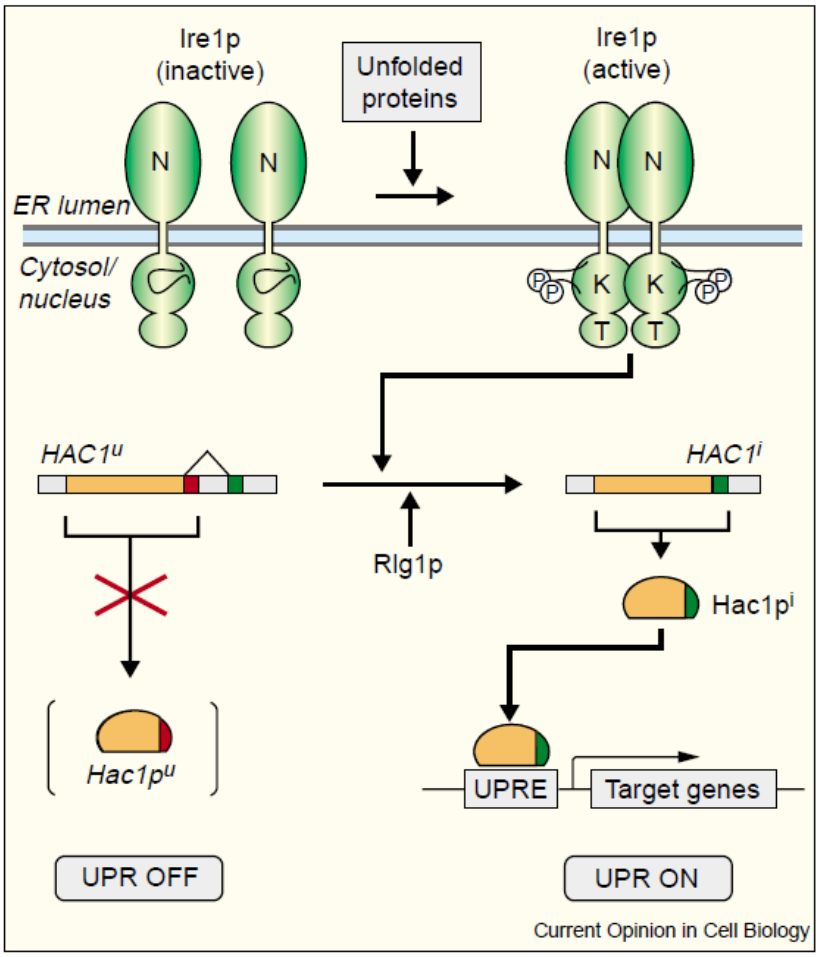


**Figure 11: When unfolded proteins accumulate in the ER, Ire1p oligomerizes, *trans*-autophosphorylates via the cytosolic kinase domain (K) and activates the endonuclease in the tail domain (T). The endonuclease Ire1p cuts *HAC1* mRNA, removing a nonclassical intron; the two exons are rejoined by Rlg1p (tRNA ligase) leading to the translation of Hac1$^{i}$, a transcriptional activator that upregulates expression of UPR target genes after binding to the unfolded protein response element (UPRE) in the promoters of genes encoding ER-resident chaperones and other proteins (Patil *et al.*, 2001).**

To date, the unique known substrate of the Ire1p endonuclease is the HAC1 mRNA, which encodes the bZIP transcription factor that ultimately activates the expression of the UPR target genes. $HAC1^{u}$ ('unspliced') mRNA is constitutively transcribed, but the encoded protein (Hac1p) is not detectable under normal conditions as a result of a non-classical intron near the 3′ end of the open reading frame (Kawahara *et al.*, 1997). Upon activation of the UPR, the intron is removed by Ire1p and the 5′ and 3′ portions of the mRNA are rejoined by tRNA ligase, generating a new mRNA ($HAC1^{i}$, 'induced') encoding a different protein in which a new 18 amino acid tail is appended. HAC1 mRNA splicing thus provides the key regulatory step in the UPR pathway in yeast (Fig. 11).

Yeast cells are able to induce the transcription of a number of ER chaperones only under ER stress via a *cis*-acting element present in their promoter regions. Besides ER chaperones, overexpression is also induced for several class of proteins functioning at various stages of secretion, specifically proteins involved in translocation, protein folding, protein degradation, glycosylation in the ER, lipid/inositol metabolism, ER-Golgi transport, glycosylation in the Golgi apparatus, vacuolar targeting, distal secretion and cell wall biogenesis. Importantly, one of the main differences between yeast and mammals seems to be the absence of attenuation in the translation under ER stress in yeast cells due to the lack of pek-1/PEK/PERK *pathway*. Moreover ER chaperones and ERAD components are transcriptionally induced simultaneously via the Ire1-Hac1 pathway owing to the absence of ATF6 in yeast cells. ER chaperones and ERAD components may deal with accumulated unfolded proteins in a competitive manner (Mori *et al.*, 2009).

Therefore in yeast the UPR is a linear, relatively well-understood pathway whereas in mammalian cells the UPR is an arborized, parallel response (or suite of responses) (Patil & Walter, 2011).

### 3.2.4 BIP/KAR2, a key element of the UPR

Unassembled or underglycosylated proteins or polypeptides that fail to fold into the correct conformation are retained in the ER, often in association with a 78-

kDa protein, termed Ig heavy chain binding protein (BiP), that is an abundant component of the organelle. BiP is the only member of the stress-70 (hsp7O) family of proteins that is located in the ER. In mammalian cells, this protein was originally described independently as the glucose-regulate protein GRP78 and as the immunoglobulin heavy-chain-binding protein that binds heavy chains in the ER of lymphocytes or hybridoma cells that lack immunoglobulin light chains (Bole *et al*., 1986). However BiP promotes productive folding and assembly of nascent polypeptides by stabilizing unfolded or partially folded structures and preventing the formation of inappropriate intra- or inter-chain interactions. The homologue in yeast is the product of *KAR2* gene and it has an amino-terminal ATPase domain close to a substrate-binding domain. Specifically, the ATPase domain is thought to regulate the interaction between the substrate-binding domain and the unfolded protein substrates (Kimata *et al*., 2003).

The *KAR2* promoter harbors different elements that control basal and stress-induced transcription. The HSE is responsible for the upregulation of expression upon a shift of cells from 24°C to 37°C. The unfolded protein response element (UPRE) is activated when unfolded proteins accumulate in the ER, e.g., when N-glycosylation or disulfide bond formation is inhibited (Fig. 12).

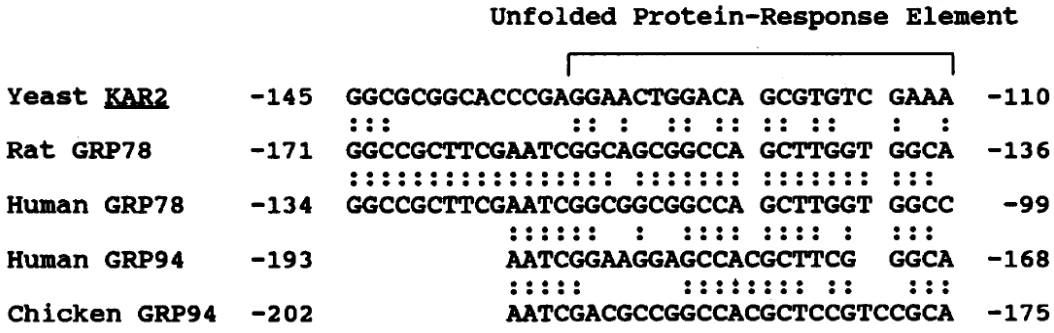


**Figure 12: Conserved sequence of mammalian and yeast Bip(Kar2) promoters. The sequence in the *S. cerevisiae* KAR2 promoter that is important for the induction by unfolded proteins in the ER is compared with sequences in the promoters of the human and rat gp78 (BiP) and human and chicken grp94 genes. (Kimata *et al*., 2003).**

To date, it is believed that Kar2 associates with Ire1 (Fig. 13). This proposed mechanism, hereafter called the Kar2-dependent Ire1 regulation, is supported by several findings in previous studies in yeast (Kohno *et al.,* 1993; Okamura *et al.,* 2000). Therefore in wild-type cells under non-stressed conditions, Kar2 binds with Ire1 and represses Ire1 activity. In ER-stressed conditions, unfolded proteins compete with Ire1 for binding to Kar2, Ire1 is then released, and in turn induces the UPR signaling pathway (Kimata *et al*., 2003).

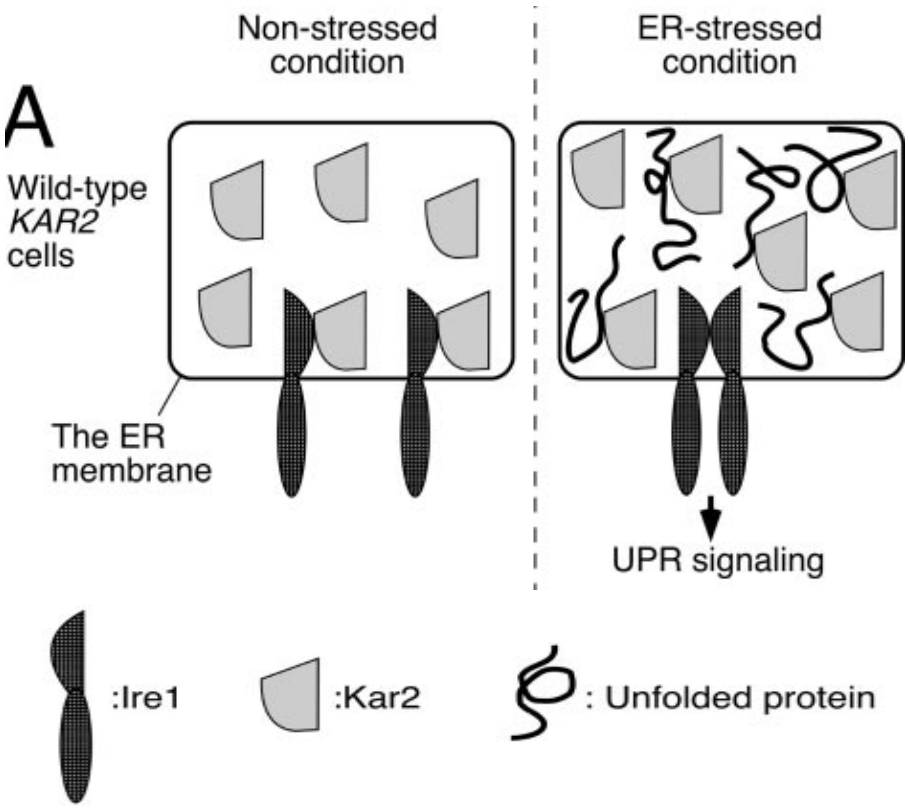


**Figure 13: A schematic model of the Kar2-Ire1p interaction. (Kimata *et al*., 2003).**

### *3.3 Cell wall stress*

As discussed earlier, fungal environments present challenges for cell survival including osmotic changes, oxidative stress, heat shock, pH changes, and chemical toxicity that, in turn, can impact on cell wall structure. Notably, the key defense to cope with environmental injuries is the fungal cell wall. Stressors can in fact damage cell wall and thus activate the repair mechanisms capable of fortifying it through cell wall biosynthesis and the integration of cell wall components into the cell wall (Fuchs & Mylonakis, 2009). Three different sensor systems can monitor the functional integrity of the yeast cell wall (Fig. 14) and modulate responses to maintain CWI upon cell wall damage: (i) The MID1-CCH1 based mechano-perception pathway; (ii) the high-osmolarity glycerol (HOG) pathway, essential for orchestrating the adaptive response of yeast cells to hyperosmotic stress and (iii) the cell wall integrity maintenance mechanism.

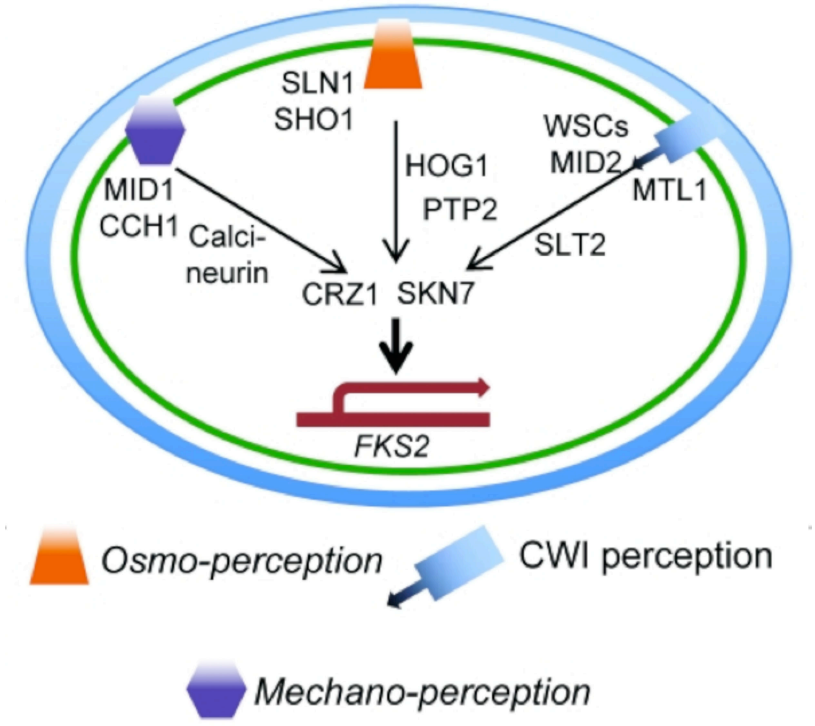


**Figure 14: Schematic overview of signaling cascades implicated in CWI maintenance in yeast (Hamann *et al.*, 2011).**

Specifically, the signal generated by the CCH1 MID1 complex upon membrane stretch is transmitted via calcineurin leading to activation of response genes like the glucan synthase FKS2 (Zhao *et al.*, 1998). The CWI pathway additionally regulates FKS2 activity. Two different sensors (SHO1; SLN1/YPD1/SSK1) perceive hyperosmotic stress and generate signals relayed to the MAPKinase HOG1 (Hohmann *et al.*, 2009). The hyperosmotic stress activated HOG pathway interacts with the CWI pathway when induced by hypo-osmotic shock thus modulating the response of the yeast cells to low pH, heat shock and zymolyase treatment (Rodríguez-Peña *et al.*, 2010).

### 3.3.1 Cell Wall

The cell wall is a cellular structure unique to fungi among eukaryotes; plant cells have a cell wall, but it is very different from the fungal cell wall. The cell wall varies between fungi, but the overall composition consists of α- and β-glucans representing the principal polysaccharides of the cell wall, *N*-acetylglucosamine, mannoproteins, and various other glycoproteins. In general, yeast cell wall comprises 10–25% of the cell mass depending on growth conditions (Smits *et al.,* 1999). It is composed of approximately 5% of proteins and 95% of polysaccharides (Fig. 15). Among them, about 40% are mannan, covalently bound to cell wall proteins. The other 60% consist mainly of β-glucans. Chitin (β-1,4-*N*-acetylglucosamine polymers) represents only 1–3% of the polysaccharides and preferentially accumulates at the bud neck and in the bud scars (Klis *et al.*, 2002). As it concerns ultrastructure analysis, yeast cell wall generally appears as a two-layered structure (Cappellaro *et al.* 1994). The inner one is less electron-dense, surrounds the plasma membrane and is composed principally of glucan polymers and chitin. This layer is composed mainly (80–90%) by β-1,3-glucan chains branched through β-1,6 linkages. Polymers of β-1,6-glucan chains make up most of the remainder of the inner layer (8–18%) with chitin chains representing the smallest fraction (1–2%). This layer is largely responsible for the mechanical strength and elasticity of the cell wall, owing primarily to the helical nature of β-1,3-glucan chains (Smits *et al.* 1999).

The outer layer is in contact with the medium, is more electron-dense and contains most of the mannoproteins (Zlotnik *et al*., 1984). This is also true for *K. lactis*, where glycosylation mutants have been shown to increase their cell wall thickness, presumably by altering the glycosylation pattern of the mannoproteins (Uccelletti *et al.*, 2000).

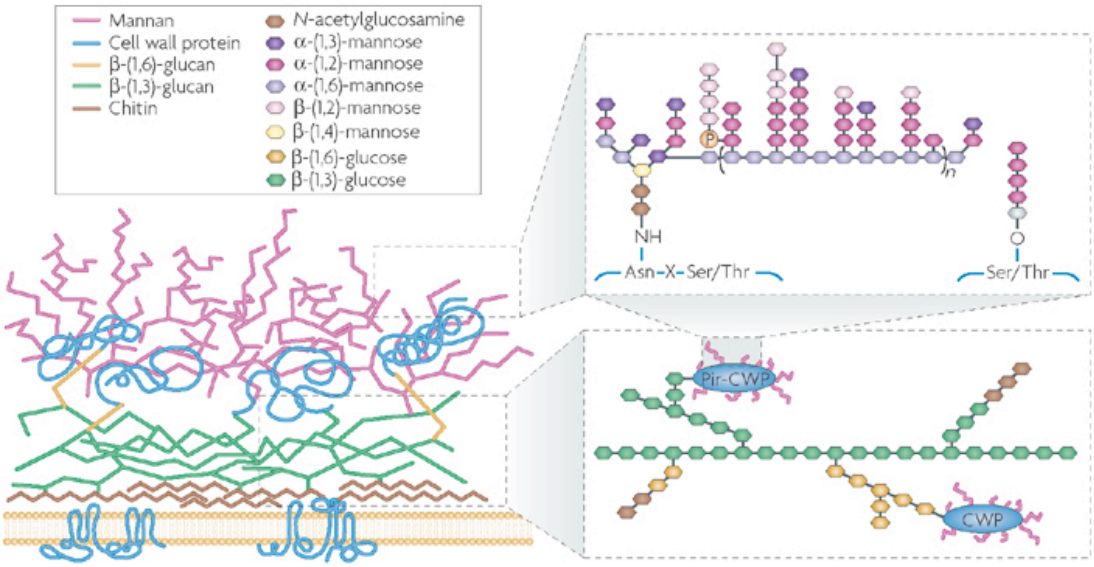


**Figure 15: The schematic shows the major components of the cell wall and their distributions. β-(1,3)-glucan and chitin are the main structural components, and these are located towards the inside of the cell wall. The outer layer is enriched with cell wall proteins (CWP) that are attached to this skeleton mainly via glycosylphosphatidylinositol remnants to β-(1,6)-glucan or, for mannoproteins with internal repeat domains (Pir-CWP), via alkali-sensitive linkages to β-(1,3)-glucan. The insets show the structure of the glucan and mannan components. (Netea *et al*., 2008)**

The outer cell wall layer is a matrix of glycoproteins. Cell wall glycoproteins (CWPs), that compose this layer, can be grouped into two main classes: (i) the majority are glycosylphosphatidylinositol (GPI) proteins and are characterized by a lipid anchor at their C termini which provides a connection to the plasma membrane but is processed further for covalent attachment of such proteins to cell wall polysaccharides. Specifically GPI proteins destined for the cell wall are liberated from the plasma membrane by cleavage of their anchors (Kollár *et al.* 1997). Lipidless GPI fragments of GPI–CWPs become linked to the external surface of the β-1,3-glucan network indirectly through β-1,6-glucan chains; (ii)

the second class includes the Pir proteins, which are named after the presence of internally repeated sequences, through which they are attached to the 1,3-β-glucan network.

Yeast cell wall possesses four principal functions:

(i) It provides protection from osmotic shock. In nature, yeast cells interplay with rapid and extreme environmental changes, particularly with respect to osmotic potential. For instance, *S. cerevisiae* cells under hypo-osmotic shock must limit the influx of water to prevent bursting (Smits *et al.* 1999; Hohmann 2002). This concern is avoided by cell wall plasticity that limits therefore cell swelling. Specifically, fungal cell creates a balance by which the force driving water across the osmotic gradient into the cell is counteracted by turgor pressure against the plasma membrane and cell wall.

(ii) Mechanical stress is avoided by cell wall strength and elasticity providing an effective barrier against sheer and compression forces.

(iii) The yeast cell wall is required to maintain cell shape (Klis *et al.* 2002), which is essential for the formation of a bud and, hence, cell division. The cell must remodel this rigid structure to provide cell expansion during vegetative proliferation and starvation-driven filamentation (pseudohyphal development) (Harold, 2002). For growth to produce cell shapes other than spheres, cell wall expansion must be focused to particular regions. *S. cerevisiae* uses an internal actin cytoskeleton for this purpose (Drubin and Nelson, 1996). During periods of polarized cell growth, the wall is loosened by digestive enzymes (*e.g.*, glucanases and chitinases) and expanded at a single point on the cell surface, a process that must be carried out in a highly regulated manner to avoid cell lysis.

(iv) The cell wall functions as a scaffold for cell-surface proteins. The polysaccharides that provide the mechanical strength of the cell wall also serve as the attachment matrix for a wide variety of glycoproteins (Klis *et al.*, 2002). These glycoproteins include sexual agglutination factors important for mating (Cappellaro *et al.*, 1994; Zhao *et al.*, 2001) and adhesins critical to cell–cell contact during filamentation, invasive growth, and biofilm formation. Cell-surface glycoproteins also limit the permeability of the cell wall to

macromolecules, thereby protecting the glucan layer from wall-degrading enzymes (Levin, 2011). These different requirements afford a rigid structure, with the capacity to be dynamically remodelled during normal cellular growth and upon extracellular stresses.

### 3.3.2 Cell Wall Integrity Pathway

Based on the importance to maintain and monitoring a functional integrity of the cell wall, yeast cells have developed a fine mechanism, namely the cell wall integrity (CWI) *pathway*, which responds to cell wall stress signals through a family of cell-surface sensors coupled to a small G protein, Rho1. The membrane-spanning sensors consist of two small sub-families (Fig. 16): (i) the Wsc-type sensors Wsc1, Wsc2 and Wsc; (ii) Mid2 and Mtl1 subclass.

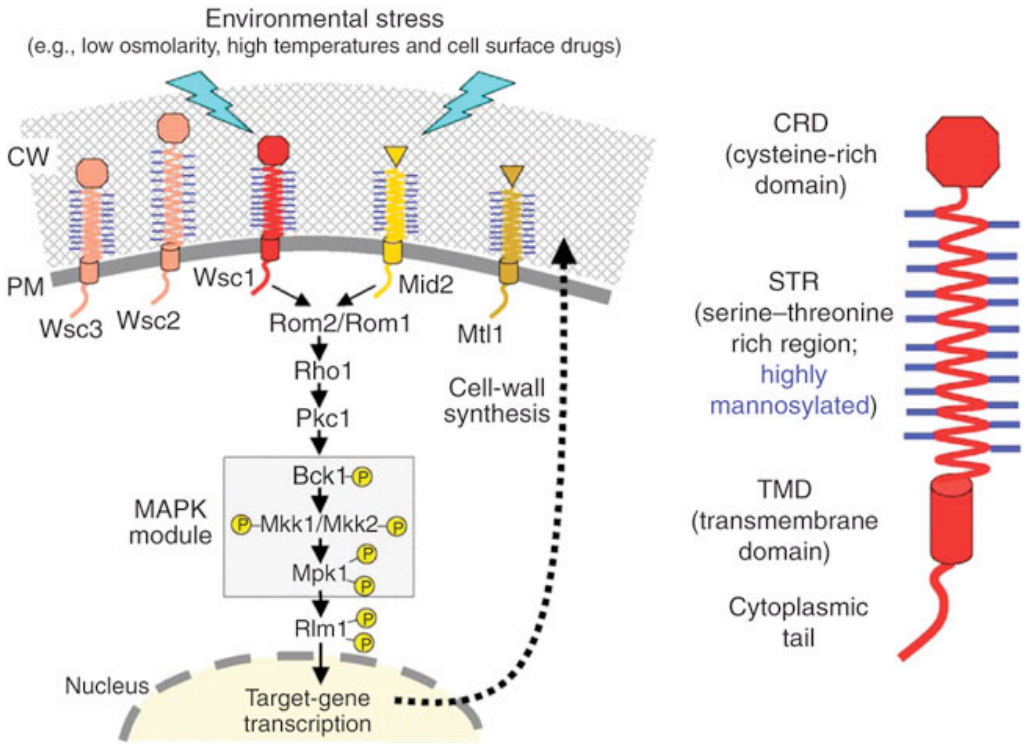


**Figure 16: The five sensors of the CWI pathway are anchored in the plasma membrane (PM) and reaching into the cell wall (CW). The first component of a conserved mitogen-activated protein kinase (MAPK) module, Bck1, is activated by Pkc1 through phosphorylation. At the right, the general structure of the Wsc1 sensor is shown, with the external region (STR) functioning as a nanospring. Octagons represent the cysteine-rich domains of the Wsc-type sensors, which may be functionally replaced by an *N*-glycosylated asparagine in the Mid-type sensors (triangles). (Heinisch *et al.*, 2009)**

It has been observed that despite little sequence identity between the deduced proteins (ca. 30% between the Wsc-type sensors and 50% between Mid2 and Mtl1), they share some common features: (i) all start with a signal peptide, which is presumably cleaved off in the secretory pathway; (ii) all five sensors contain a single predicted transmembrane domain (TMD), connecting the proteins' large extracellular regions; (iii) relatively short cytoplasmic tails (CT); (iv) the extracellular regions contain sequences rich in serines and threonines (STR), which are highly *O*-mannosylated (Lommel *et al.*, 2004); (v) in addition, the sensors from the Wsc-family are characterized by a cysteine-rich domain (CRD) at their aminoterminal end.

Classifications of the two subfamilies are based on the additional CRD (cysteine-rich domain; also referred to as the Wsc-domain) at the aminoterminal end of the Wsc-type sensors in face of an N-glycosylated asparagine, which characterizes the other sensor subclass. It has been suggested that the CWI sensors work as mechanosensors (Levin, 2011). Thus, the TMD anchors the sensors in the plasma membrane, whereas the head groups would provide a dynamic interaction with the cell wall. The connecting STR region would adopt a rod-like structure, owing to its *O*-mannosylation (Heinisch *et al.*, 2010). Consequently, a pressure either on the cell wall or on the plasma membrane should produce a mechanical force on the extracellular part of the sensors that, in turn, undergo conformational changes, transmitted then to the cytoplasmic tails. In such a way the intracellular response is triggered. The CRD domain apparently mediates protein–protein interactions, resulting in the sensors clustering and thus generating a ‘sensosome’. The two sensors Mid2 and Mtl1 lack a CRD domain. However, Mid2 was shown to depend on an *N*-glycosylated asparagine (N35) near the aminoterminal end for its function (Hutzler *et al.*, 2008). In analogy to the CRD of the Wsc-type sensors, it may provide a ‘head group’ contacting the cell wall glucans. An asparagine at position 42 in Mtl1 could also be *N*-glycosylated and could serve a similar function. Three homologous sensors could be identified in the milk yeast *K. lactis* (KlWsc1, KlWsc2/3 and KlMid2), where they ensure cell integrity (Rodicio *et al.*, 2008).

Specifically, sensors are capable of recruiting Rom2 to sites near the cell surface where cell wall remodelling is required and of catalyzing the exchange of GDP to GTP in the nucleotide binding pocket of the small GTPase Rho1. Hence the induced Rho1 binds to and activate the protein kinase C, Pkc1 (Fig. 17).

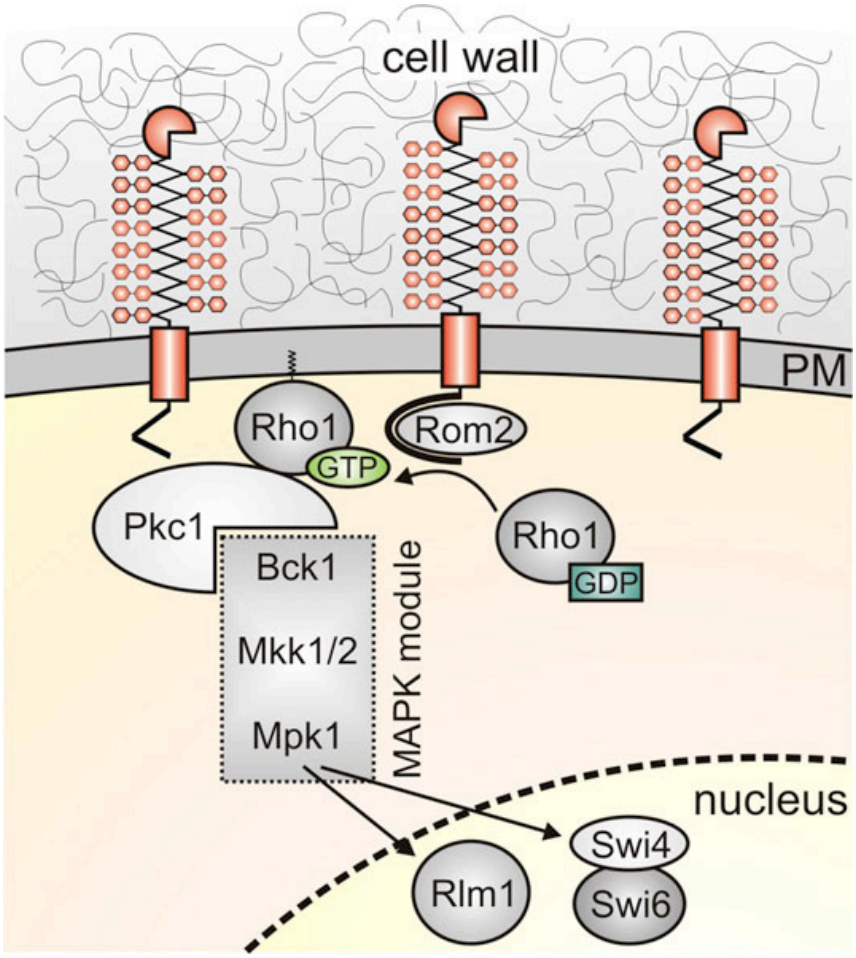


**Figure 17: Simplified scheme of the CWI signaling pathway in *S. cerevisiae*. The plasma membrane (PM) spanning sensors interact with their cytoplasmic tails with Rom2, which in turn activates Rho1 and recruits it to the membrane. Rho1 then interacts with and activates Pkc1, which phosphorylates Bck1, the upstream kinase of the MAPK module. Phosphorylation of the dual pair of MAPKKs finally activates the MAPK Mpk1 by a dual phosphorylation at a threonine and a tyrosine residue. Two transcription factors, Rlm1 and the SBF complex consisting of Swi4 and Swi6, have been identified as the targets of Mpk1. They regulate the nuclear expression of genes involved either in cell wall biosynthesis and remodelling, or in cell cycle progression, respectively. (Jendretzki *et al.*, 2011)**

Rho1 is considered to be the master regulator of CWI signaling and its various effectors include the β-1,3-glucan synthase encoded by the FKS1 and FKS2 genes, β-1,6-glucan synthase activity. Calcineurin participates also in cell wall biosynthesis. In fact, *FKS1* is also induced by calcineurin and experimental evidences indicate interplay between the CWI pathway and calcineurin (Fuchs & Mylonakis, 2009). One target of the activated protein kinase C is Bck1, the upstream kinase of a conserved MAPK (*m*itogen *a*ctivated *p*rotein *k*inase) module. This cascade (also comprising the protein kinases Mkk1/Mkk2 and Mpk1) presumably regulates the nuclear localization and thus the activity of two known transcription factors, the SBF complex (consisting of Swi4 and Swi6) and Rlm1, which have been implicated in the expression of cell wall biosynthetic genes and in regulating the cell cycle.

# *4. PROTEIN GLYCOSYLATION*

Proteins of all living organisms are generally modified in many different ways. The most complex and at the same time energetically most-costly protein modification is the glycosylation of proteins. Glycoproteins are implicated in a multitude of cellular processes including the immune response, intracellular targeting, intercellular recognition, and protein folding and stability (Varki, 1993).

The known cases of compromised glycosylation of proteins provoke very severe health problems in children and typically result in multisystemic presentation such as abnormal development of the brain and functions of the nerve-, liver-, stomach-, and intestinal systems. Specifically, such congenital disorders of glycosylation (CDG) are genetic diseases owing to deficient or increased protein glycosylation (Jaeken, 2010).

Glycoproteins, the end products of such a modification, are proteins containing covalently linked oligosaccharides that consist of different monomers and are mostly branched. The carbohydrate moiety tipically represents 20 % of the molecular weight, but can be as much as 90 % in some cases (Lehle *et al.*, 2006).

Glycoproteins are typically produced as mixtures of glycoforms possessing the same polypeptide backbone but differing in the site of glycosylation and/or in the structures of pendant glycans (Wang & Lomino, 2012). The different sugars, which are either N- or O-glycosidically linked to the amino acid asparagine or to the hydroxy amino acids threonine, serine, hydroxyproline, hydroxylysine, and tyrosine (Fig. 18) reflect the complexity of protein glycosylation. In addition, there is a large variety of more or less highly branched oligo- and polysaccharides of varying composition that decorate the proximal sugar of the protein with *e.g.*, sialic acids, and noncarbohydrate functional groups such as sulfate, phosphate, and acetate.

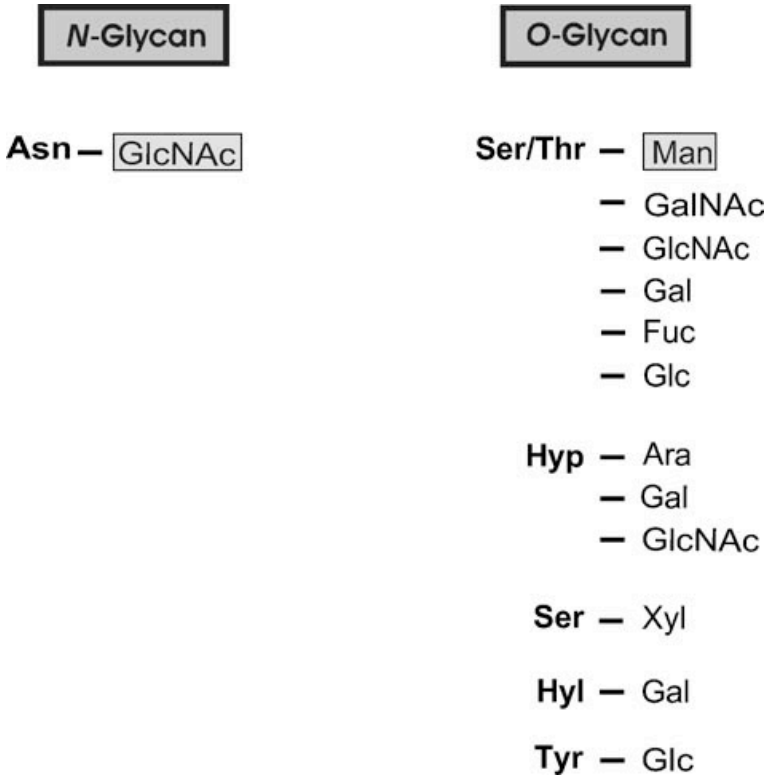


**Figure 18: Types of sugar-peptide bonds in eukaryotes. Asn=asparagine, Ser=serine, Thr=threonine, Hyl=hydroxylysine, Hyp=hydroxyproline, Tyr=tyrosine, GlcNAc=*N*-acetylglucosamine, GalNAc=*N*-acetylgalactosamine, Glc=glucose, Gal=galactose, Rha=rhamnose, Xyl=xylose, Ara=arabinose, Man=mannose, Fuc=fucose. (Lehle *et al.*, 2006)**

Glycosylation patterns are regulated by many factors such as amino acid sequences, local peptide conformations at the glycosylation sites, as well as the accessibility and localization of activated substrates, enzymes, and cofactors (Wang & Lomino, 2012).

N-glycosylation is evolutionary conserved from yeast to man. Yeast cells only possess two kinds of protein glycosylation; N-glycosylation of asparagine residues and O-mannosylation of threonine and serine residues. For the formation of the glycan chains, more than 100 gene products are required (Lehle *et al.*, 2006). Notably, most of the CGDs in humans are related to failure in exactly these two pathways of protein glycosylation.

### *4.1 N-Glycosylated Proteins*

In particular, the N-glycosylated proteins contain oligosaccharides that are N-glycosidically linked to the γ-amido group of asparagines. This type of glycoprotein has been most intensively studied with respect to their structure, biosynthesis, and function; they occur in all eukaryotes and in many archaea but only exceptionally in bacteria (Lechner & Wieland, 1989). Commonly, N-glycosylated proteins are secretory proteins and thus move along the secretory pathway to the cell surface where they either get exported or anchored to the plasma membrane, to the extracellular matrix, or to the cell wall.

It was demonstrated that the formation of the highly variable *N*-linked oligosaccharides originates in each case from the transfer of the $Glc_3Man_9GlcNAc_2$ unit. The so-called core oligosaccharide is relocated from a lipid carrier to the protein. Subsequently the protein-bound oligosaccharide is modified in a protein- and tissue-specific manner by splitting off definite sugar residues and by adding others.

The structure and synthesis of the core oligosaccharide $Glc_3Man_9GlcNAc_2$ in N-glycosylation are highly conserved. The molecule capable of assembling such precursor is a lipid poly-isoprenoid named dolichol pyrophosphate (Dol-PP). It functions as a carrier on which the $Glc_3Man_9GlcNAc_2$ oligosaccharide is synthesized. Because of its highly hydrophobicity, dolichol remains firmly associated with ER membrane while some enzymes, both cytosolic both resident in the ER, add several sugar residues.

The oligosaccharide-protein-transferase (OST) complex catalyzes the subsequent oligosaccharide relocation on asparagine residues (in the sequences Asn-X-Ser or Asn-X-Thr) of the nascent polypeptide (fig 19).

Although the reactions of oligosaccharide maturation are substantially different along organisms, in each case occurs the removal or addition of sugar residues to newly-sinthesized glycoproteins.

Thus, N-linked protein glycosylation pathway in eukaryotes can be divided into two different processes: the assembly of the lipid-linked oligosaccharide at the

membrane of the endoplasmic reticulum and the transfer of the oligosaccharide from Dol-PP to selected asparagine residues of nascent polypeptides.

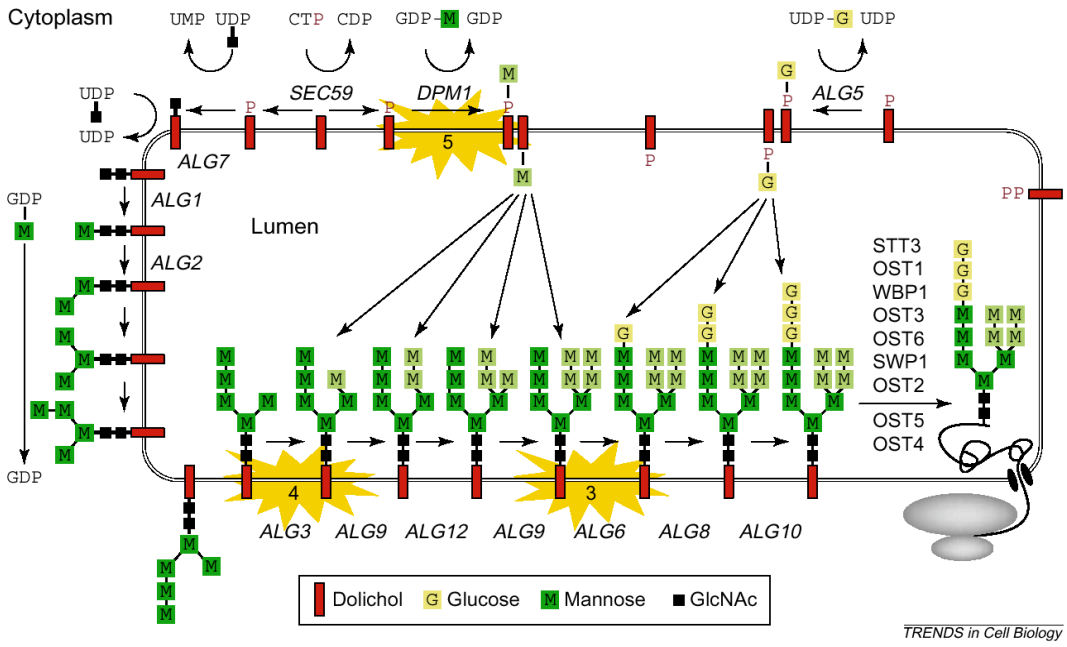


**Figure 19: The biosynthesis of lipid-linked oligosaccharide and its transfer to protein in the process of N-linked protein glycosylation in the ER in the yeast *Saccharomyces cerevisiae*. A schematic view of the ER membrane is shown, where the lipid dolichol (red bar) is phosphorylated and then serves as a carrier in the synthesis of the core oligosaccharide. At the stage of $Man_5GlcNAc_2$, the lipid-linked oligosaccharide is flipped into the lumen of the ER and further extended by dolichylphosphomannose (DolP-Man) and dolichylphosphoglucose (DolP-Glc)-dependent glycosyltransferases. The oligosaccharyltransferase complex transfers the oligosaccharide to selected asparagine residues of translocating polypeptide chains. (Aebi *et al.*, 2001)**

The consensus sequence or sequon, asparagine-X-serine/threonine (X can be any amino acid except proline) within the proteins to be glycosylated are recognized by OST. Since only 66 % of the sequons are glycosylated, additional structural requirements have to be satisfied for N-glycosylation to occur. Basically, the amino acids adjacent to the sequon, its position in the aminoacidic chain, the rate of protein folding and the availability of the dolichol precursor saccharide, all impact the efficiency of glycosylation (Lehle *et al.*, 2006). Following transfer of the core oligosaccharide to the asparagine residue, three glucose moieties and one terminal α-1,2-mannose moiety are removed by glucosidase I and glucosidase II, and an ER-residing α-1,2-mannosidase,

respectively. The resulting $Man_8GlcNAc_2$-containing glycoprotein is then transported to the Golgi apparatus where *N*-glycan processing differs markedly between yeast and mammals (Fig. 20).

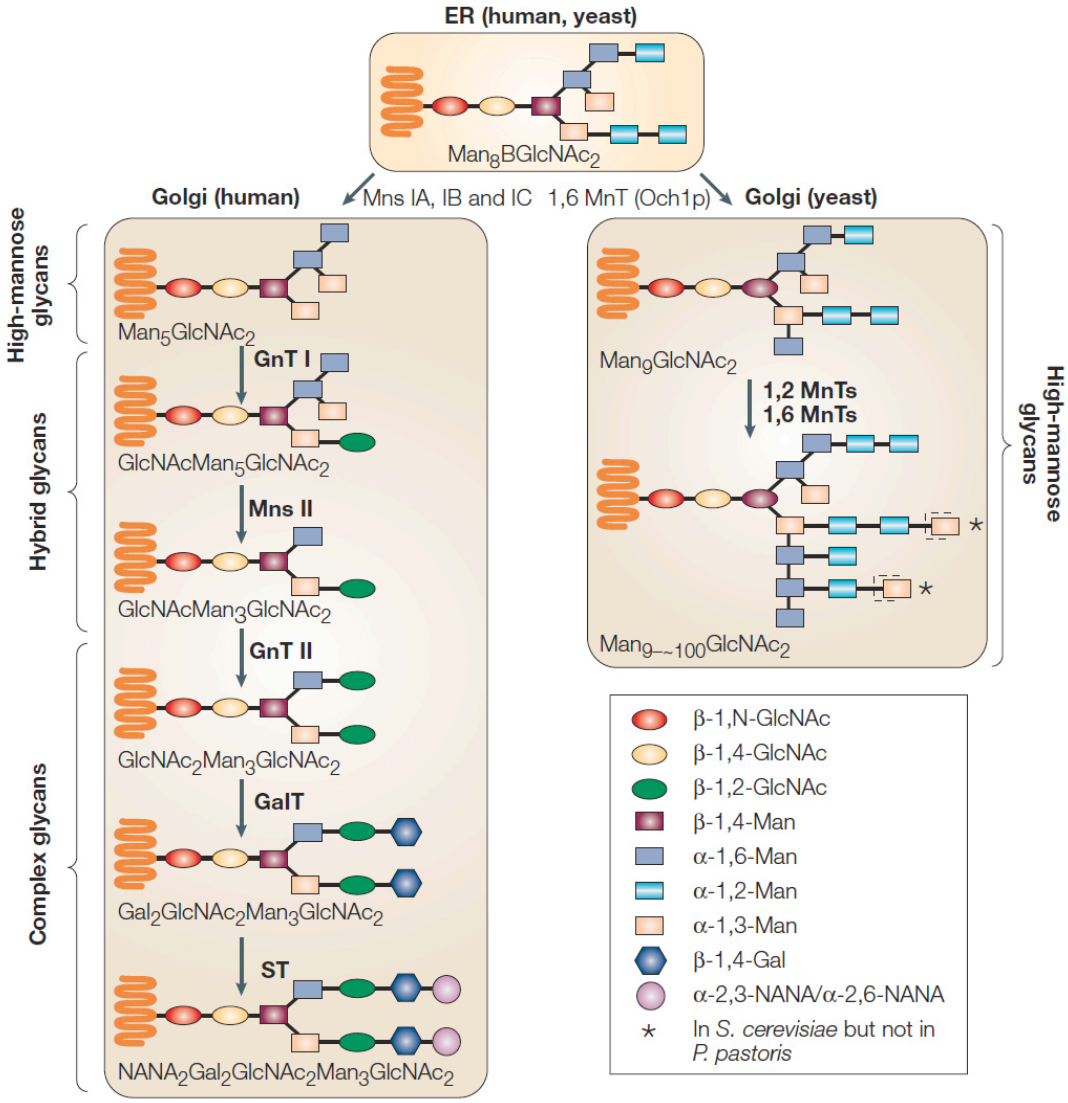


**Figure 20: Representative pathway of *N*-glycosylation pathways in humans (left) and yeast (right). (Wildt *et al.*, 2005)**

This is due to the fact that a series of different sugars and their transferases exist in mammalian cells that do not exist in yeast. Notably it has been observed that some yeasts such as *Schizosaccharomyces pombe* and *K. lactis* seem to lack

ER-specific α-1,2-mannosidase activity, resulting in the transport of $Man_9GlcNAc_2$-containing glycoproteins to the Golgi (Gemmill *et al.*, 1999).

The Golgi apparatus is made up of flattened cisternae that usually organize into a stack and compartmentalize the enzymes that modify the proteins and lipids synthesized in the endoplasmic reticulum (Czlapinski *et al.*, 2006).

Human *N*-glycan processing involves the removal of mannose followed by the addition of GlcNAc, galactose, fucose and NANA. In such a way, the enormous diversity of glycan structures of the so-called "complex type" arises. If the number of mannoses is not reduced, the glycan chain is defined as an "oligomannose type", which only exists in yeast, but, dependent on the protein, it may be further extended in the Golgi apparatus with more than 100 mannose units forming the so-called outer chain (Ballou, 1990). In fact, early *N*-glycan processing in yeast is limited to the addition of mannose and mannosylphosphate sugars. The Golgi apparatus of *S. cerevisiae* contains α-1,2-, α-1,3- and α-1,6-mannosyltransferases as well as mannosylphosphate transferases, which produce *N*-glycan structures that are mannosylated and hyper-mannosylated to varying extents.

In the yeast *S. cerevisiae* the maturation of N-linked oligosaccharides in the Golgi consists entirely of mannose additions (Fig. 21). Some N-linked oligosaccharides are extended to form hypermannosylated glycoproteins with outer chains that may contain up to 200 mannose units. The linear backbone of the outer chain contains 50 or more mannoses in an α-1,6-linkage. Addition of α1,2- and α1,3-linked mannoses results in a highly branched structure. The outer chain also contains several mannosylphosphate residues that endow the oligosaccharide with a net negative charge. These polymannose structures are primarily found on secreted or cell wall mannoproteins and may contribute up to 95% of the molecular mass of these glycoproteins (Dean *et al.*, 1999).

In *K. lactis*, *H. polymorpha* and *P. pastoris*, a similar set of mannosyltransferases exists, resulting in the production of mostly high-mannose structures that resemble those produced in *S. cerevisiae* but which are typically smaller in size (Wildt *et al.*, 2005).

Synthesis of the outer chain begins when a single mannose is added onto the $Man_8GlcNAc_2$ core structure in the Golgi, a reaction catalyzed by the Och1 protein (Fig. 21). This mannose then serves as the scaffold for the further extension of the outer chain.

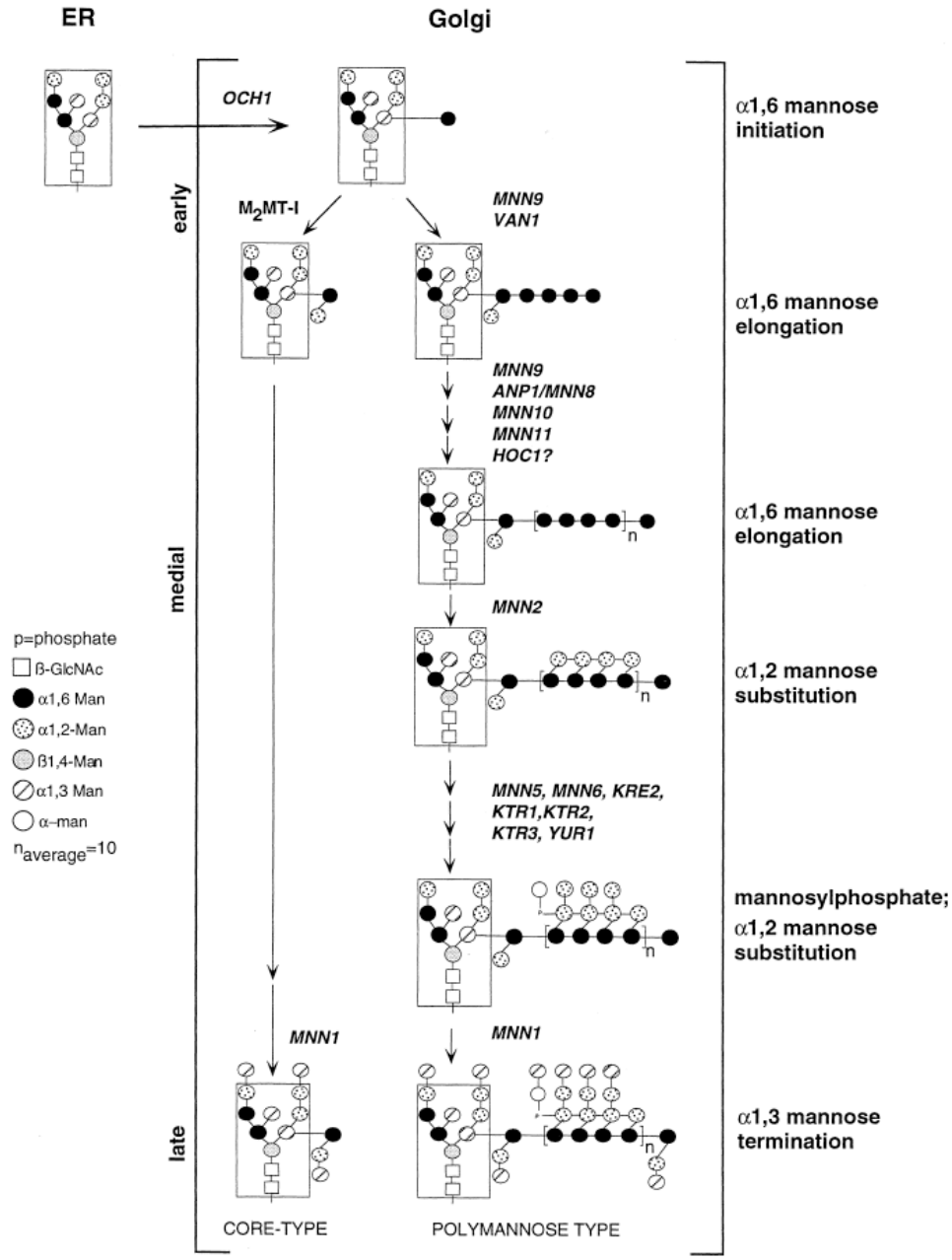


**Figure 21: Biosynthetic pathway of yeast N-linked oligosaccharides in the Golgi (Ballou, 1990).**

A multi-step process has been proposed for the elongation of the α-1,6 backbone, where several α-1,6-mannoses and a single α-1,2-mannose are first added in a reaction catalyzed by a protein complex that contains both Mnn9p and Van1. The elaboration of the backbone may also occur in several stages by complexes that contain other α-1,6-mannosyltransferases. The order of addition of mannosylphosphate and secondary α-1,2-mannose residues is not known. The Och1p-catalyzed initiation reaction is taken to define the *cis*-most compartment and the Mnn1p-catalyzed termination reaction is taken to define a late processing compartment (Ballou, 1990).

## *4.2 Vanadate Glycosylation Affected mutants*

In a previous study from our lab several glycosylation mutants of *K. lactis* have been isolated (Uccelletti *et al.*, 1999), taking advantage of the knowledge that, in *S. cerevisiae*, the orthovanadate-resistant mutants usually show defects in protein glycosylation (Ballou, 1990).

The isolated mutants belong to at least four complementation groups. All mutant strains were analyzed for the ability to extend the chains of mannose present on invertase. Since they are also altered in the N-glycosylation, as well as in sensitivity to vanadate, they have been termed vga (Vanadate Glycosylation Affected) 1 to 4.

Defective N-glycosylation is often associated with a reduced ability to correctly organize the structure of the cell wall, since the enzymes involved in its assembly undergo modifications in the secretion apparatus.

Among the different isolated mutants, VGA3 was finely characterized and it was found that the gene of *Kluyveromyces lactis* VGA3 corresponded to *KlOCH1* gene, functionally homologous to *OCH1* gene of *Saccharomyces cerevisiae*.

This gene codes for the $\alpha$-1,6 mannosyltransferase that localized in the Golgi apparatus. This enzyme catalyzes the addition of the first mannose to the oligosaccharide core of newly synthesized glycoproteins, coming from the endoplasmic reticulum. The point mutation characterizing this strain causes the substitution of a G with an A in position 735 of the ORF of the *KlOCH1* gene, with the subsequent formation of the stop codon (TGA). As a result, the truncated protein is unstable in the cells.

N-glycosylation efficiency was strongly reduced in this mutant strain with respect to wild type. By contrast, the *O*-glycosilation process is not affected. Besides the N-glycosylation defects, *Kloch1-1* cells display alterations in the structure and composition of the cell wall as well as growth defects. Nonetheless, mutant secretory capacity is increased compared to the wild type strain. Concerning heterologous proteins production, *Kloch1-1* cells can be

considered as an outstanding "cell factory". Specifically its hypersecretor capacity was demonstrated by employing two different recombinant proteins such as the Human Serum Albumin (HSA) and Glucoamylase (GAA) from *Arxula adeninivorans*. Moreover, as discussed before, *Kloch1-1* cells display alteration in cell wall organization since they are sensitive to calcofluor, a molecule known to interfere with chitin deposition. Electron microscope photographs (Fig. 22) showed, in addition, that mutant cell wall (panels A and C) is thicker than its parental counterpart (panels B and D) and it is evident an accumulation of fragments of electron-dense material in the layer containing the glucans (Uccelletti *et al.*, 2000).

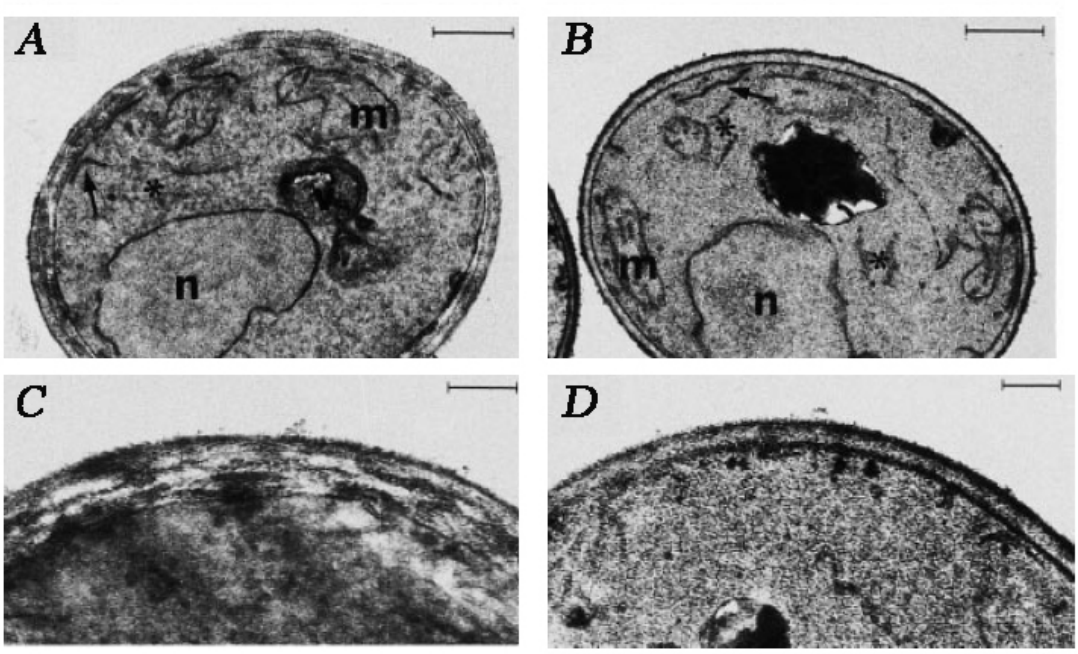


**Figure 22: Ultrathin sections of mutant (A and C) and wild type strains (B and D). (Uccelletti *et al.*, 2000).**

# AIM OF THE PROJECT

Natural environments are complex and often vary significantly in space and time, posing challenges for the organisms living within them. Single-cell organisms are particularly vulnerable, since variation in external conditions can directly impact internal homeostasis. Physiological adaptation to changing environmental conditions is an essential feature of all cells. In fact, when faced with stressful conditions, cells have to trigger a molecular response that allows them to adapt and survive or, alternatively, cause cell death. The existence of molecular mechanisms responsible for repair and adaptation, many of which are greatly conserved across nature, give rise to the cellular stress response (Zdralević *et al.*, 2012).

Calcium ion ($Ca^{2+}$) may be the most universal between the second messengers capable of triggering several cell responses, as it can be spatially and temporally controlled with remarkable finesse, interacting with a dizzying array of proteins to execute its many cellular regulatory functions in both prokaryotic and eukaryotic organisms. Given the broad physiological roles of $Ca^{2+}$, intracellular $Ca^{2+}$ concentrations ($[Ca^{2+}]_i$) must be controlled and maintained at the appropriate level (Santella & Carafoli, 1997). The secretion machinery organelles, such as the ER and the Golgi apparatus, play an important role in the equilibrium of intracellular calcium homeostasis.

Given that calcium regulates and controls several processes, its altered regulation could lead to different severe diseases. Thus, it results clear that understanding calcium homeostasis mechanisms is a critical topic from a research point of view.

Nowadays, an ever-growing interest is moving towards stresses, such as the ER and the oxidative ones, which are reported to be associated with important human diseases including Alzheimer, Parkinson, diabetes mellitus,

atherosclerosis, and ischemia, as well as liver and heart diseases (Yoshida, 2007).

Besides that calcium plays a key role in maintaining ER homeostasis, it is well known that accumulation of misfolded proteins in the ER can disrupt the organelle function. In the ER, a complex orchestra of chaperones helps proteins acquire their final form (Trombetta and Parodi, 2003; Anelli and Sitia, 2008). Proteins that are translocated into the ER lumen undergo post-translational modification, such as glycosylation, necessary for protein folding and thus for optimal function.

N-glycosylation is essential for numerous fundamental and intracellular events. In fact, N-glycosylation plays a key role in the protein trafficking across the secretory apparatus to the cell surface (Conti *et al*., 2002), and in the recognition of mis-folded proteins in the ER (O'Connor & Imperiali, 1996).

To date, the known cases of congenital underglycosylation of proteins cause very severe health problems in children and typically result in multisystemic presentation involving interference with normal development of the brain and functions of the nerve-, liver-, stomach-, and intestinal systems. As far as protein N-glycosylation is involved, the disease is called CDG-syndrome (*c*ongenital *d*isorders of *g*lycosylation) and the whole phenomenon demonstrates most convincingly the enormous biological importance of protein glycosylation (Jaeken, 2010).

However, the interplay between calcium metabolism and glycosylation in yeast remains still largely unknown. In order to clarify this relationship, this project is aimed to figure out if and how defective glycosylation process can impact on calcium-related stress onset. Moreover, it has been reported that defects in protein *N*-glycosylation can cause mitochondrial deficiencies and loss of tolerance to oxidative stress (Nakamura *et al.*, 2007). However, in most of the cases the mechanisms linking glycosylation and mitochondrial dysfunctions need to be elucidated.

In this study, the effect of the mutation of the *KlOCH1* gene on calcium homeostasis and stress onset was investigated in the yeast *Kluyveromyces lactis*.

This gene codes for the α-1,6-mannosyltransferase, which is the first enzyme in the Golgi Apparatus responsible for the oligosaccharide core elongation of new-synthesized peptides by the addition of the first mannose to the N-glycan chains. Specifically the attention was focused on the analysis of the interplay between calcium signaling executors in relation to oxidative and ER stress responses in this N-glycosylation mutant.

# RESULTS

## *1. Altered mitochondrial biogenesis in Kloch1-1 cells*

The *K. lactis KlOCH1* gene encodes the α-1,6-mannosyltransferase localized in the Golgi apparatus and involved in the glycosylation process and in cell wall morphogenesis. From a biotechnological point of view, the *Kloch1-1* mutant strain showed a strikingly enhanced heterologous protein secretion as demonstrated in a previous work (Uccelletti *et al.*, 2006). However, as a bottleneck in its employment as a 'cell factory', the *Kloch1-1* cells displayed in fermenter a higher generation time in rich fermentable medium than wild type cells under optimal growth conditions.

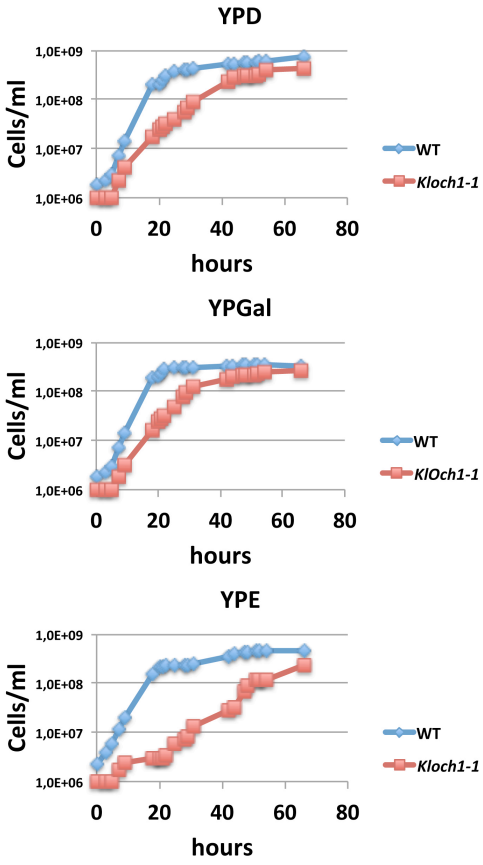


**Figure 1: Growth of *K. lactis* strains in fermenter in rich media containing different carbon sources such as glucose (YPD), galactose (YPGal) or ethanol (YPE).**

Nevertheless the biomass yield was strongly reduced in the presence of a respiratory carbon source such as ethanol with respect to fermentable carbon sources including glucose and galactose (Fig. 1). Indeed, fermenter data prompted us to investigate if the lack of α-1,6-mannosyltransferase activity in *K. lactis* cells could be associated with mitochondrial alteration. To this aim we performed DASPMI staining, a fluorescent probe that is taken up by mitochondria of live cells as a result of membrane electrochemical potential and thus considered as an indicator of mitochondrial functionality. Once cells were incubated with this dye, we observed a different distribution of the fluorescence in the two strains: in the *Kloch1-1* background, cells showed a punctuate pattern and some ring structures in face of the regular tubular network of the wild type counterpart (Fig. 2A).

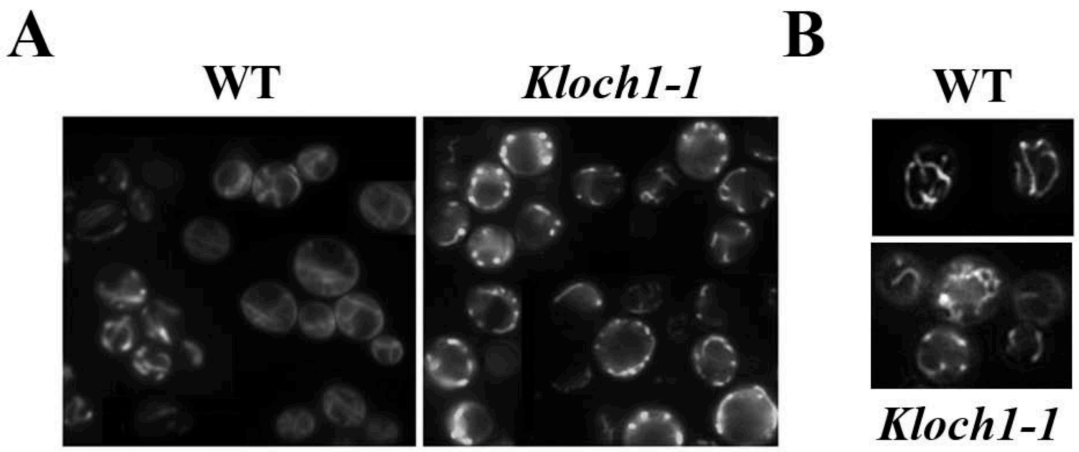


**Figure 2: Morphological and functional analysis of mitochondria in cells lacking α-1,6-mannosyltransferase activity. (A) DASPMI staining of *Kloch1-1* cells and the parental strain. (B) GFP fluorescence of mitochondrial matrix of wt and mutant strains harboring pCXJ3-mtGFP vector.**

In order to figure out if alterations in the mitochondrial network morphology could occur, we transformed the mutant and wild type strains with a plasmid carrying the GFP fused to the mitochondrial signal sequence from the subunit 9 of the F0-ATPase from *Neurospora crassa*; this construct has been demonstrated to correctly deliver GFP into yeast mitochondria (Westermann & Neupert, 2000). Taking into account that mitoGFP can not give us indication of

mitochondria functionality, mitoGFP fluorescence in the mutant cells revealed a hyper-branched mitochondrial net in face of the fragmented phenotype visualized by DASPMI. By contrast for the wild-type cells, GFP-fluorescence resulted identical to the DASPMI one. This data demonstrated that just a few portions of the *Kloch1-1* mitochondrial network are functional in comparison with the wild type. To further study the altered mitochondrial morphology, the mutant strain and its isogenic wild type counterpart were analyzed by electron microscopy. In ultrathin sections of the parental strain, mitochondria appeared as round structures, with regular morphology and typical cell peripheral distribution (Fig. 3). By contrast, the *Kloch1-1* cells showed mitochondria appearing stretched; crests were not visible in the middle part and mitochondria ends resembled round swollen, in agreement with the altered morphology observed by DASPMI staining.

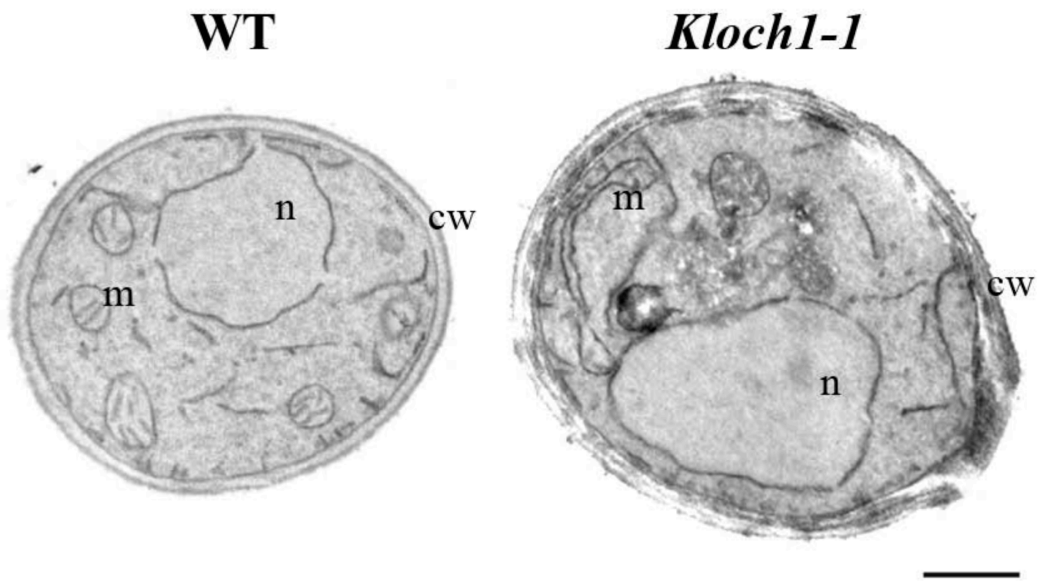


**Figure 3: Mitochondrial analysis by electron microscopy of *Kloch1-1* cells and the parental strain. Cultures were grown to exponential phase into YPD medium. n, nucleus; m, mitochondrion; cw, cell wall; bar 1 µm.**

Since mitochondrial dysfunction is often associated with accumulation of reactive oxygen species (ROS), we therefore evaluated the amount of ROS by using the fluorescent dye 123 dihydrorhodamine (DHR). Such compound

accumulates inside the cells and it is oxidized to the corresponding fluorescent chromophore by ROS. The fluorescence microscope observation revealed that 28% of *Kloch1-1* cells accumulated ROS as compared to 5% of the parental strain (Fig. 4); these values increased up to 48% and 18% in the mutant and wild type cells respectively after challenge with a generator of oxidative stress, such as the hydrogen peroxide ($H_2O_2$).

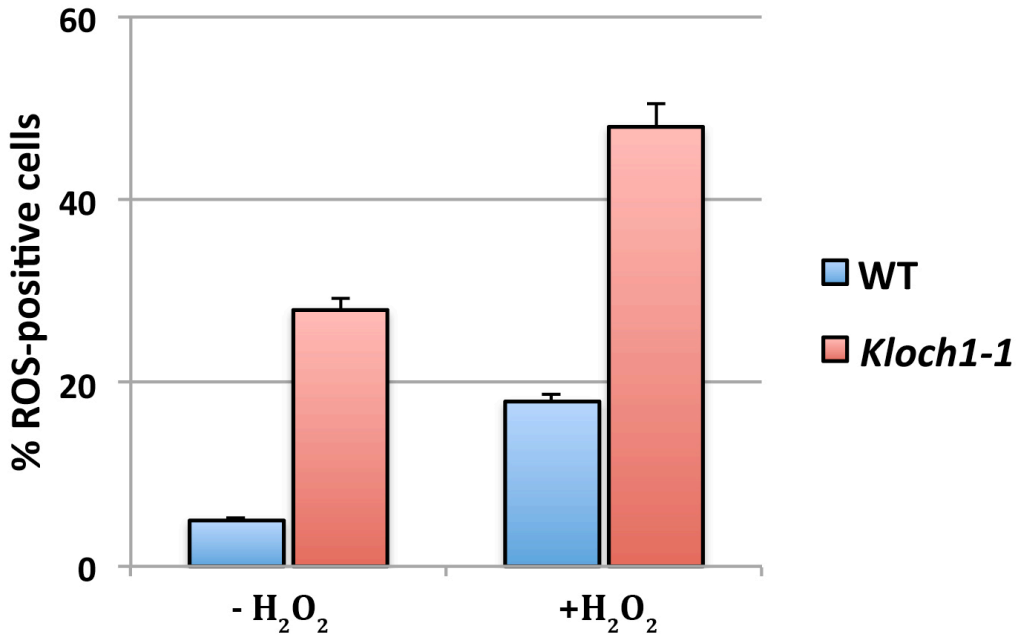


**Figure 4: Estimation of ROS accumulation in the indicated strains by DHR-staining after growth to exponential phase in YPD medium. Measurements were also obtained after exposure to $H_2O_2$ for 2 h.**

To further investigate the cellular response to oxidative stress taking place in the mutant strain, *K. lactis* cells were challenged for 2 and 5 h with a cytotoxic concentration of $H_2O_2$ (Fig. 5). A strong reduction of the survival rate was observed after a 5 h treatment in cells lacking the α-1,6-mannosyltransferase activity. Specifically only 41% of mutant cells survived versus 93% of the parental ones.

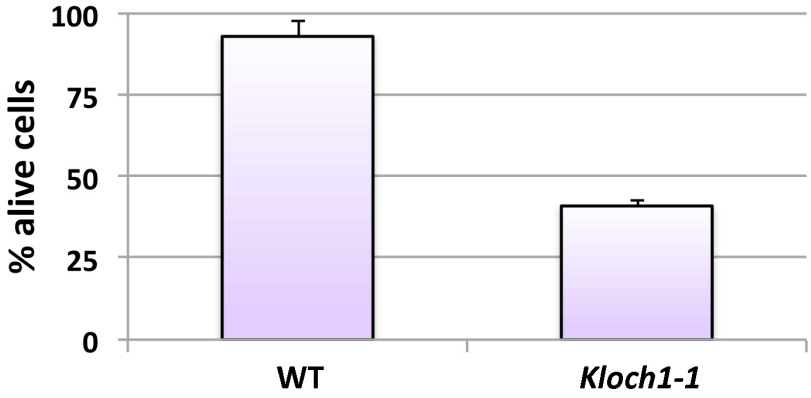


**Figure 5: Cell viability after $H_2O_2$ exposure: parental strain and cells lacking α-1,6-mannosyltransferase activity, grown to exponential phase on YPD medium, were challenged with 20 mM $H_2O_2$ for 5 h. The viability was evaluated plating the samples on YPD and was expressed as the CFU percentage of the corresponding untreated cultures. The values were the mean of three independent experiments and showed an SD < 10%.**

Oxidative stress was also assessed in *K. lactis* cells by analyzing the growth sensitivity onto rich medium containing $H_2O_2$; the mutant strain, in fact, was not capable of growing in the presence of 4 mM hydrogen peroxide as shown in figure 6.

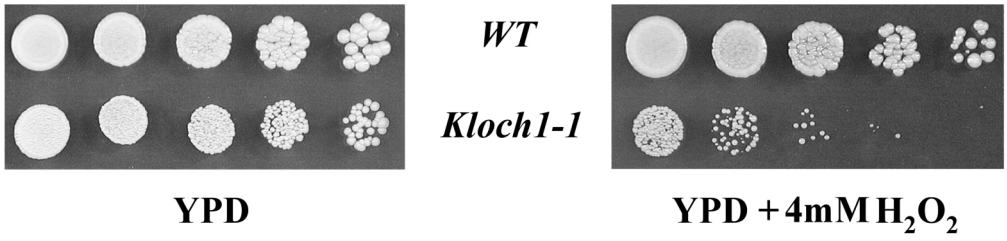


**Figure 6: Growth of indicated yeast strains onto solid medium supplemented with 4 mM $H_2O_2$.**

## *2. Isolation of KlCMD1 as extragenic suppressor of oxidative stress occurring in Kloch1-1 cells*

In order to highlight genetic interactions underlying *Kloch1-1* alterations, we performed a screen to identify multicopy suppressors able to relieve the growth sensitivity on $H_2O_2$-containing media (Fig. 7).

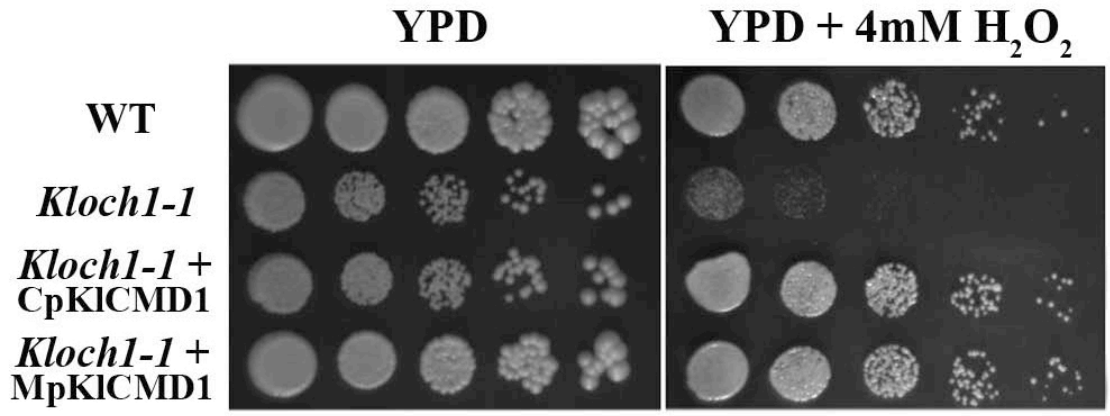


**Figure 7: Genetic screen to identify suppressor(s) able to rescue the growth defect of *Kloch1-1* cells. The *KlCMD1* gene, responsible to allow again the growth of the mutant cells in medium containing the hydrogen peroxide was subcloned into centromeric and multicopy plasmids, CpKlCMD1 and MpKlCMD1 respectively. The growth at 28°C was monitored after 3 days; three independent transformants have been checked, obtaining identical results.**

Three of the plasmids, isolated from the corresponding clones that survived the selection procedure, resulted to be identical and were further analyzed. Sequencing analysis revealed that the *K. lactis* DNA fragment present in the plasmid contained an ORF of 441 bp with 1000 bp upstream of the putative ATG start codon and 100 bp downstream of the putative stop codon. The protein encoded by this ORF resulted to be KlCmd1p, the homologue of the *S. cerevisiae* calcium sensor calmodulin (Rayner & Stark, 1998). This gene was able to restore the growth defect of *Kloch1-1 cells* on $H_2O_2$ also when cloned in a centromeric plasmid (CpKlCMD1).

Possible transcriptional variations of *KlCMD1* gene are thus investigated in the *Kloch1-1* mutant cells. A strong reduction of calmodulin mRNA levels was effectively observed as revealed by northern blotting analysis (Figure 8).

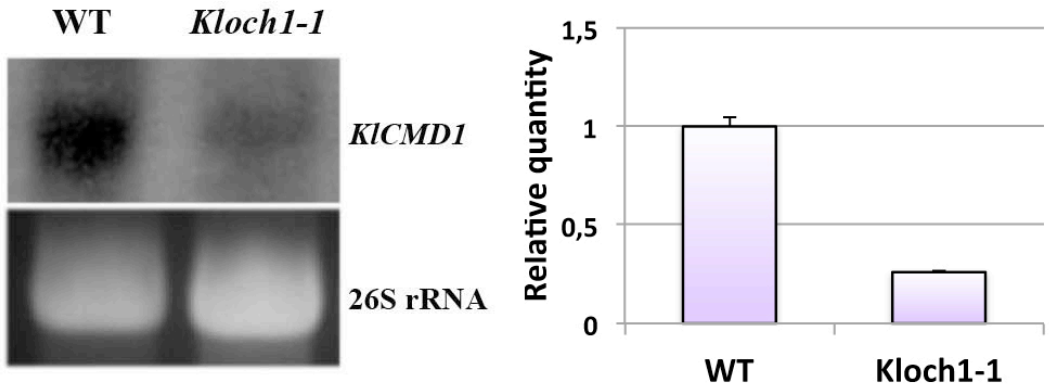


**Figure 8: Comparison of transcript levels of calmodulin in parental and mutant strains by Northern blot analysis. RNAs were extracted from cells after growth for 48 h in SD minimal medium. The same amount of total RNA from the strains was loaded on each lane; the ethidium bromide-stained gel of the autoradiogram is shown in the bottom part of the figure and the mRNA loading was normalized using the 26S rRNA bands. Quantification, by densitometric analysis, of the radiolabeled signal on the blot is shown in the right part of the figure. The hybridization signal for wild type strain was set as 1.**

Moreover the impact of *KlCMD1* overexpression on ROS and mitochondria alterations was explored. The analysis revealed that the presence of *KlCMD1* gene on a centromeric plasmid was able to reduce the oxidative stress of these cells as revealed by the DHR staining; the amount of positively stained cells of the transformants, in fact, was significantly reduced in comparison with untransformed cells: 8% versus 28% respectively (Figure 9A). Unexpectedly, the *Kloch1-1* cells transformed with CpKlCMD1 or MpCMD1 did not show an increase in the survival capabilities with respect to the mutant cells, when challenged for 5 hours with 20 mM (Fig. 9B). This result suggests that calmodulin alone is not sufficient to trigger a quick cellular response to oxidative stress.

In addition the mitochondrial functionality of the *Kloch1-1* cells carrying the calmodulin either on a centromeric (CpKlCMD1) either on a multicopy plasmid (MpKlCMD1) was analyzed by DASPMI staining (Fig. 9C).

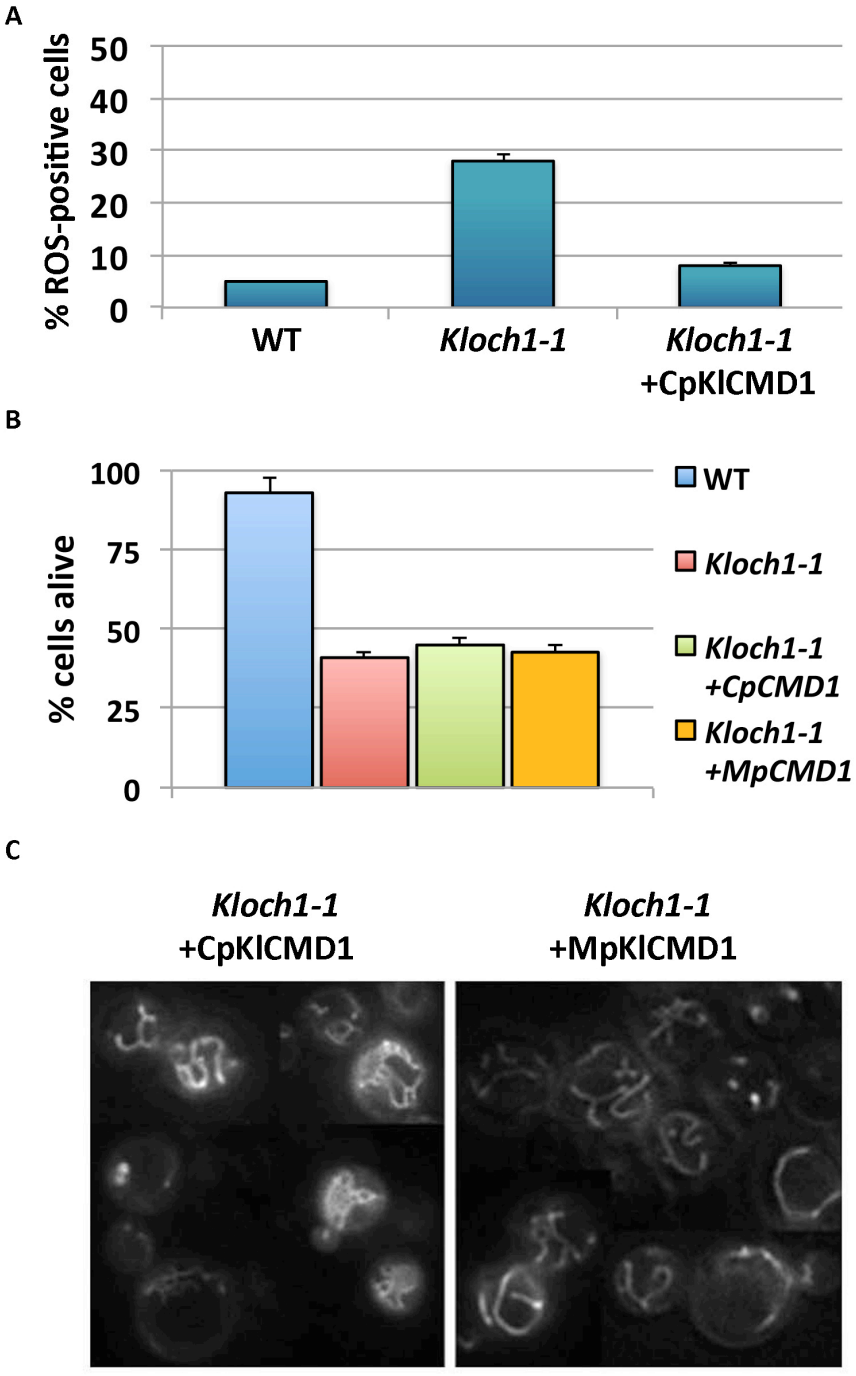


**Figure 9: (A) Estimation of ROS accumulation in WT cells and *Kloch1-1* mutant strain harboring empty or CpKlCMD1 vectors by DHR-staining. (B) Cell viability after a 5 h $H_2O_2$ exposure of indicated strains. (C) DASPMI staining of mutant cells transformed with centromeric (left side) or multicopy (right side) plasmids containing *KlCMD1* gene.**

In *Kloch1-1* cells carrying the CpKlCMD1 vector, DASPMI fluorescence showed a hyper-branched mitochondrial net in spite of the dotting phenotype of the

mutant strain (see Fig. 2A). This indicates that in *Kloch1-1* cells the hyper-branched mitochondrial net visualized by mitoGFP (see Fig. 2B) that has been proved to be not completely functional (see Fig. 2A) – DASPMI binds potentially active membranes – became able to fully establish a membrane electrochemical potential just by adding a few copies of calmodulin in these cells through the centromeric plasmid. On the other hand, the mitochondrial alteration was completely abolished when the mutant cells were transformed with the multicopy vector MpKlCMD1; in those cells DASPMI staining, in fact, revealed a tubular mitochondrial network similar to wild type cells, even if in some cases ring structures were still present (Fig. 9C).

Besides the generation of cellular energy, mitochondria play a critical role also in regulating calcium homeostasis (Babcock *et al.*, 1997). As a result, we explored possible calcium homeostasis alterations in *Kloch1-1* cells, taking into account the oxidative stress suppression by calmodulin. We thus investigated if cells lacking α-1,6-mannosyltransferase activity could grow in the presence of EGTA, a cationic chelator. This perturbing agent makes calcium unavailable in YPD medium, resulting in lack of growth for cells with impaired calcium homeostasis.

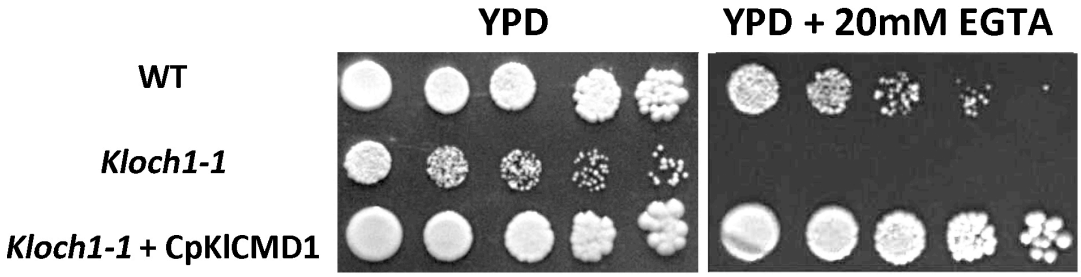


**Figure 10: Growth of indicated yeast strains onto solid medium supplemented with 20 mM EGTA.**

As reported in figure 10, growth was strongly inhibited in the mutant cells when YPD plates were supplemented with this chelating agent. However, such sensitivity was completely suppressed in the mutant strain as a result of calmodulin overexpression, indicating that an altered calcium homeostasis effectively occurs. These findings prompted us to determine the intracellular

calcium content by using Fura-2AM, a membrane-permeable derivative of the ratiometric calcium indicator Fura-2 (Poenie & Tsien, 1986). When added to cells, Fura-2AM crosses cell membranes and once inside the cell, the acetoxymethyl groups are removed by cellular esterases. Removal of the acetoxymethyl esters regenerates "Fura-2", the calcium indicator. Bond of $Ca^{2+}$ increases the fluorescence of Fura-2 when excited at 340 nm and decreases the fluorescence from excitation at 380 nm. Measurement of $Ca^{+2}$-induced fluorescence at both 340 nm and 380 nm allows for calculation of calcium concentrations based 340/380 ratios.

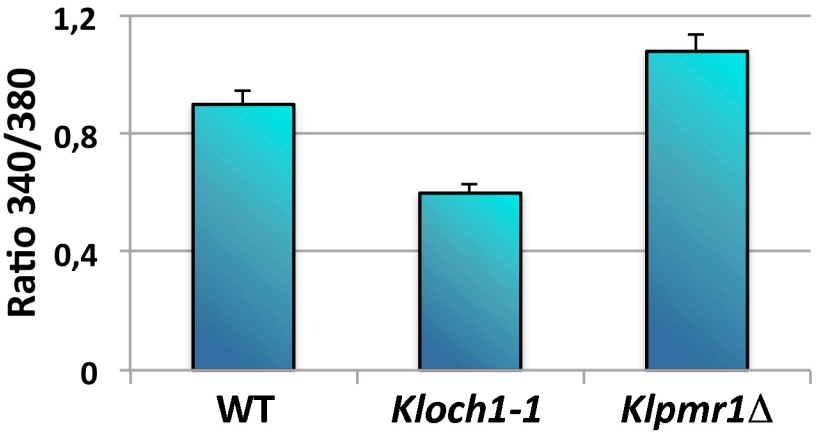


**Figure 11: Intracellular calcium content in WT and *Kloch1-1* cells measured with FURA-2 AM, expressed as the ratio of fluorescence excitation intensities (340/380 nm). $Ca^{2+}$ ion measurement of *Klpmr1*Δ strain was also reported as a control. p<0,001**

Indeed Fura analysis showed that the calcium content of *Kloch1-1* cells was significantly reduced with respect to the cation concentration of wild-type cells (Fig. 11). Measurements employing cells deleted for the Golgi $Ca^{2+}$-ATPase, KlPmr1p, previously reported to have increased cytosolic calcium content, were used as additional calibration control.

## *3. Increased calcineurin activity is required in Kloch1-1 cells for normal mitochondrial and cell wall structure*

Since calmodulin acts as a mediator of calcium signals in eukaryotic cells mainly through the activation of $Ca^{2+}$/calmodulin-dependent phosphatase calcineurin, we investigated its possible role in the mitochondrial phenotypes of *Kloch1-1* cells. Given that calcineurin requires both the regulatory and the catalytic subunits for full activity, the *KlCNB1* and *KlCNA1* trancriptional levels were investigated. Cells lacking the α-1,6-mannosyltransferase activity effectively showed a decrease of *KlCNB1* transcript in comparison with wild type cells (Fig. 12A); a similar result was also observed for the catalytic subunit (Fig. 12B).

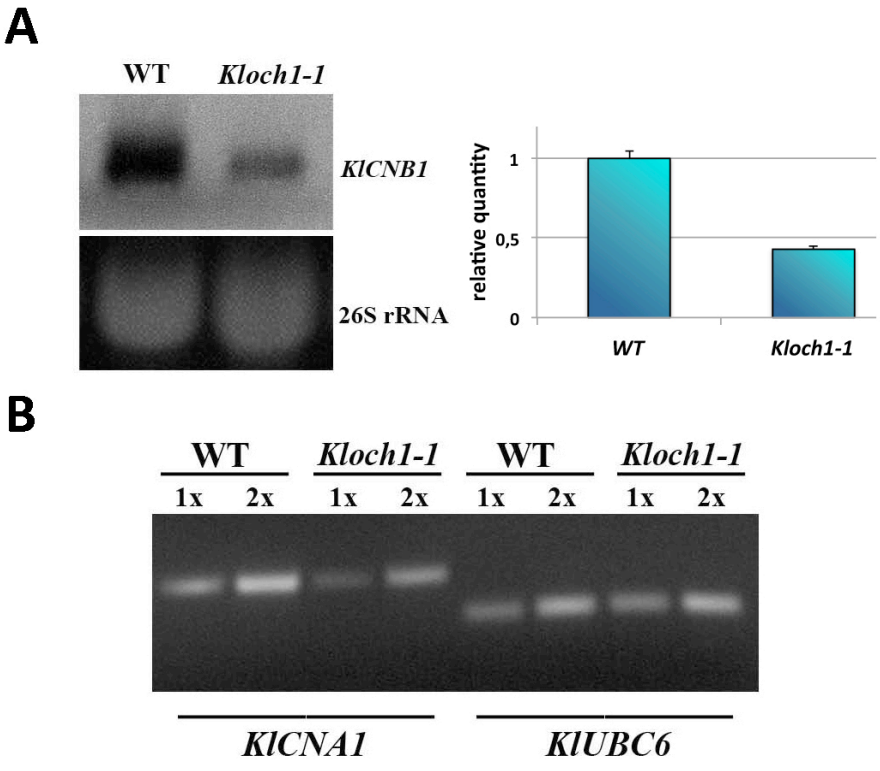


**Figure 12: (A) Northern Blotting analysis of *KlCNB1* in WT and *Kloch1-1* cells. (B) RTPCR semi-quantitative analysis of *KlCNA1* gene. It is shown the electrophoresis in a 2% agarose gel of 10 µl of each PCR reaction with 5 µl (1X) and 10 µl (2X) of cDNA as template. RT-PCR of the *KlUBC6* gene was performed as an internal control.**

In order to achieve the expressional balance of both regulatory and catalytic subunits of calcineurin, we transformed *Kloch1-1* strain with the plasmids

harboring *KlCNB1* (pKlCNB1) and *KlCNA1* (pKlCNA1) genes. Surprisingly, the impact on the EGTA sensitivity of the increased dosage of the regulatory subunit alone was identical when overexpressing both subunits (Fig. 13). Similar results were also obtained when the amount of ROS was analyzed: 15% of the *Kloch1-1* cells transformed with pKlCNB1 alone or together with pKlCNA1 were positive to the staining with DHR as compared to 28% of the cells harboring the empty vector. However, in this case the suppression was not complete if compared to 8% of *Kloch1-1* cells overexpressing calmodulin gene.

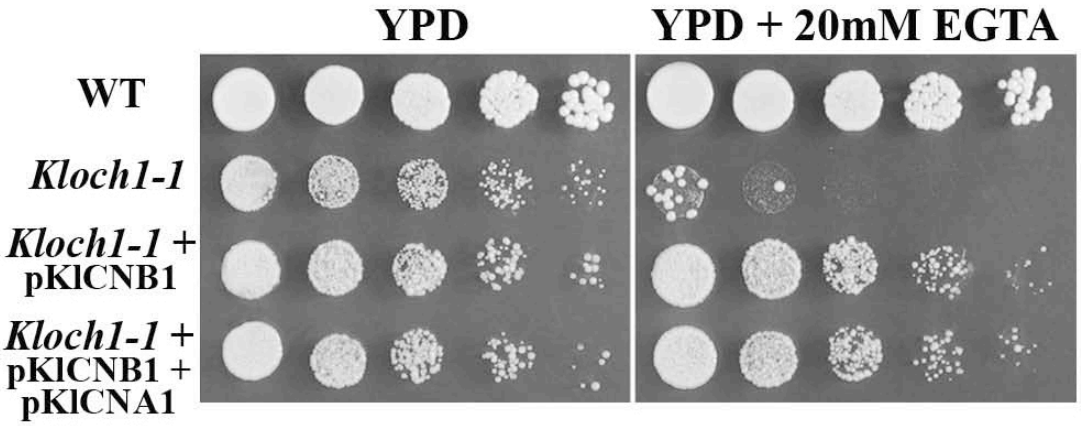


**Figure 13: Growth of indicated yeast strains onto solid medium supplemented with 20 mM EGTA.**

We then looked up to the mitochondrial structures and functionality by DASPMI staining of the transformants. Mutant cells carrying pKlCNB1 vector alone showed a partial recovery of the tubular phenotype. A reduced amount of dots with the concomitant appearance of tubules was detected, whereas the same cells transformed also with the pKlCNA1 plasmid showed the representative tubular wild type-like network, even if with a peripheral distribution (Fig. 14A). Electron microscopy analysis highlighted only a partial recovery of round mitochondria in *Kloch1-1* cells harboring only the pKlCNB1 vector (Fig. 14B). However, when in the same strain we co-overexpressed also the catalytic subunit of calcineurin, the relief was almost complete; mitochondria seemed to be similar to wild type cells and mitochondrial cristae were visible, in agreement with the morphology observed by DASPMI fluorescence analysis.

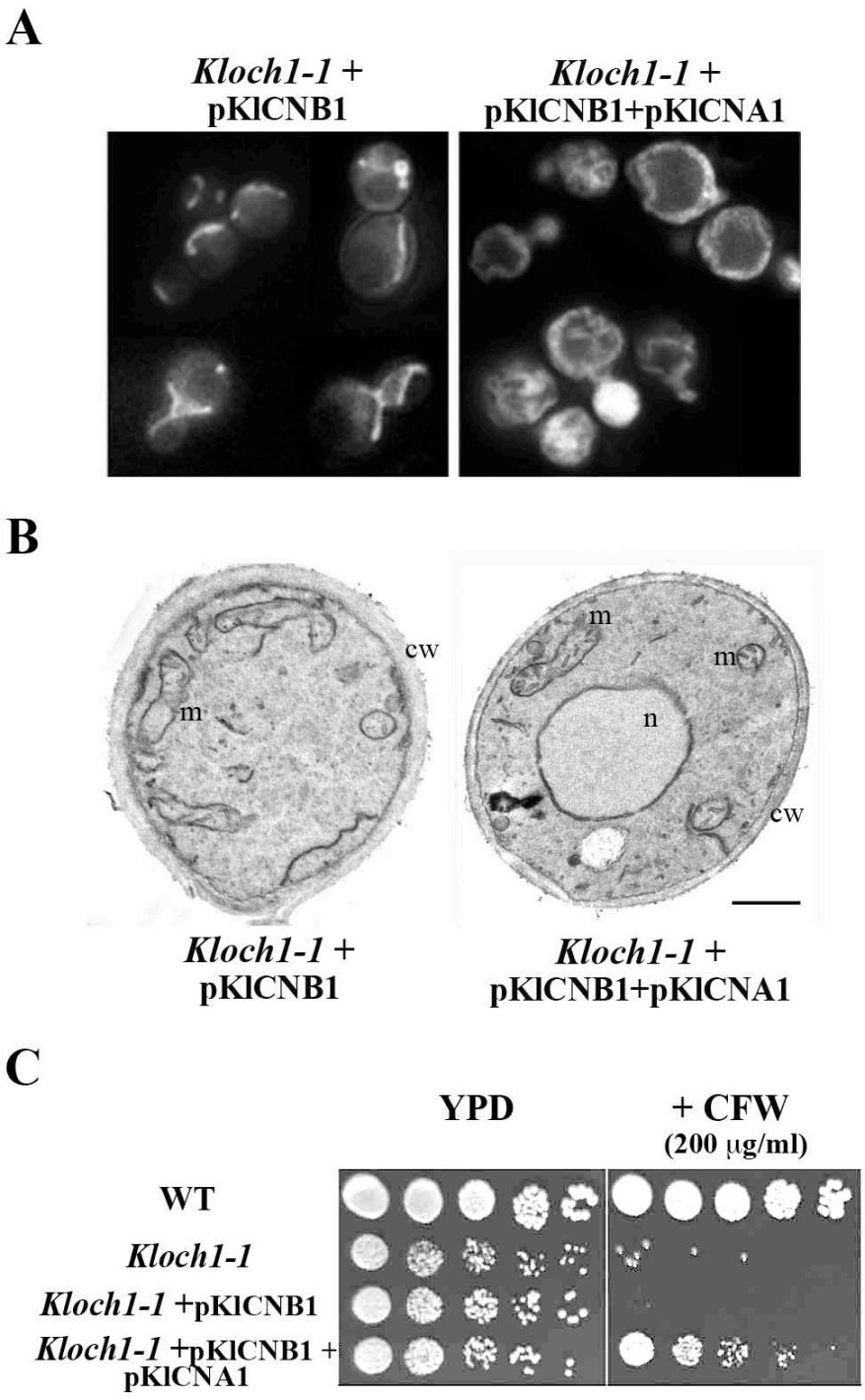


**Figure 14: (A) DASPMI staining of the *Kloch1-1* cells harboring pKlCNB1 plasmid alone or with the pKlCNA1 plasmid. (B) Ultra-thin sections of indicated strains. n, nucleus; m, mitochondrion; cw, cell wall; bar 2 μm. (C) Serial dilutions of cultures from the same strains onto YPD agar plates supplemented with the cell wall interfering agent calcofluor white (CFW).**

It was previously reported that the *Kloch1-1* mutant had increased cell wall thickness and some dark-stained rims were present within the amorphous layer

in comparison with wild-type cells (Uccelletti *et al.*, 2006). Although KlCnb1p overexpression did not produce any effect, in the mutant cells transformed with both the pKlCNB1 and pKlCNA1 plasmids, the thickness of the cell wall resembled that of the wild type cells (Fig. 14B). In agreement with the electron microscopy observations, we found that the ability of the mutant cells to grow in the presence of the cell wall-perturbing agent calcofluor white was completely restored only when the cells were transformed with both subunits of calcineurin (Fig. 14C).

Identical results were also obtained when congo red, another molecule interfering with the cell wall, was used (data not shown). This phenotype could be ascribed to the increased activation of the calcineurin signaling pathway that generates a rescue of a normal biogenesis of the cell wall.

## *4. Increased KlMID1 gene dosage is able to suppress calcium-related defects in Kloch1-1*

As discussed before, calcium homeostasis is normally achieved by a small subset of $Ca^{2+}$ transporters present in the cytoplasmic membrane and membranous organelles. Specifically, the *S. cerevisiae* plasma membrane contains Mid1p, a putative stretch-activated nonselective cation channel component (Kanzaki *et al*., 1999) that interacts with a second subunit, Cch1p, to catalyze high-affinity $Ca^{2+}$ influx into cells (Locke *et al.,* 2000; Iida *et al.,* 1994). Taking into account that calcium transporters respond to the calmodulin/calcineurin signaling pathway, our hypothesis has been based on the possibility that a defective Mid1/Cch1 calcium membrane channel could account for the impaired calcium metabolism of this N-glycosylation mutant. In fact, in *S. cerevisiae* it has been reported that Mid1p requires a full glycosylation to correctly localize and assembly at the plasma membrane (Ozeki-Miyawaki *et al.*, 2005).

A Northern blotting analysis was thus performed in *K. lactis* cells lacking mannosyltransferase activity, revealing a decreased level of the *KlMID1* transcript with respect to wild type cells (Fig. 15).

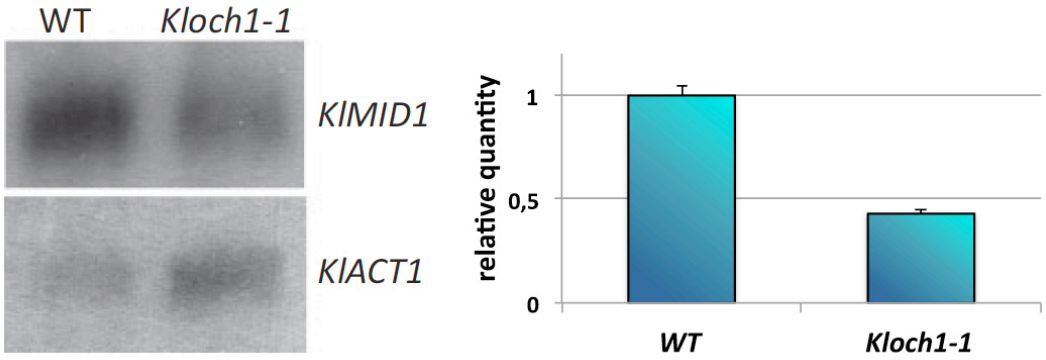


**Figure 15: Expression of *KlMID1* gene in *K. lactis* cells. Northern blotting analysis on *KlMID1* transcript in wild type and mutant strains grown on SD medium until exponential phase. Signals were normalized by using *KlACT1* mRNA and quantified in the right part of the panel by the Phoretix 1D software.**

Supported by this result, we wondered whether an increase in *KlMID1* gene dosage could relieve the phenotypes showed by the mutant cells. To this purpose, the *KlMID1* gene was cloned in the pCXJ18 centromeric vector resulting in pMID1 plasmid, since *KlMID1* on a multicopy vector resulted toxic to the cells. After transforming *Kloch1-1* cells with pMID1 plasmid, the calcium homeostasis was examined and a sensitivity assay to EGTA was thus performed. As shown in figure 16, cells carrying the mutation in the *OCH1* gene were able to grow in the presence of EGTA when transformed with pMID1.

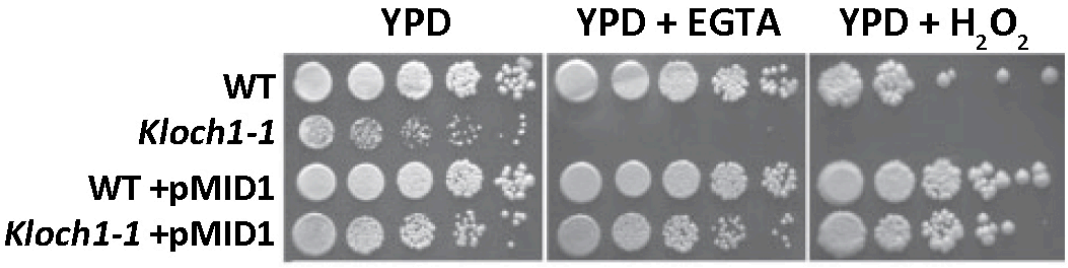


**Figure 16: YPD plates containing or not the perturbing agents, 20 mM EGTA or 4 mM $H_2O_2$, were spotted with 5 µl of 5-fold serial dilutions of cells and growth at 28°C was monitored after 3 days.**

As previously observed, the N-glycosylation mutant resulted sensitive to oxygen peroxide. In order to explore whether calcium homeostasis modulation could influence oxidative stress in *Kloch1-1* cells, the response to this oxidant agent was analyzed. No sensitivity to this strong ROS generator was detected in the mutant strain harboring pMID1 plasmid (Fig. 16).

To further examine in *Kloch1-1* mutant the cellular response to oxidative stress conditions when Mid1p is overexpressed, a challenge assay was performed. Cells were thus treated with a cytotoxic concentration of $H_2O_2$ and after 5 h only 41 % of the mutant cells were viable with respect to 93 % of the wild type counterpart (Fig. 17). Notably, the survival rate increased up to 68 % as a result of *MID1* overexpression.

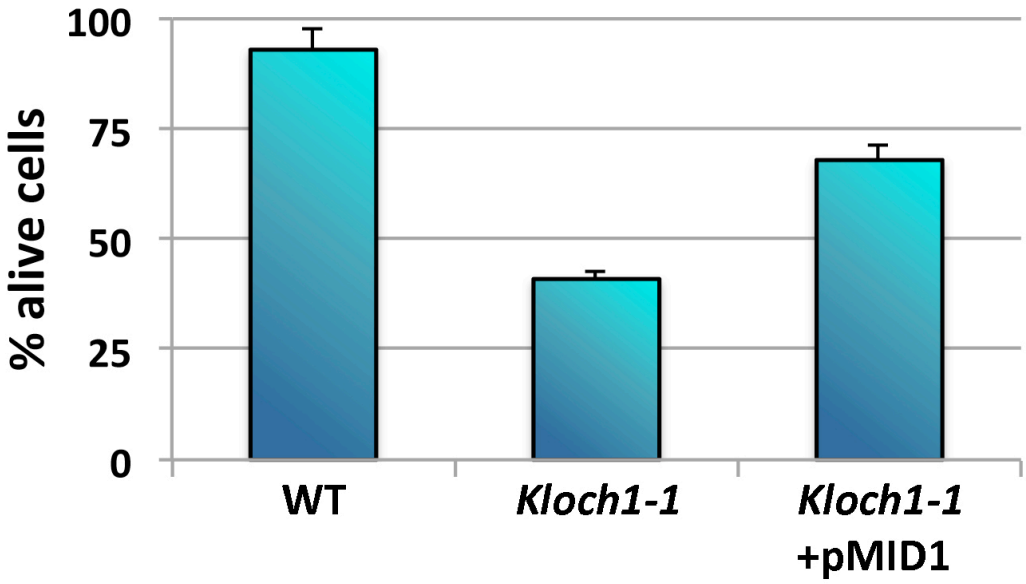


**Figure 17: Cell viability after $H_2O_2$ exposure of parental strain, cells lacking α-1,6-mannosyltransferase activity and *Kloch1-1* cells transformed with pMID1. Strains were grown to exponential phase on SD minimal medium and challenged with 20 mM $H_2O_2$ for 5 h. The viability was evaluated by plating the samples on YPD and was expressed as the CFU percentage of the corresponding untreated cultures.**

Given that oxidative stress and ROS accumulation play a pivotal role in mitochondrial morphology and biogenesis, mitochondria functionality was then investigated in these strains by DASPMI staining. As shown in figure 18, in most mutant cells carrying pMID1 the mitochondrial tubular network appeared almost identical to the wild type counterpart; the punctuate phenotype, as a

result of the mutation in the *KlOCH1* gene, was detectable only in a few cells.

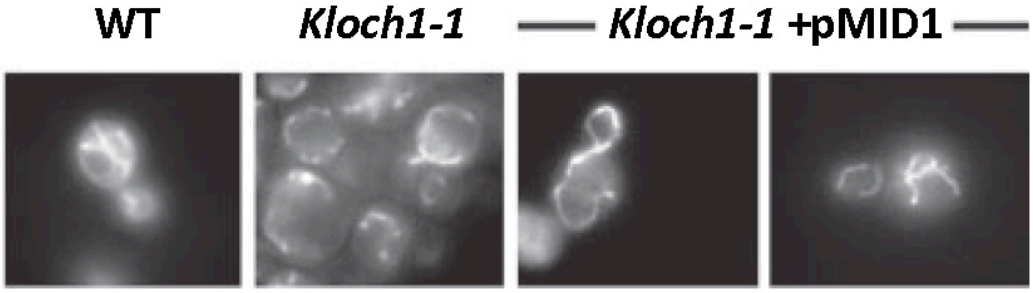


**Figure 18: Fluorescence micrographs taken at 100X magnification showed DASPMI staining of mutant cells transformed or not with the centromeric plasmid containing *KlMID1* gene.**

## *5. KlMID1 is able to modulate calcium signalling and cell wall organization*

In our lab, it has been previously demonstrated that the *Kloch1-1* mutant strain displayed a significantly thicker and mis-organized cell wall with respect to the wild type (Uccelletti *et al.*, 2006). To analyze the effect of *KlMID1* overexpression on cell wall-related defects, we assayed the sensitivity to congo red, a molecule known to interfere with the cell wall organization (Kopecká & Gabriel, 1992). As reported in figure 19, the presence of pMID1 conferred to *Kloch1-1* cells the ability to grow on the medium containing the drug (panel A). In parallel, calcofluor white (CFW) fluorescent dye was also exploited to investigate the cell wall structure because of its property to specifically bind chitin (Roncero & Duran, 1985). After CFW staining, wild type cells showed the normal chitin deposition localized only at the bud scars. By contrast, in the mutant strain the fluorescence was abnormally distributed across the entire cell wall (Uccelletti *et al*., 2000). Moreover, we observed a chitin distribution at the bud emergence sites in *Kloch1-1* cells transformed with pMID1 vector (Fig. 19B). Additionally we found that both size and shape of the cells were almost indistinguishable from the wild type ones.

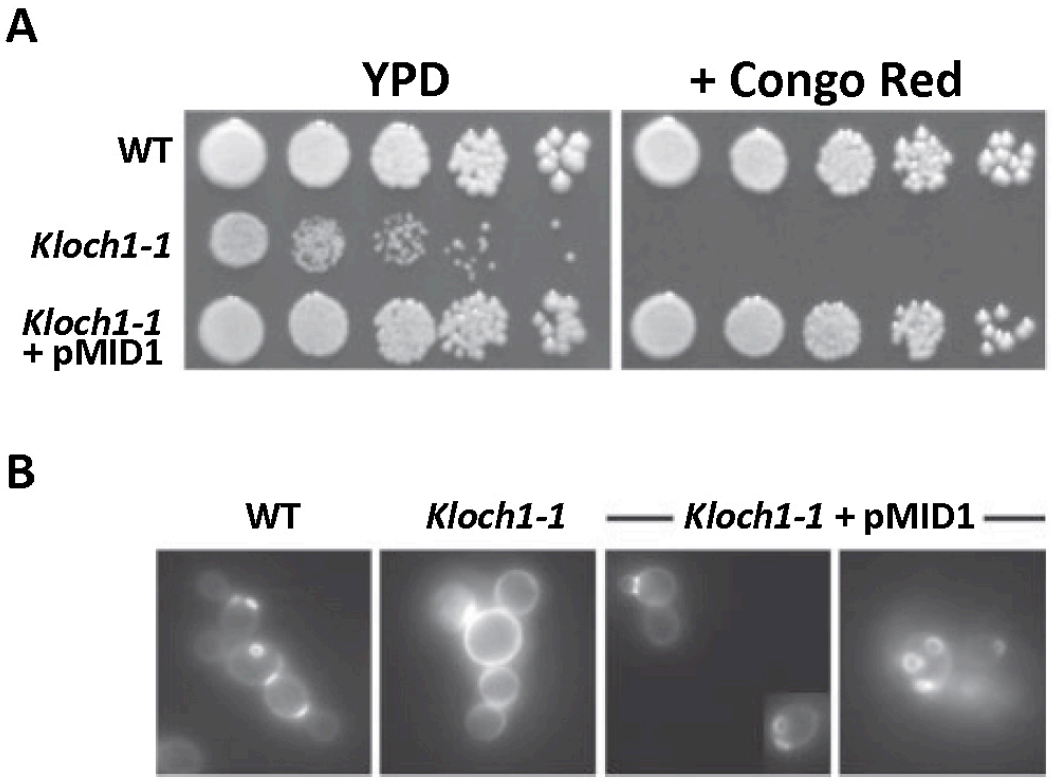


**Figure 19: (a) Serial dilutions of cultures were spotted onto YPD agar plates supplemented or not with 200 μg/ml Congo red and grown at 28°C for 3 days. (b) Chitin distribution was analyzed by calcofluor white staining. Indicated strains were grown to late exponential phase in 2% glucose minimal medium. All the pictures were taken at the same magnification.**

Since calcineurin overexpression restores the cell wall defects in the mutant cells, we attempted to explore if an increased dosage of *KlMID1* was able to induce the cell wall integrity pathway (CWI) by modulating the expression of calcineurin in the mutant strain. Indeed *KlCNB1* transcripts resulted in a 2-fold increase in *Kloch1-1* cells transformed with pMID1 in comparison to the wild type counterpart (Fig. 20); similar results were also observed for the catalytic subunit, *KlCNA1*.

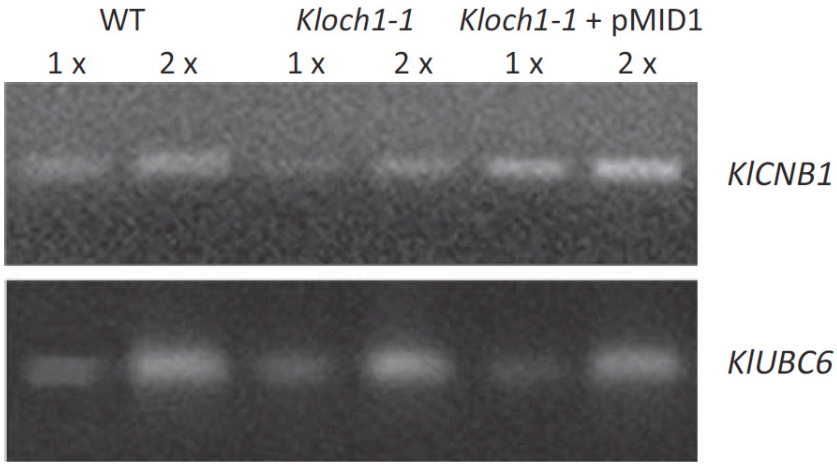


**Figure 20: RT-PCR semi-quantitative analysis of the *KlCNB1* gene. Exponentially growing cells were collected and RNA was isolated. Reverse transcription and PCR reactions with the specific primers described in materials and methods were performed. The electrophoresis in a 1% agarose gel of 15 µl of each PCR reaction performed with 2 µl (1×) and 4 µl (2×) of cDNA as template was reported. RT-PCR of the *KlUBC6* gene was performed as an internal control.**

## *6. Perturbed ER homeostasis in K. lactis is responsible for reduced transcription of KlMID1*

In *S. cerevisiae* cells, Mid1p, together with Cch1p, is required for the high affinity $Ca^{2+}$ influx system; the expression analysis of the *K. lactis CCH1* gene was thus performed in *Kloch1-1* cells. As reported in figure 21, the mutant strain showed a 2-fold *KlCCH1* transcript reduction that reverted to wild type level by overexpressing the *KlMID1* gene.

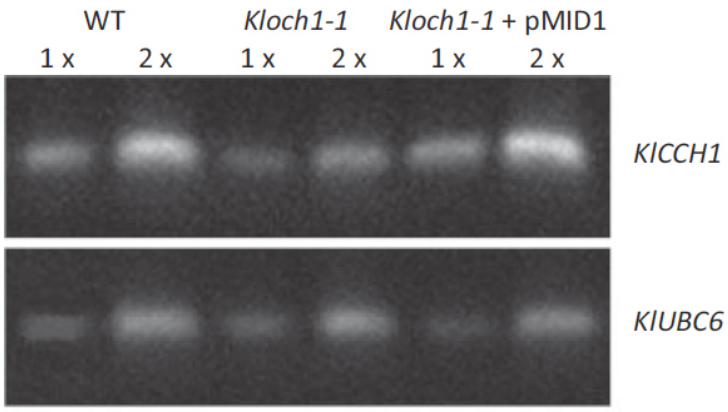


**Figure 21: RT-PCR semi-quantitative analysis of *KlCCH1* gene. PCR reaction was obtained from 2 µl (1×) and 4 µl (2×) of cDNA as template.**

Given that both components of the unique calcium influx system were downregulated in the mutant cells, the calcium uptake was evaluated. Surprisingly, a noticeable 10-fold increase in calcium influx was highlighted in the mutant strain with respect to the wild type one. Such increase was completely abolished in the mutant cells transformed with the pMID1 vector (Fig. 22A). On the other hand, in the FURA-2AM calcium analysis, it has been found a reduced cytosolic calcium content in *Kloch1-1* cells. In order to explain these conflicting results, a possible alteration of vacuolar calcium homeostasis was hypothesized. So that, the expression of the *KlPMC1* gene encoding the vacuolar calcium pump was investigated. Indeed, the mutant cells exhibited a 8-fold increase in the *KlPMC1* transcript compared to wild type ones. Such alteration was completely restored by enhancing *KlMID1* expression in the mutant cells (Fig. 22B).

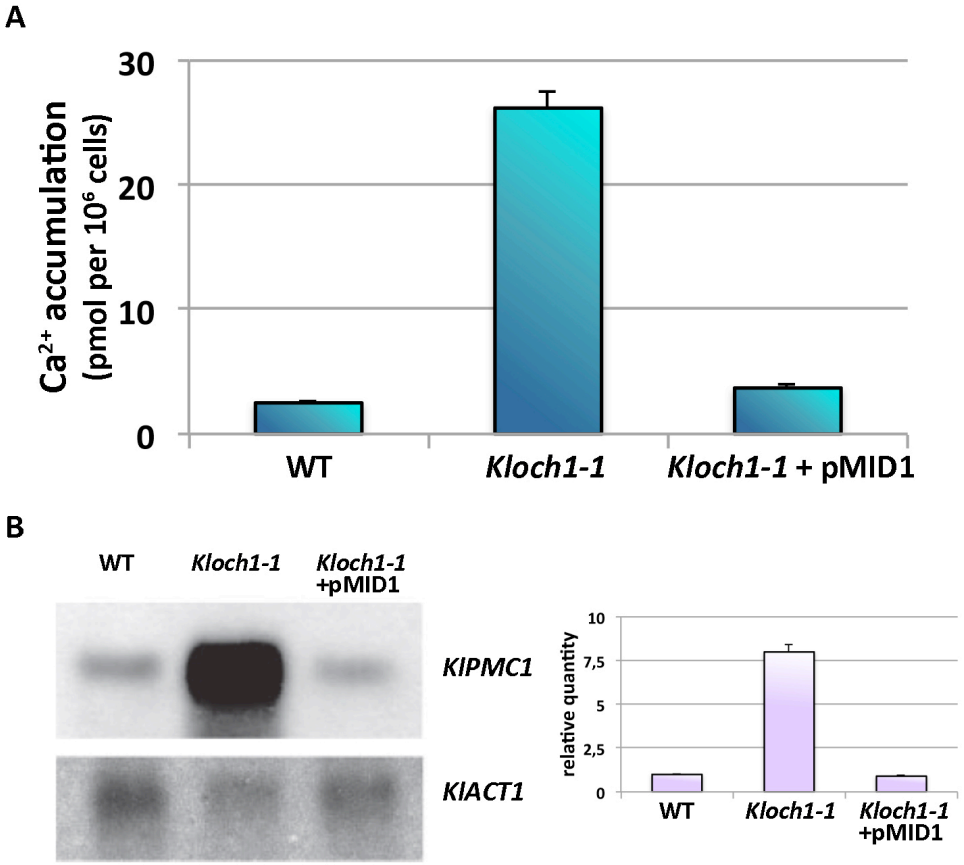


**Figure 22: (a) $Ca^{2+}$ accumulation of cells in SD.Ca100 medium. (b) Northern blotting analysis on *KlPMC1* transcript of the indicated strains. Signals were normalized by using *KlACT1* mRNA and quantified in the right part of the panel by the Phoretix 1D software.**

In *S. cerevisiae* a calcium cell survival (CCS) pathway is activated under ER stress when calcineurin activity is inhibited leading to calcium accumulation (Bonilla *et al.,* 2002). We thus investigated if this mechanism could occur also in the *K. lactis* strains. Given that in the *Kloch1-1* cells an increased calcium uptake is associated with a down-modulation of calcineurin, a possible ER homeostasis perturbation was investigated. To this aim, a Northern blotting analysis directed to an ER stress marker gene was performed. In particular, we found that the *KlKAR2* transcript amount rose up to 2.4 folds in the *Kloch1-1* strain with respect to the wild type counterpart (Fig. 23A). In addition, we made use of the reducing agent dithiothreitol (DTT), a well-known ER stressor. It has been demonstrated that this molecule can cross membranes and promote accumulation of misfolded proteins in the ER by preventing disulfide bond formation, thus triggering the ER stress response (Simons *et al.*, 1995; Cox *et al.*, 1993). Effectively, when DTT was added to the medium the mutant cells exhibited a growth-sensitive phenotype (Fig. 23B). Taken together these findings support the idea that the CCS pathway might be activated in *Kloch1-1* cells.

In order to understand if the altered calcium homeostasis and the mitochondrial dysfunction taking place in the mutant strain were caused by ER stress *per se* or by the defective glycosylation, we challenged the *K. lactis* wild type cells with DTT. The first analysis revealed that such treatment not only resulted in reduced transcription of *KlMID1*, but also led to down-modulation of the calmodulin transcript (Fig. 23C).

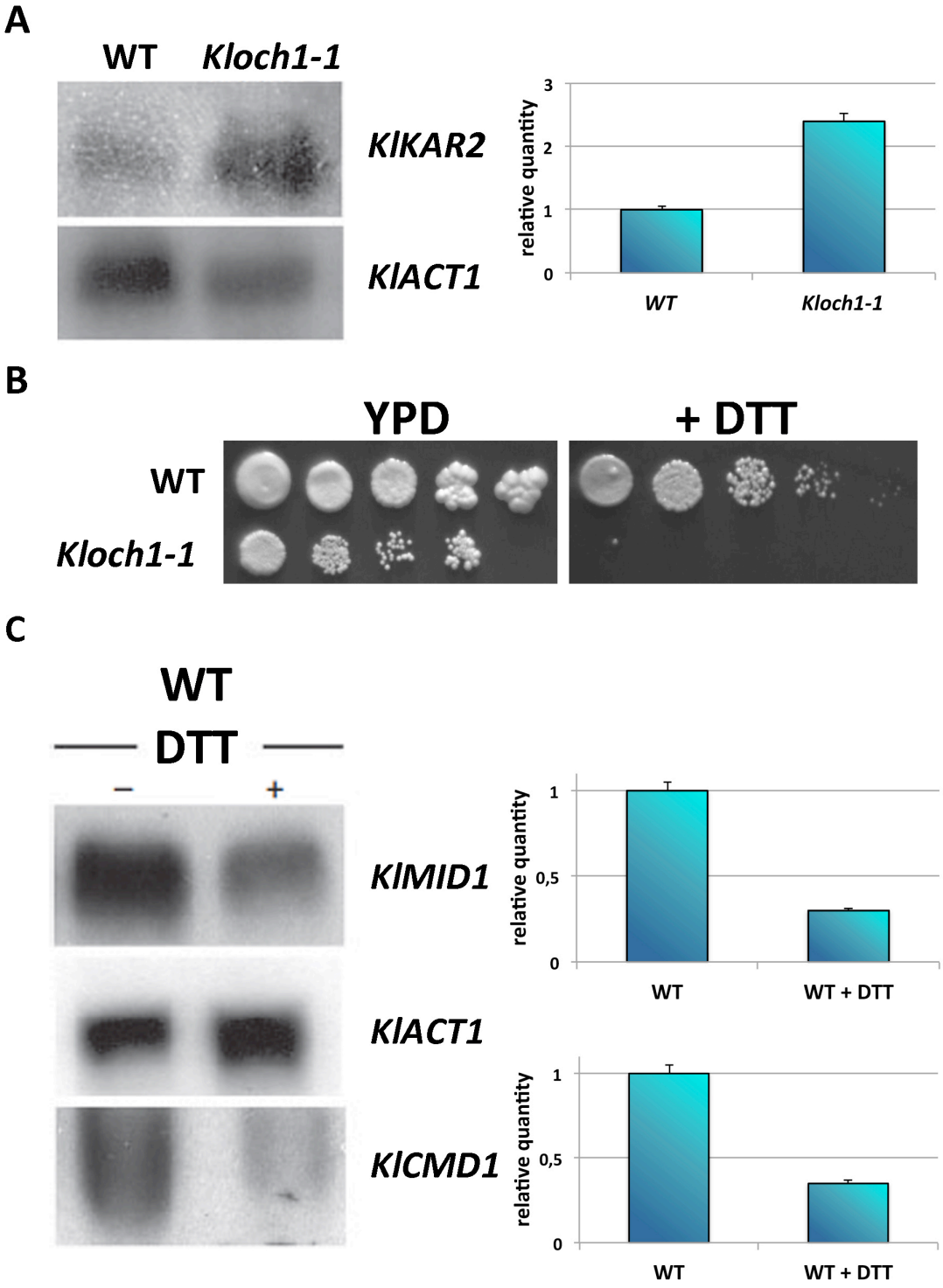


**Figure 23: (a) Northern blot analysis of *KlKAR2* in *Kloch1-1* cells. The same amount of RNA was loaded on each lane. (b) Serial dilutions of cultures were spotted onto YPD agar plates supplemented or not with 20 mM DTT and grown at 28°C for 3 days. (c) Northern analysis of *KlMID1* and *KlCMD1* genes in wild type cells treated with 10 mM DTT for 3h.**

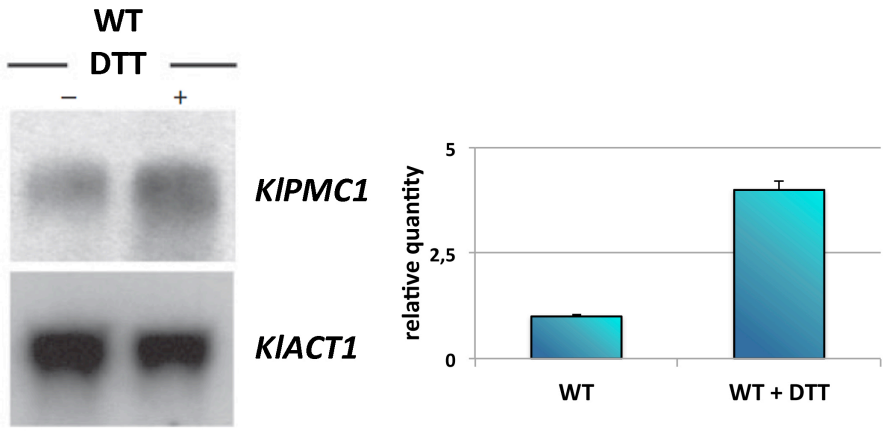


**Figure 24: *KlPMC1* transcript analysis of DTT-treated wild type cells by Northern blotting. Densitometric quantification of mRNA was performed by the Phoretix 1D software and showed in the right part of each panel.**

In addition, in wild type cells under ER stress the transcriptional profile of *KlPMC1* was up-regulated, similarly to *Kloch1-1* cells, although not at the same extent (Fig. 24); 4-fold versus 8-fold of the N-glycosylation mutant.

A DASPMI staining after DTT treatment was also performed in wild type cells. After only 3 h this reducing agent provoked a dotted mitochondrial network, nearly identical to *Kloch1-1* counterpart, in the 42% of the cells (Fig. 25).

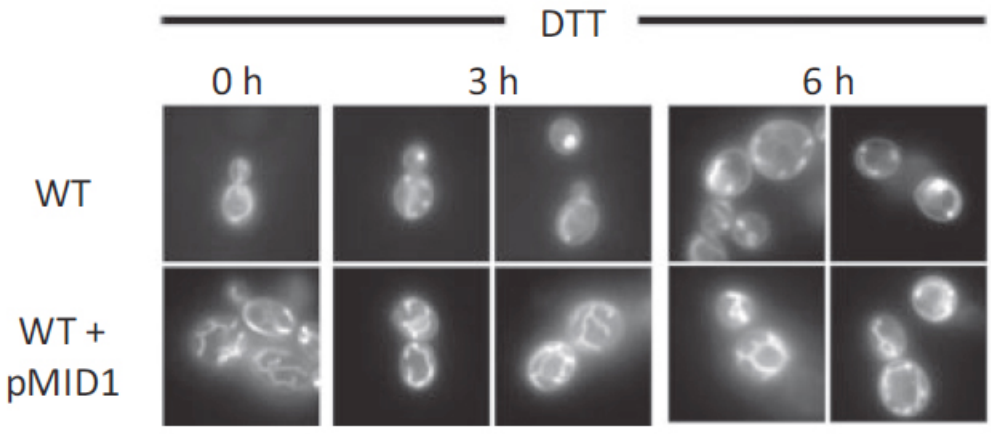


**Figure 25: Fluorescence micrographs of DASPMI-stained cells after exposure to DTT.**

Nevertheless such phenotype became more severe after 6 h of treatment, resulting evident in 67% of the population. By contrast, long-term exposure was

not sufficient to determine an alteration of the mitochondrial functionality in 92% of the wild type cells overexpressing *KlMID1* gene (Fig. 25). The cell wall and the ER stress responses are coordinately regulated in *S. cerevisiae* (Krysan, 2009). Recently it has been demonstrated in *K. lactis* that DTT treatment affects the clustering of the cell wall sensor wsc1p by breaking the disulfide bridges (Dupres *et al.*, 2011) and therefore inducing the CWI pathway. We thus investigated if the DTT effect, observed on both calcium homeostasis and mitochondrial functionality, could be related to its action on the cell wall. To this aim, cells were treated with CFW as a cell wall structure perturbing agent and the modulation of the calcium signaling was evaluated (Fig. 26).

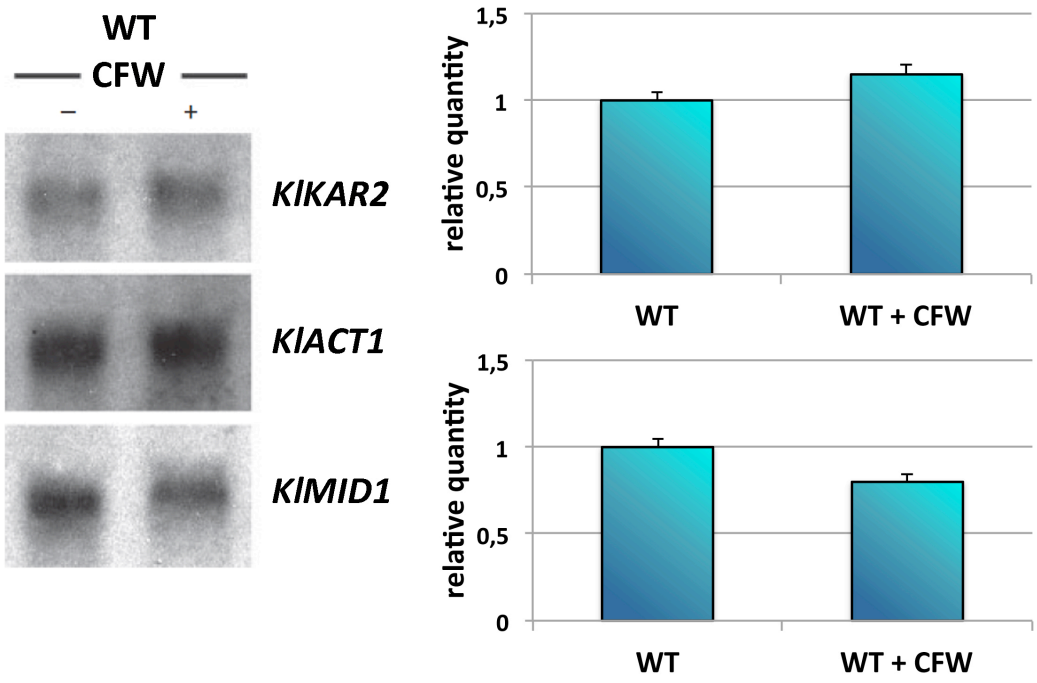


**Figure 26: Cell wall alteration and calcium signaling in *K. lactis* cells. Northern blot analysis of *KlKAR2* and *KlMID1*genes in wild type cells exposed to 200 µg/ml CFW for 3h. The same amount of RNA was loaded on each lane. Densitometric quantification of mRNA was performed by the Phoretix 1D software, normalized using the *KlACT1* transcript, as a housekeeper gene, and showed in the right part of each panel.**

Such treatment was not able to induce the ER stress response, since the cells did not show enhanced transcription of *KlKAR2*. Northern blotting analysis revealed only a slight decrease in the *KlMID1* transcript, while no variation was observed

in the case of *KlCMD1* (not shown), suggesting that the cell wall stress is not a major component responsible for the down modulation of calcium signaling in *Kloch1-1* cells.

# DISCUSSION

Eukaryotic proteins that enter the secretory pathway in the endoplasmic reticulum are glycosylated by distinct sets of enzymes that catalyze either the formation of N- or O-linked glycans. Glycosylation can influence the folding of proteins, their biological activity and half-life. The Och1 proteins of yeasts are α-1,6-mannosyltransferases that initiate a distinct branch in the N-glycan core thereby providing the platform for the subsequent formation of a large poly-mannosylated outer chain in the Golgi complex (Nakayama *et al.,* 1992; Bates *et al.,* 2006; Uccelletti *et al.*, 2006).

Protein *N*-glycosylation is one of the fundamental metabolic pathways in cell fate. Deciphering how *N*-glycosylation controls specific metabolic and signaling events has become important to unraveling the underlying basis of cellular behavior. In this study, we reported that altered mitochondrial functionality and oxidative stress take place in *K. lactis* cells carrying a mutation in the *KlOCH1* gene. The mutant cells showed also a reduction in the cytosolic calcium content and in the expression of genes related to calcium signalling.

Although a direct link between *N*-glycosylation defects and mitochondrial functionality has not been reported, underglycosylation of proteins destined for the mitochondria could interfere with, or abolish, the import of these proteins into the organelle. Indeed, a 45 kDa *N*-glycoprotein has been identified in rat liver inner mitochondrial membranes that physically interacts with complex I and the F1F0-ATP synthase (Babcock *et al.*, 1997); Tim11p, its yeast homologue, has one potential *N*-glycosylation site. Also, mutations in the signal recognition particle (SRP) receptor have been shown to disrupt the reticular structure of both the ER and mitochondria in yeast (Prinz *et al.*, 2000), suggesting that a proper ER structure and/or functionality are required for maintaining the mitochondrial network. It is conceivable that the underglycosylation of proteins

has adverse effects on the structure and functionality of the early secretory compartments, which, in turn, influences mitochondria characteristics.

Moreover, we isolated *KlCMD1* gene as a suppressor in *Kloch1-1* cells of either ROS accumulation either sensitivity to the oxidative stress, when $H_2O_2$ was added in the growth medium. On the other hand, enhanced dosage of this $Ca^{2+}$-signaling gene was not able to increase the survival rate of the mutant cells undergoing a treatment with cytotoxic concentration of the same oxidant agent. These findings suggest that, in the mutant cells, the altered defense mechanisms against high concentration of a ROS generator were not fixed by calmodulin itself.

The *Kloch1-1* cells also showed a reduction in the cytosolic calcium content displayed by FURA-2AM, accompanied by a reduction in the expression of the *KlCMD1*, *KlCNA1* and *KlCNB1* genes, encoding for key components of the calmodulin/calcineurin signaling pathway. On the other hand, a 10-fold increase in calcium influx was observed in the mutant strain by performing calcium accumulation analysis. However we attempted to explain these conflicting results by demonstrating an up-modulation of *KlPMC1* gene, responsible for calcium sequestering inside the vacuole.

In fungi, conserved signal transduction pathways control fundamental aspects of growth, development and reproduction. Two important classes of fungal signaling pathways are the mitogen-activated protein kinase (MAPK) cascades and the calcium-calcineurin pathway. They are triggered by an array of stimuli and target a broad range of downstream effectors such as transcription factors, cytoskeletal proteins, protein kinases and other enzymes, thereby regulating processes such reproduction, morphogenesis and stress response (Cyert, 2003; Qi & Elion, 2005). We can thus hypothesize a possible activation of a MAPK signaling in *Kloch1-1* cells that, in turn, could down modulate calcium signaling. It has been found that in *K. lactis* cells deleted in *PMR1* gene and sharing phenotypes with the *Kloch1-1* mutant, such as cell wall defects, oxidative stress and altered calcium homeostasis, the HOG1 MAPK cascade resulted activated (Uccelletti *et al.*, 2005).

*S. cerevisiae* calmodulin, a $Ca^{2+}$ binding protein, regulates many cell processes both depending or not upon the intervention of $Ca^{2+}$ ions. Among those $Ca^{2+}$-dependent is the organization of the actin cytoskeleton; moreover mutations in *CMD1* resulted colethal, suggestive of functional interactions, with the inactivation of genes encoding components of the glycosylation pathways like ANP1, CWH8 and MNN10 (Sekiya-Kawasaki, 1998).

Mitochondrial plasticity and functionality strongly depend on the interactions between mitochondria and cytoskeleton. Several shape-related proteins have been described in *S. cerevisiae*, localized on the mitochondria surface and reported to interact with actin (Boldogh *et al.*, 1998; Kuznetsov *et al.*, 2009); however the individual role and the underlying mechanisms are still not characterized.

Another unsolved question is how cells change the mitochondrial shape upon cell signals. In the case of calcium signaling, a relevant player could well be Gem1p, a member of the Miro GTPase family (Frederick *et al.*, 2004); Gem1p is also localized on the outer mitochondrial membrane with its GTPase domain and, most notably, its EF-hand calcium binding domain exposed in the cytosol.

In mammalian cells $Ca^{2+}$ influx through voltage-dependent $Ca^{2+}$ channels (VDCCs) causes a rapid halt in mitochondrial movement and induces mitochondrial fission. VDCC-associated $Ca^{2+}$ signaling stimulates phosphorylation of dynamin-related protein 1 (Drp1) at serine 600 via activation of $Ca^{2+}$/calmodulin-dependent protein kinase Iα (CaMKIα). In neurons and HeLa cells, phosphorylation of Drp1 at serine 600 and dephosphorylation at serine 637, both calcineurin-dependent, are associated with increase in Drp1 translocation to mitochondria (Han *et al.*, 2008; Cereghetti *et al.*, 2008).

Our efforts are thus been addressed to speculate if the altered calcium availability could be originated by a defective calcium membrane channel Mid1/Cch1 and the role of *MID1* as a key player in the calcium related defects taking place in the mutant cells was also investigated.

In *S. cerevisiae* the glycoprotein Mid1p is one component of the plasma membrane Mid1/Cch1 $Ca^{2+}$ channel (Iida *et al.*, 1994). Mid1 is probably activated by membrane stretching and mediates the subsequent opening of the Cch1 channel, thus leading to localized $Ca^{2+}$ influx. On the other hand, there are indications that under some conditions Mid1p alone is able to form a functional $Ca^{2+}$ channel without the contribution of Cch1p (Kanzaki *et al.*, 1999; Courchesne & Ozturk, 2003). In addition, a full glycosylation of Mid1p is required for proper localization of the calcium uptake system at the plasma membrane (Ozeki-Miyawaki *et al.*, 2005). Based on this, our attempt was to investigate the functioning of *MID1* in the *K. lactis* glycosylation mutant.

Although a down modulation of both *KlMID1* and *KlCCH1* genes occurred in the mutant cells, a striking increase in calcium uptake was highlighted. Notably, a co-regulation of the two sub-units seems to exist in *K. lactis*. In fact, the wild type cells carrying pMID1 showed an increased transcription of the *KlCCH1* gene. We can thus hypothesize that the reduced transcription of the two sub-units in *Kloch1-1* cells involves a compensatory mechanism in response to the activation of the channel. In *S. cerevisiae* the activity of the high affinity calcium system (HACS), composed essentially by Mid1 and Cch1 proteins, is stimulated in wild-type strains overexpressing the vacuolar $Ca^{2+}$-ATPase Pmc1p (Locke *et al*., 2000). Notably, the overexpression of *KlPMC1* also occurs in the *Kloch1-1* cells.

Increased dosage of *KlMID1* in *Kloch1-1* cells was able, through the modulation of calcium signaling to suppress mitochondria related defects. Moreover, we reported that overexpressing MID1 restored cell wall alterations in the N-glycosylation mutant. This strongly suggests that Mid1p could influence the apparatus responsible for the synthesis and the deposition of chitin, probably by increasing calcineurin activity and thus inducing the CWI pathway.

Surprisingly, we found that the down modulation of *KlMID1* occurring in the mutant strain is probably to be ascribed to ER stress rather than to the impaired glycosylation *per se*. In fact, *Kloch1-1* cells showed sensitivity to DTT and increased *KAR2* transcript as compared to wild type cells. In addition, under ER

stress conditions, *KlOCH1* cells showed a reduction in the *KlMID1* mRNA and concomitantly altered mitochondrial functionality.

Notably, in the *Pichia pastoris* yeast a down modulation of *MID1* transcript also occurs when the cells are treated with DTT or the UPR is activated by overexpression of the transcription factor *HAC1* (Graf *et al.,* 2008). It has been recently reported that also down-regulation of expression of the nucleotide sugar transporters of the Golgi apparatus induced endoplasmic reticulum stress in mammalian cells (Xu *et al.,* 2010). If this is also accompanied by altered calcium homeostasis will deserve further investigations.

To date, the involvement of $Ca^{2+}$ signaling in a multitude of cellular pathways has been well documented (Berridge *et al.,* 2003); however, little is known about the role of $Ca^{2+}$ signaling in restoring ER homeostasis once ER stress has been triggered. Yeasts respond to ER insults by initiating $Ca^{2+}$ influx across their plasma membrane through the high affinity $Ca^{2+}$ channel, assembled with the subunits Cch1 and Mid1; the latter has been suggested to be the one responsible for mediating the influx (Bonilla *et al.,* 2002*;* Hong *et al.,* 2010). We can hypothesize that in *K. lactis* cells a similar mechanism occurs, although it can not be excluded the functioning of an additional $Ca^{2+}$ channel/transporter rather than the involvement of Mid1p and Cch1p that are even down modulated in *Kloch1-1* background. Currently, several reports propose the existence of a calcium influx system, not yet identified, that could operate as a substitute when the well-characterized HACS is inactivated (Cui *et al.,* 2009; Groppi *et al.*, 2011).

Intriguingly, it has been reported that fully glycosylated Mid1p is present at the plasma membrane and also at the ER membrane, where it may be functional to release $Ca^{2+}$ from the ER under stress (Yoshimura *et al.,* 2004). Recently, discrete sites of close apposition between ER and mitochondria facilitating inter-organelle calcium and phospholipid exchange have been characterized also in yeast (Kornmann *et al.,* 2009). We attempt to speculate that in *K. lactis* cells Mid1p is required for, or participate to, such interactions to ensure proper $Ca^{2+}$ homeostasis between ER and mitochondria. Further study will be

performed to elucidate in *K. lactis* cells the role of *KlMID1* in the ER/mitochondria homeostasis.

# MATERIALS AND METHODS

## *1. STRAINS*

Strains of *Kluyveromyces lactis* :

**MW278-20C**: MAT a, *ade2*, *leu2*, *uraA*),

*Kloch1-1* (MAT a, *ade2*, *leu2*, *uraA, Kloch1-1*)

*Klpmr1*Δ **(**MAT a, *ade2, leu2, uraA*, *KlPMR1::Kan* R).

## *2. MEDIA*

**LB**:

- 1 % Bacto Triptone
- 0,5 % Bacto Yeast Extract
- 1 % NaCl

**YPD**:

- 1 % Yeast Extract
- 1 % Bacto Peptone
- 2 % Glucose

**YPE**:

- 1 % Yeast Extract
- 1 % Bacto Peptone
- 2 % Ethanol

**YPGal**:

- 1 % Yeast Extract
- 1 % Bacto Peptone
- 2 % Galactose

**SD minimal medium:**

- 2 % Glucose
- Yeast Nitrogen Base

For solid media 2% agar was added.

For the dithiothreitol (DTT) treatment, cells were grown to exponential phase and then exposed to the reducent agent at a final concentration of 10 mM for 3 or 6 hours. Untreated cultures were incubated in parallel over the same periods.

## *3. DRUGS SENSITIVITY ASSAY*

Fivefold serial dilution from concentrated suspensions of exponentially growing cells (5 × $10^6$ cell/ml) were spotted onto synthetic YPD agar plates supplemented or not with drugs and the plates were incubated at 30°C for 72 h. Concentrations of the perturbing agents were listed below:

- 4 mM $H_2O_2$
- 20 mM EGTA
- 200 µg/ml Congo red
- 50 µg/ml CFW
- 10 mM DTT

## *4. PLASMIDS CONSTRUCTION*

**Construction of the pCXJ3-U and pCXJ6-L plasmids**: the kanamycin-resistance encoding gene (*kan*) was excised by PstI digestion from pCXJ3 and pCXJ6 plasmids (Chen, 1996), giving muticopy vectors with the selectable marker URA3 or LEU2, respectively.

Construction of the pCXJ3-K plasmid: the URA3 gene was excised by BglII digestion from pCXJ3 plasmid, obtaining muticopy vector with the selectable marker KAN.

**Construction of the pCXJ3-mtGFP plasmid**: the open reading frame encoding

for the green fluorescent protein (GFP) was isolated as a *Eco*RI-*Xho*I fragment from plasmid pYX232 (Westermann & Neupert, 2000) and was ligated into *Eco*RI-*Sal*I-restricted pCXJ3 multicopy plasmid (Chen, 1996).

**Construction of the CpKlCMD1 and MpKlCMD1 plasmids**: the 1545 bp fragment containing the full ORF (444 bp) of *KlCMD1* plus 1000 bp upstream and 100 bp downstream was amplified by PCR, using primers modified with the recognition site for the restriction endonuclease BamHI. The PCR fragment encoding the KlCmd1p was cloned into the pGEM-T-Easy vector (Promega) according to the manufacturer's instructions, giving pGEM-KlCMD1 and the gene correctness was confirmed by DNA sequencing (MWG Biotech, Martinsried, Germany). The fragment was excised by BamHI digestion from pGEM-KlCMD1 and was ligated into the centromeric (pCXJ20) or multicopy (pCXJ6-L) vectors, linearized by the same endonuclease, to obtain the CpKlCMD1 and MpKlCMD1 plasmids respectively.

**Construction of the pKlCNB1 and pKlCNA1 plasmids**: the *KlCNB1* and *KlCNA1* genes were PCR amplified from *K. lactis* DNA genome using the primers 5'-CG**GGATCC**GGGCAGAGAGCAGGTTCAAC-3' and 5'-CG**GGATCC**GCTGCTTCACATTCATACGCGC-3', 5'-CG**GGATCC**CGTCAGCCCCAGCTTCCTCATC-3' and 5'-CG**GGATCC**CCGGTGCCGTTGTTGACAAGGG-3' respectively (the BamHI restriction site is underlined). The PCR products were ligated into the pGEM-T-Easy vector (Promega) giving the pGEM-KlCNB1 and pGEM-KlCNA1 plasmids.
After sequencing (MWG Biotech, Ebersberg, Germany) the fragments were successively cloned in BamHI-digested pCXJ3-U and pCXJ3-K plasmids, obtaining pKlCNB1 and pKlCNA1 vectors, respectively.

**Construction of the pMID1 plasmid**: the 2796 bp fragment containing the full ORF (1653 bp) of *KlMID1* plus 1000 bp upstream and 100 bp downstream was amplified by PCR, using primers modified with the recognition site for the restriction endonuclease EcoRI, 5'-CGGAATTCTGGGTGAGGTGCACCGATGC-3' and 5'-CGGAATTCGCAGAGGAAACACCGACTGGC-3'. The PCR fragment encoding the KlMid1p was cloned into the pGEM-T-Easy vector (Promega) according to

the manufacturer's instructions, giving pGEM-MID1 and the gene correctness was confirmed by DNA sequencing (MWG Biotech, Martinsried, Germany). The fragment was excised by EcoRI digestion from pGEM-MID1 and was ligated into the centromeric vector (pCXJ18) (Chen, 1996) linearized by the same endonuclease, to obtain the pMID1 plasmid.

## *5. YEAST TRANSFORMATION WITH GENOMIC LIBRARY*

The *Kloch1-1* strain was transformed to saturation with the yeast genomic library constructed in the pKep6 multicopy vector (kindly provided by Wesolowsky-Louvel) by electroporation method described in Sambrook (2001). All the $Ura^+$ transformants were replicated onto YPD medium supplemented with 4 mM $H_2O_2$. The plasmids isolated from the $Ura^+/H_2O_2{}^R$ transformants were used to transform the *Kloch1-1* strain. Plasmids capable of restoring the $H_2O_2{}^R$ phenotype to the *Kloch1-1* after retransformation were analyzed. Restriction enzymes analysis of the genomic fragments from the isolated plasmids showed that one of these plasmids carrying an insert of about 8000 bp was able to restore the $H_2O_2{}^R$ phenotype. The plasmid was then sequenced (MWG Biotech). The 1600 bp fragment contained the full ORF (444 bp) of *KlCMD1* plus 1000 bp upstream and 100 bp downstream.

## *6. CHALLENGE WITH HYDROGEN PEROXIDE AND VIABILITY*

Yeast cells were grown aerobically at 28°C in liquid medium for 24 h and were challenged with hydrogen peroxide. This was directly added to the growth medium to the final concentration of 20 mM. Untreated cultures were incubated in parallel over the same periods. Viability was determined by colony counts on YPD plates after 2 and 5 h of incubation at 28°C and was expressed as the percentage of the corresponding control cultures. The values are the mean of three independent experiments with a SD < 10%.

## *7. MEASUREMENT OF INTRACELLULAR OXIDATION LEVELS*

The oxidant-sensitive probe dihydrorhodamine 123 (DHR Sigma) was used to measure intracellular oxidation levels in yeast. Yeast cells were grown aerobically at 28°C in liquid medium for 24 h and were concentrated by centrifugation and resuspended in 1 ml of fresh medium. Cells were then treated for 2 h with 20 mM oxygen peroxide and subsequently washed. 2 microliters of DHR (5 μg/ml) was added to the medium. After 2 h of incubation, 5 μl of stained cells were loaded onto slides and observed immediately under epifluorescence microscopy (excitation at 488 nm and emission at 530 nm). At least 300 cells per sample were scored manually as fluorescent or nonfluorescent.

## *8. FLUORESCENCE MICROSCOPY*

Epifluorescence microscopy was carried out with a Zeiss Axiophot microscope fitted with a 100× immersion objective.

**For DASPMI staining:** Cells grown in 2% glucose medium were harvested in exponential growth phase (6 × $10^7$ cells/ml), washed with water and then incubated for 30 min in the presence of 5 μM of 2-(4-(dimethylamino)styryl)- 1-methylpyridinium iodide (DASPMI). Cells were then observed with a FITC filter.

**For mitoGFP localization**: Cells containing the mitoGFP plasmid were grown at 28°C and harvested in logarithmic phase. The GFP was detected by fluorescence microscopy, and cells were then observed with a FITC filter directly from the culture.

**For CFW staining:** Cell pellets derived from exponential cultures were resuspended in 100 μl calcofluor white (1 mg/ml; Sigma) and incubated for 10 min at room temperature. The cells were then washed three times with 1 ml PBS and resuspended in 500 μl of distilled water. Aliquots were applied to slides and observed with an UV filter in a fluorescence microscope.

## *9. ELECTRON MICROSCOPY*

Exponential-phase cultures of cells were fixed with 2 % glutaraldehyde in distilled water for 1 h at room temperature. Cells were washed five times with water and post-fixed with freshly prepared 4% $KMnO_4$, in $H_2O_{dd}$ for 2 h at 4 °C. After five washes with water, cells were incubated with 2 % uranyl acetate for 2 h at room temperature, then were washed five times with water and dehydrated in increasing (30-100 %) concentrations of ethanol. The samples were infiltrated overnight at 4°C in a 1:1 mixture of ethanol and Epon 812 embedding medium. The mixture was replaced with pure Epon 812 and the samples allowed to polymerize at 60°C for 48 h. Ultrathin sections were cut with a Reichert automatic ultramicrotome, stained with lead citrate and examined with a CM 10 Philips electron microscope at 80 kV.

## *10. RNA EXTRACTION*

Cells grown in 2% glucose medium were harvested in exponential growth phase and washed with RNAse free water (DEPC treatment). After 1h at -80 °C, 400 µl of AE buffer (50 mM NaAc pH 5,3; 10 mM EDTA), 40 µl of SDS 10% and an equal volume of Phenol (pre-heated at 65° C) were added. Sample were mixed for 1 minute and then incubated at 65° C for 2 minutes (three times). Subsequently, samples were immediately frozen. The purification with phenol/chloroform and phenol/chloroform/isoamilic alcohol (25:24:1) was then carried out. Afterwards the top (aqueous) layer was transferred into new tubes and 1/10 of the total volume of NaAc 3M pH 5,3 and 2,5 times volumes of ethanol 96% were added. Incubation overnight was performed at -80º C to precipitate. Finally the pellet concentrated by centrifugation was then washed with ethanol 75% and resuspended in 20 µl of RNAse free water.

## *11. NORTHERN BLOT ANALYSIS*

The RNAs were quantified by absorption ($OD_{260}$) and separated by denaturing agarose electrophoresis. After electrophoresis the RNAs were transferred to nylon membranes and hybridized with $^{32}P$-labeled random primed probes

(Roche, Lewes, East Sussex, United Kingdom). All the probes were PCR amplified from the *K. lactis* DNA genome. The 1300-bp PCR product of *KlCMD1* was obtained using primers 5'-CGGGATCCCGTACCCTGATAGCTCTACC-3' and 5'-CGGGATCCGTGCGTAATTTGAGCGATGG-3'. The fragment of 410 bp containing the *KlCNB1* gene was obtained with primers 5'-GAATTGAAATGGGAGCAGCA-3' and 5'-CTTGAAAATCAACATCTCCGC-3'. The densitometric analysis was done with an image analyzer (Phoretix 1D; Non Linear Dynamics Ltd.). The fragment of 1653 bp containing the *KlMID1* gene was obtained with primers 5'-GCATGATAGTGCAGTTACCAG-3' and 5'CGGAATTCGCAGAGGAAACACCGACTGGC-3'. The 1300 bp PCR product of *KlCMD1* gene was obtained using primers 5'-CGGGATCCCGTACCCTGATAGCTCTACC-3' and 5'-CGGGATCCGTGCGTAATTTGAGCGATGG-3'. The 800 bp *KlKAR2* probe was PCR amplified using primers 5'-AAAAAGTTCAGTGGGATGGC-3' and 5'-CATGGCTTTGTCATTCTTGG-3'. The *KlPMC1* fragment of 876 bp was obtained with primers 5'-CGACTTGTGTGGGAAGCATTC-3' and 5'-AACCCTCTGGAACAGCAACC-3'.

## *12. SEMI QUANTITATIVE RT-PCR*

Total RNAs were subjected to TURBO™ DNase treatment according to manufacture's instructions (Ambion, USA). Reverse transcription was performed using Promega Reverse Transcription System with 1 µg total RNA to yield 20 µl cDNA. PCRs were then performed to determine the linear range of amplification for the genes that would allow a semi-quantitative assessment of expression levels. The primers used for *KlCNA1* were 5'-GTTAATGCAGCTCTGCGAGTC-3' and 5'-CACGTGATAGTCGTCCTTCT-3', while for *KlCNB1* were 5'-TGCATATTCGGTACCATCCTCG-3' and 5'-CTTTTCGAGGGATCCTCGATT-3'. *KlCCH1* fragment was amplified with primers 5'-CAGACGGCCACTCAGAAAGA-3' and 5'-GACGATGGAGCACTGAAATC-3' whereas for *KlUBC6* were 5'-ATTACGTGATTACCGGTCCA-3' and 5'-GCCTCT GGATGATAATCACT-3'. The optimal parameters determined for each PCR were

95°C, 30 s; 52°C, 30 s; 72°C, 30 s; and 20 cycles for all genes. The primers used were designed to yield small amplicons (from 170 bp to 500 bp) to improve the efficiency and reproducibility of the PCR. 15 µl of each PCR reaction with 2 µl (1×) and 4 µl (2×) of cDNA diluted 1:20 as template were separated on a 1% agarose gel, stained with ethidium bromide and photographed.

## *13. SPHEROPLASTS PREPARATION*

Cells corresponding to exponential phase were harvested by centrifugation and resuspended in 3 ml of spheroplast buffer (SB) containing 1 M sorbitol, 50 mM Tris buffer, pH 7.5, 10 mM $Mg^{2+}$, and 30 mM dithiothreitol (DTT). After a 15-min incubation at 28°C, the suspension was centrifuged, and the resulting pellets were resuspended in 5 ml of SB containing 2 mg of zymolyase 20T. The suspensions were then incubated at 30°C for 40–60 min, until the conversion to spheroplasts was observed. The spheroplast suspension was then centrifuged and washed twice with SB devoided of DTT.

## *14. $Ca^{2+}$ MEASUREMENTS BY FURA-2AM ANALYSIS*

Suspension of 50 µl freshly prepared spheroplasts were diluted in 1 ml of SB and left into a polylysine-coated plate in agitation at 4°C overnight. Plates were washed twice with 1 ml of SB. Spheroplasts were incubated for 60 min at 37°C in standard reaction medium (125 mM sucrose, 65 mM KCl, 10 mM HEPES, pH 7.2 and 500 µM ethanol) in the presence of 0.1 mg/ml bovine serum albumin (Sigma) and 10 µM Fura-2AM (Molecular Probes, Eugene, OR). To measure fluorescence changes, a Hamamatsu Argus 50 computerized analysis system was used, recording every 6 sec the ratio between the values of light intensity at 340 and 380 nm stimulation.

## *15. $Ca^{2+}$ ACCUMULATION ASSAYS*

Cells were grown to approximately 2 x $10^6$ cells/ml in SD.Ca100 medium at 30˚C and incubated for additional 2 h with 185 kBq/ml $^{45}CaCl_2$ (1.8 kBq/nmol; PerkinElmer, Cat. No. NEZ013). Samples (100 µl) were filtered with Millipore

filters (type HA; 0.45 μm) presoaked with 5 mM $CaCl_2$ and washed five times with the same solution and dried. Radioactivity retained on each filter was counted with a liquid scintillation counter. Data are means $\pm$ SD from three independent experiments.

# REFERENCES


1. Santella L, Carafoli E. Calcium signaling in the cell nucleus. *FASEB J* 1997; **11**, 1330.

2. Berridge MJ, Lipp P, Bootman MD. The versatility and universality of calcium signalling. *Nature Rev. Mol. Cell Biol.* 2000; **1**, 11–21.

3. Berridge MJ, Bootman MD, Roderick HL. Calcium signalling: dynamics, homeostasis and remodelling. Nat Rev Mol Cell Biol. 2003; **4**:517-29.

4. Brini M, Carafoli E. Calcium pumps in health and disease. Physiol Rev. 2009; **89**:1341-78.

5. Berridge MJ. Inositol trisphosphate and calcium signalling. *Nature* 1993; **361**, 315–325

6. Clapham, DE. Calcium signaling. *Cell* 1995; **80**, 259–268.

7. Bootman MD, Berridge MJ, Roderick HL. Calcium signalling: more messengers, more channels, more complexity. *Curr. Biol.* 2002; **12**, R563–R565.

8. Saunders CM, Larman MG, Parrington J, Cox LJ, Royse J, Blayney LM, Swann K, Lai FA. PLC zeta: a sperm-specific trigger of $Ca^{2+}$ oscillations in eggs and embryo development. *Development* 2002; **129**, 3533–3544 ().

9. Brini M, Carafoli E. Calcium Pumps in Health and Disease *Physiol Rev* 2009; **89**: 1341–1378

10. Carafoli E. The calcium-signalling saga: tap water and protein crystals *Nature Reviews Molecular Cell Biology* 2004; **4**: 326-332.

11. Bootman MD, Lipp P. Calcium signalling: Ringing changes to the 'bell-shaped curve'. *Curr. Biol*. 1999; **9**: R876–R878

12. Pozzan T, Rizzuto R, Volpe P, Meldolesi J. Molecular and cellular physiology of intracellular calcium stores. *Physiol. Rev.* 1994; **74**: 595–636.

13. Blaustein MP, Lederer WJ. Sodium/calcium exchange: Its physiological implications. *Physiol. Rev.* 1999; **79**: 763–854.

14. Rizzuto R, Brini M, Murgia M, Pozzan T. Microdomains with high $Ca^{2+}$ close to IP3-sensitive channels that are sensed by neighboring mitochondria. *Science* 1993; **262:** 744–747.

15. Walker K, Skelton H, Smith K. Cutaneous lesions showing giant yeast forms of Blastomyces dermatitidis. *Journal of Cutaneous Pathology* 2002; **29**: 616–618.

16. Tenreiro S, Outeiro TF. Simple is good: yeastmodels of neurodegeneration *Fems* 2010; **10**:970-979.

17. Sugiyama M, Yamagishi K, Kim, YH, Kaneko Y, Nishizawa M, Harashima S. Advances in molecular methods to alter chromosomes and genome in the yeast *Saccharomyces cerevisiae*. *Appl Microbiol Biotechnol*. 2009; **84:**1045-52

18. Faraco V, Ercole C, Festa G, Giardina P, Piscitelli A, Sannia G. Heterologous expression of heterodimeric laccase from *Pleurotus ostreatus* in *Kluyveromyces lactis*. *Appl Microbiol Biotechnol*. 2008; **77**:1329-35.

19. van Ooyen AJ, Dekker P, Huang M, Olsthoorn MM, Jacobs DI, Colussi PA, Taron CH. Heterologous protein production in the yeast *Kluyveromyces lactis*. *FEMS Yeast Res*. 2006; **6**:381-92.

20. Swinkels BW, van Ooyen AJ, Bonekamp FJ. The yeast *Kluyveromyces lactis* as an efficient host for heterologous gene expression. *Antonie Van Leeuwenhoek* 1994; **64**, 187-201

21. Das S, Kellermann E, Hollenberg CP. Transformation of *Kluyveromyces fragilis*. *J Bacteriol*. 1984; **158**, 1165-7.

22. van den Berg JA, van der Laken KJ, van Ooyen AJ, Renniers TC, Rietveld K, Schaap A, Brake AJ, Bishop RJ, Schultz K, Moyer D, et al. *Kluyveromyces* as a host for heterologous gene expression: expression and secretion of prochymosin. *Biotechnology* 1990; **8,** 135-9.

23. Uccelletti D, De Jaco A, Farina F, Mancini P, Augusti-Tocco G, Biagioni S, Palleschi C. Cell surface expression of a GPI-anchored form of mouse acetylcholinesterase in Klpmr1Delta cells of *Kluyveromyces lactis* . *Biochem Biophys Res Commun*. 2002; **298**:559-65.

24. Dujon B, Sherman D, Fischer G, Durrens P, Casaregola S, Lafontaine I, De Montigny J, Marck C, Neuvéglise C, *et al*. Genome evolution in yeast. *Nature*. 2004; **430**:35-44.

25. Functional expression of heterologous proteins in yeast: insights into $Ca^{2+}$ signaling and $Ca^{2+}$-transporting ATPases. Ton VK, Rao R. Am J *Physiol Cell Physiol*. 2004; **287**:580-9.

26. Iida H, Yagawa Y, Anraku Y. Essential role for induced $Ca^{2+}$ influx followed by $[Ca^{2+}]_i$ rise in maintaining viability of yeast cells late in the mating pheromone response pathway. A study of $[Ca^{2+}]_i$ in single *Saccharomyces cerevisiae* cells with imaging of fura-2. *J Biol Chem.* 1990; **265**:13391-9.

27. Bonilla M, Nastase KK, Cunningham KW. Essential role of calcineurin in response to endoplasmic reticulum stress. *EMBO J*. 2002; **21**:2343-53.

28. Pinton P, Pozzan T, Rizzuto R. The Golgi apparatus is an inositol 1,4,5-trisphosphate-sensitive $Ca^{2+}$ store, with functional properties distinct from those of the endoplasmic reticulum. EMBO J. 1998; **17**:5298-308.

29. Strayle J, Pozzan T, Rudolph HK. Steady-state free Ca(2+) in the yeast endoplasmic reticulum reaches only 10 microM and is mainly controlled by the secretory pathway pump pmr1. *EMBO J.* 1999; **18**:4733-43.

30. Matsumoto TK, Ellsmore AJ, Cessna SG, Low PS, Pardo JM, Bressan RA, and Hasegawa PM. An osmotically induced cytosolic $Ca^{2+}$ transient activates calcineurin signaling to mediate ion homeostasis and salt tolerance of Saccharomyces cerevisiae. *J Biol Chem* 2002; **277**:33075–33080.

31. Garrett-Engele P, Moilanen B, and Cyert MS. Calcineurin, the $Ca^{2+}$/calmodulin-dependent protein phosphatase, is essential in yeast mutants with cell integrity defects and in mutants that lack a functional vacuolar $H^+$-ATPase. *Mol Cell Biol* 1995; **15**:4103–4114.

32. Bonilla M, Cunningham KW. Mitogen-activated protein kinase stimulation of Ca(2+) signaling is required for survival of endoplasmic reticulum stress in yeast. *Mol Biol Cell.* 2003; **14**: 4296-305.

33. Courchesne WE, Ozturk S. Amiodarone induces a caffeine-inhibited, MID1-depedent rise in free cytoplasmic calcium in Saccharomyces cerevisiae. *Mol Microbiol.* 2003; **47**:223-34

34. Cunningham KW. Acidic Calcium Stores of *Saccharomyces cerevisiae. Cell Calcium.* 2011; **50**:129–138.

35. Locke EG, Bonilla M, Liang L, Takita Y, Cunningham KW. A Homolog of Voltage-Gated Ca2+ Channels Stimulated by Depletion of Secretory Ca2+ in Yeast. *Mol Cell Biol.* 2000; **20**: 6686–6694.

36. Denis V, Cyert MS. Internal Ca2+ release in yeast is triggered by hypertonic shock and mediated by a TRP channel homologue. *J Cell Biol.* 2002; **156**: 29–34.

37. Cagnac O, Aranda-Sicilia MN, Leterrier M, Rodriguez-Rosales MP, Venema K. Vacuolar Cation/H+ Antiporters of Saccharomyces cerevisiae. *J Biol Chem*. 2010; **285**: 33914–33922.

38. Cyert MS. Genetic analysis of calmodulin and its targets in Saccharomyces cerevisiae. *Annu Rev Genet*. 2001; **35**:647-72.

39. Falke JJ, Snyder EE, Thatcher KC, Voertler CS. Quantitating and engineering the ion specificity of an EF-hand-like Ca2+ binding. *Biochemistry.* 1991; **30**:8690-7.

40. Rusnak F, Mertz P. Calcineurin: form and function. *Physiol Rev*. 2000; **80**:1483-521.

41. Nakajima-Shimada J, Sakaguchi S, Tsuji FI, Anraku Y, Iida H. $Ca^{2+}$ signal is generated only once in the mating pheromone response pathway in *Saccharomyces cerevisiae*. *Cell Struct Funct*. 2000; **25**:125-31.

42. Withee JL, Mulholland J, Jeng R, Cyert MS. An essential role of the pheromone-dependent $Ca^{2+}$ signal is to activate yeast calcineurin. *Mol. Biol. Cell* 1997; **8**:263–77

43. Ohya Y, Kawasaki H, Suzuki K, Londesborough J, Anraku Y. Two yeast genes encoding calmodulin-dependent protein kinases: isolation, sequencing and bacterial expression of CMK1 and CMK2. *J. Biol. Chem.* 1991; **266**:12784–94

44. Morano KA, Grant CM, Moye-Rowley WS. The response to heat shock and oxidative stress in Saccharomyces cerevisiae. *Genetics*. 2011; **190**:1157-95.

45. Zdralević M, Guaragnella N, Antonacci L, Marra E, Giannattasio S. Yeast as a tool to study signaling pathways in mitochondrial stress response and cytoprotection. *Scientific World Journal.* 2012; **2012**:912147.

46. Tu BP, Weissman JS. Oxidative protein folding in eukaryotes: mechanisms and consequences. *J Cell Biol* 2004; **164**: 341–346.

47. Riemer J, Bulleid N, Herrmann JM. Disulfide formation in the ER and mitochondria: two solutions to a common process. *Science* 2009; **324**: 1284–1287.

48. Ayer A, Fellermeier S, Fife C, Li SS, Smits G, Meyer AJ, Dawes IW, Perrone GG. A genome-wide screen in yeast identifies specific oxidative stress genes required for the maintenance of sub-cellular redox homeostasis. *PLoS One*. 2012; **7**:44278.

49. Barnham KJ, Masters CL, Bush. Neurodegenerative diseases and oxidative stress. *Nat Rev Drug Discov* 2004; **3**: 205–214

50. Murphy MP, Holmgren A, Larsson NG, Halliwell B, Chang CJ, Kalyanaraman B, Rhee SG, Thornalley PJ, Partridge L, Gems D, Nyström T, Belousov V, Schumacker PT, Winterbourn CC. Unraveling the biological roles of reactive oxygen species. *Cell Metab.* 2011; **13**:361-6.

51. Harrison DG, Gongora MC, Guzik TJ, Widder J. Oxidative stress and hypertension. *J Am Soc Hypertens*. 2007; **1:** 30-44.

52. Halliwell B. Free radicals and antioxidants: updating a personal view. *Nutr Rev.* 2012; **70**:257-65.

53. Giugliano D. Dietary antioxidants for cardiovascular prevention. *Nutr Metab Cardiovasc Dis*. 2000;**10**:38-44

54. Facecchia K, Fochesato LA, Ray SD, Stohs SJ, Pandey S. Oxidative toxicity in neurodegenerative diseases: role of mitochondrial dysfunction and therapeutic strategies. *J Toxicol.* 2011; **2011**:683728

55. Jimenez-Del-Rio M, Velez-Pardo C. The Bad, the Good, and the Ugly about Oxidative Stress. *Oxid Med Cell Longev.* 2012; **2012**: 163913.

56. Barber SC, Mead RJ, Shaw PJ. Oxidative stress in ALS: a mechanism of neurodegeneration and a therapeutic target. *Biochim Biophys Acta.* 2006; **1762**: 1051-67.

57. Rizzetto L, Zanni E, Uccelletti D, Ferrero I, Goffrini P. Extension of Chronological Lifespan by Hexokinase Mutation in *Kluyveromyces lactis* Involves Increased Level of the Mitochondrial Chaperonin Hsp60. *J Aging Res*. 2012; **2012**:946586.

58. Veal E, Day A. Hydrogen peroxide as a signaling molecule. *Antioxid Redox Signal.* 2011; **15**:147-51.

59. Kregel KC, Zhang HJ. An integrated view of oxidative stress in aging: basic mechanisms, functional effects, and pathological considerations. *Am J Physiol Regul Integr Comp Physiol.* 2007; **292**:18-36.

60. Willcox JK, Ash SL, Catignani GL. Antioxidants and prevention of chronic disease. *Crit Rev Food Sci Nutr* 2004; **44**: 275–295.

61. Liochev SI, Fridovich I. The effects of superoxide dismutase on H2O2 formation. *Free Radic Biol Med*. 2007; **42**: 1465-9

62. Herrero E, Ros J, Bellí G, Cabiscol E. Redox control and oxidative stress in yeast cells. *Biochim Biophys Acta*. 2008; **1780**:1217-35.

63. Moraitis C, Curran BP. Reactive oxygen species may influence the heat shock response and stress tolerance in the yeast Saccharomyces cerevisiae. *Yeast.* 2004; **21**: 313-23.

64. Fridovich I. Oxygen toxicity: a radical explanation. *J Exp Biol.* 1998; **201**: 1203-9.

65. Halliwell B, Cross CE. Oxygen-derived species: their relation to human disease and environmental stress. *Environ Health Perspect.* 1994; **102**: 5-12.

66. Avery SV. Molecular targets of oxidative stress. *Biochem J.* 2011; **434**:201-10.

67. Cecarini V, Gee J, Fioretti E, Amici M, Angeletti M, Eleuteri AM, Keller JN. Protein oxidation and cellular homeostasis: Emphasis on metabolism. *Biochim Biophys Acta*. 2007 **1773**:93-104.

68. Lushchak VI. Adaptive response to oxidative stress: Bacteria, fungi, plants and animals. *Comp Biochem Physiol C Toxicol Pharmacol.* 2011; **153**: 175-90.

69. Toledano MB, Delaunay A, Monceau L, Tacnet F. Microbial H2O2 sensors as archetypical redox signaling modules. *Trends Biochem Sci.* 2004; **29**: 351-7.

70. Isoyama T, Murayama A, Nomoto A, Kuge S. Nuclear import of the yeast AP-1-like transcription factor Yap1p is mediated by transport receptor Pse1p, and this import step is not affected by oxidative stress. *J Biol Chem.* 2001; **276**: 21863-9.

71. Carmel-Harel O, Stearman R, Gasch AP, Botstein D, Brown PO, Storz G. Role of thioredoxin reductase in the Yap1p-dependent response to oxidative stress in Saccharomyces cerevisiae. *Mol Microbiol*. 2001; **39**: 595-605.

72. Trombetta ES, Parodi AJ. Quality control and protein folding in the secretory pathway. *Annu Rev Cell Dev Biol.* 2003; **19**: 649-76.

73. Anelli T, Sitia R. Protein quality control in the early secretory pathway. *EMBO J.* 2008; **27:** 315-27.

74. Walter P, Ron D. The unfolded protein response: from stress pathway to homeostatic regulation. *Science*. 2011; **334**: 1081-6.

75. Moreno AA, Orellana A. The physiological role of the unfolded protein response in plants. *Biol Res*. 2011; **44**: 75-80.

76. Ron D, Walter P. Signal integration in the endoplasmic reticulum unfolded protein response. *Nat Rev Mol Cell Biol*. 2007; **8**: 519-29.

77. Yoshida H. ER stress and diseases. *FEBS J.* 2007; **274:** 630–658

78. Tu BP, Ho-Schleyer SC, Travers KJ, Weissman JS. Biochemical basis of oxidative protein folding in the endoplasmic reticulum. *Science.* 2000; **290:** 1571-4.

79. Penninckx MJ. An overview on glutathione in Saccharomyces versus non-conventional yeasts. *FEMS Yeast Res*. 2002; **2**: 295-305.

80. Hwang C, Sinskey AJ, Lodish HF. Oxidized redox state of glutathione in the endoplasmic reticulum. *Science*. 1992; **257**: 1496-502.

81. Delic M, Mattanovich D, Gasser B. Monitoring intracellular redox conditions in the endoplasmic reticulum of living yeasts. *FEMS Microbiol Lett.* 2010; **306**: 61-6.

82. Kohno K. Stress-sensing mechanisms in the unfolded protein response: similarities and differences between yeast and mammals. *J. Biochem* 2010; **147:** 27–33

83. Papanikou E, Glick BS. The yeast Golgi apparatus: insights and mysteries. *FEBS Lett*. 2009; **583:** 3746–3751

84. Mori K. Signalling pathways in the unfolded protein response: development from yeast to mammals. *J Biochem*. 2009; **146**:743-50.

85. Rasheva VI, Domingos PM. Cellular responses to endoplasmic reticulum stress and apoptosis. *Apoptosis*. 2009; **14**: 996-1007.

86. Tirasophon W, Welihinda AA, Kaufman RJ. A stress response pathway from the endoplasmic reticulum to the nucleus requires a novel bifunctional protein kinase/endoribonuclease (Ire1p) in mammalian cells. *Genes Dev*. 1998; **12:** 1812-24.

87. Iwawaki T, Hosoda A, Okuda T, Kamigori Y, Nomura-Furuwatari C, Kimata Y, Tsuru A, Kohno K. Translational control by the ER transmembrane kinase/ribonuclease IRE1 under ER stress. *Nat Cell Biol*. 2001; **3**: 158-64.

88. Yoshida H, Matsui T, Yamamoto A, Okada T, Mori K. XBP1 mRNA is induced by ATF6 and spliced by IRE1 in response to ER stress to produce a highly active transcription factor. Cell. 2001; 107: 881-91.

89. Harding HP, Zhang Y, Ron D. Protein translation and folding are coupled by an endoplasmic-reticulum-resident kinase. *Nature*. 1999; **397**: 271-4.

90. Patil C, Walter P. Intracellular signaling from the endoplasmic reticulum to the nucleus: the unfolded protein response in yeast and mammals. *Curr Opin Cell Biol.* 2001; **13**: 349-55.

91. Shamu CE, Walter P. Oligomerization and phosphorylation of the Ire1p kinase during intracellular signaling from the endoplasmic reticulum to the nucleus. *EMBO J*, 1996; **15**: 3028–3039

92. Kawahara T, Yanagi H, Yura T, Mori K. Endoplasmic reticulum stress-induced mRNA splicing permits synthesis of transcription factor Hac1p/Ern4p that activates the unfolded protein response. *Mol Biol Cell*. 1997; **8:** 1845-62.

93. Bole DG, Hendershot LM, Kearney JF. Posttranslational association of immunoglobulin heavy chain binding protein with nascent heavy chains in nonsecreting and secreting hybridomas. *J Cell Biol*. 1986; **102**: 1558-66.

94. Kimata Y, Kimata YI, Shimizu Y, Abe H, Farcasanu IC, Takeuchi M, Rose MD, Kohno K. Genetic evidence for a role of BiP/Kar2 that regulates Ire1 in response to accumulation of unfolded proteins. *Mol Biol Cell.* 2003; **14**: 2559-69.

95. Kohno K, Normington K, Sambrook J, Gething MJ, Mori K. The promoter region of the yeast KAR2 (BiP) gene contains a regulatory domain that responds to the presence of unfolded proteins in the endoplasmic reticulum. *Mol Cell Biol.* 1993; **13**: 877-90.

96. Okamura K, Kimata Y, Higashio H, Tsuru A, Kohno K. Dissociation of Kar2p/BiP from an ER sensory molecule, Ire1p, triggers the unfolded

protein response in yeast. *Biochem Biophys Res Commun*. 2000; **279**: 445-50.

97. Fuchs BB, Mylonakis E. Our paths might cross: the role of the fungal cell wall integrity pathway in stress response and cross talk with other stress response pathways. *Eukaryot Cell*. 2009; **8**: 1616-25.

98. Hamann T, Denness L. Cell wall integrity maintenance in plants: lessons to be learned from yeast? *Plant Signal Behav*. 2011; **6**: 1706-9.

99. Zhao C, Jung US, Garrett-Engele P, Roe T, Cyert MS, Levin DE. Temperature-induced expression of yeast FKS2 is under the dual control of protein kinase C and calcineurin. *Mol Cell Biol.* 1998;**18**: 1013–22.

100. Hohmann S. Control of high osmolarity signalling in the yeast *Saccharomyces cerevisiae. FEBS Lett*. 2009; **583**: 4025–9.

101. Rodríguez-Peña JM, Garcia R, Nombela C, Arroyo J. The high-osmolarity glycerol (HOG) and cell wall integrity (CWI) signalling pathways interplay: a yeast dialogue between MAPK routes. *Yeast*. 2010; **27**: 495–502.

102. Smits GJ, Kapteyn JC, van den Ende H, Klis FM. Cell wall dynamics in yeast. *Curr Opin Microbiol*. 1999; **2**: 348-52.

103. Klis FM, Mol P, Hellingwerf K, Brul S. Dynamics of cell wall structure in Saccharomyces cerevisiae. *FEMS Microbiol Rev*. 2002; **26**: 239-56.

104. Cappellaro C, Baldermann C, Rachel R, Tanner W. Mating type-specific cell-cell recognition of Saccharomyces cerevisiae: cell wall attachment and active sites of a- and alpha-agglutinin. *EMBO J.* 1994; **13**: 4737-44.

105. Zlotnik H, Fernandez MP, Bowers B, Cabib E. Saccharomyces cerevisiae mannoproteins form an external cell wall layer that determines wall porosity. *J Bacteriol.* 1984; **159**: 1018-26.

106. Uccelletti D, Pacelli V, Mancini P, Palleschi C. vga Mutants of Kluyveromyces lactis show cell integrity defects. *Yeast*. 2000; **16**: 1161-71.

107. Netea MG, Brown GD, Kullberg BJ, Gow NA. An integrated model of the recognition of Candida albicans by the innate immune system. *Nat Rev Microbiol*. 2008; **6**: 67-78.

108. Kollár R, Reinhold BB, Petráková E, Yeh HJ, Ashwell G, Drgonová J, Kapteyn JC, Klis FM, Cabib E. Architecture of the yeast cell wall. Beta(1-->6)-glucan interconnects mannoprotein, beta(1-->)3-glucan, and chitin. *J Biol Chem.* 1997; **272**: 17762-75.

109. Harold FM. Force and compliance: rethinking morphogenesis in walled cells. Fungal Genet Biol. 2002 Dec;37(3):271-82.

110. Drubin DG, Nelson WJ. Origins of cell polarity. *Cell*. 1996; **84**: 335-44.

111. Levin DE. Regulation of cell wall biogenesis in Saccharomyces cerevisiae: the cell wall integrity signaling pathway. *Genetics*. 2011; **189**: 1145-75.

112. Lommel M, Bagnat M, Strahl S. Aberrant processing of the WSC family and Mid2p cell surface sensors results in cell death of *Saccharomyces cerevisiaeO*-mannosylation mutants. *Mol Cell Biol* 2004; **24**: 46–57.

113. Heinisch JJ, Dupres V, Alsteens D, Dufrêne YF. Measurement of the mechanical behavior of yeast membrane sensors using single-molecule atomic force microscopy. *Nat Protoc*. 2010; **5**: 670-7.

114. Hutzler F, Gerstl R, Lommel M, Strahl S. Protein N-glycosylation determines functionality of the *Saccharomyces cerevisiae* cell wall integrity sensor Mid2p. *Mol Microbiol* 2008; **68**: 1438–1449.

115. Rodicio R, Buchwald U, Schmitz HP, Heinisch JJ. Dissecting sensor functions in cell wall integrity signaling in Kluyveromyces lactis. *Fungal Genet Biol* 2008; **45**: 422–435.

116. Jendretzki A, Wittland J, Wilk S, Straede A, Heinisch JJ. How do I begin? Sensing extracellular stress to maintain yeast cell wall integrity. *Eur J Cell Biol*. 2011; **90**: 740-4.

117. Jaeken J. Congenital disorders of glycosylation. *Ann N Y Acad Sci*. 2010; **1214**: 190-8.

118. Lehle L, Strahl S, Tanner W. Protein glycosylation, conserved from yeast to man: a model organism helps elucidate congenital human diseases. *Angew Chem Int Ed Engl.* 2006; **45**: 6802-18.

119. Wang LX, Lomino JV. Emerging technologies for making glycan-defined glycoproteins. *ACS Chem Biol.* 2012; **7**: 110-22.

120. Varki A. Biological roles of oligosaccharides: all of the theories are correct. *Glycobiology*. 1993; **3**: 97-130.

121. Lechner J, Wieland F. Structure and biosynthesis of prokaryotic glycoproteins. *Annu Rev Biochem.* 1989; **58**: 173-94.

122. O'Connor SE, Imperiali B. A molecular basis for glycosylation-induced conformational switching. *Chem Biol.* 1998; **5**: 427-37.

123. Aebi M, Hennet T. Congenital disorders of glycosylation: genetic model systems lead the way. *Trends Cell Biol*. 2001; **11**: 136-41.

124. Gemmill TR, Trimble RB. Schizosaccharomyces pombe produces novel Gal0-2Man1-3 O-linked oligosaccharides. *Glycobiology*. 1999; **9**: 507-15.

125. Czlapinski JL, Bertozzi CR. Synthetic glycobiology: Exploits in the Golgi compartment. *Curr Opin Chem Biol.* 2006; **10**: 645-51.

126. Wildt S, Gerngross TU.The humanization of N-glycosylation pathways in yeast. *Nat Rev Microbiol.* 2005; **3**: 119-28.

127. Ballou CE. Isolation, characterization, and properties of Saccharomyces cerevisiae mnn mutants with nonconditional protein glycosylation defects. *Methods Enzymol*. 1990; **185**: 440-70.

128. Dean N. Asparagine-linked glycosylation in the yeast Golgi. *Biochim Biophys Acta.* 1999; **1426**: 309-22.

129. Uccelletti D, Farina F, Morlupi A, Palleschi C. Mutants of Kluyveromyces lactis with altered protein glycosylation are affected in cell wall morphogenesis. *Res Microbiol*. 1999; **150**: 5-12.

130. Nakamura T, Ando A, Takagi H, Shima J. EOS1, whose deletion confers sensitivity to oxidative stress, is involved in N-glycosylation in Saccharomyces cerevisiae. *Biochem Biophys Res Commun* 2007; **353**: 293-298.

131. Uccelletti D, Farina F, Rufini S, Magnelli P, Abeijon C, Palleschi C. The Kluyveromyces lactis α1,6-mannosyltransferase KlOch1p is required for cell-wall organization and proper functioning of the secretory pathway. *FEMS Yeast Res* 2006; **6**: 449-457.

132. Westermann B, Neupert W. Mitochondria-targeted green fluorescent proteins: convenient tools for the study of organelle biogenesis in Saccharomyces cerevisiae. *Yeast*. 2000; **16**: 1421-7.

133. Rayner TF, Stark MJ. Identification and characterization of the KlCMD1 gene encoding Kluyveromyces lactis calmodulin. *Yeast*. 1998; **14**: 869-75.

134. Babcock DF, Herrington J, Goodwin PC, Park YB, Hille B. Mitochondrial participation in the intracellular $Ca^{2+}$ network. *J Cell Biol* 1997; **136**: 833-844.

135. Kanzaki M, Nagasawa M, Kojima I, Sato C, Naruse K, Sokabe M, Iida H. Molecular identification of a eukaryotic, stretch-activated nonselective cation channel. *Science*. 1999; **285**: 882-6.

136. Poenie M, Tsien R. Fura-2: a powerful new tool for measuring and imaging $[Ca^{2+}]_i$ in single cells. *Prog Clin Biol Res*. 1986; **210**: 53-6.

137. Iida H, Nakamura H, Ono T, Okumura MS, Anraku Y. MID1, a novel Saccharomyces cerevisiae gene encoding a plasma membrane protein, is required for Ca2+ influx and mating. *Mol Cell Biol.* 1994; **14**: 8259-71.

138. Ozeki-Miyawaki C, Moriya Y, Tatsumi H, Iida H, Sokabe M. Identification of functional domains of Mid1, a stretch-activated channel component,

necessary for localization to the plasma membrane and Ca2+ permeation. *Exp Cell Res*. 2005; **311**: 84-95.

139. Kopecká M, Gabriel M. The influence of congo red on the cell wall and (1---3)-beta-D-glucan microfibril biogenesis in Saccharomyces cerevisiae. *Arch Microbiol*. 1992; **158**: 115-26.

140. Roncero C, Durán A. Effect of Calcofluor white and Congo red on fungal cell wall morphogenesis: in vivo activation of chitin polymerization. J Bacteriol. 1985; 163: 1180-5.

141. Simons JF, Ferro-Novick S, Rose MD, Helenius A. BiP/Kar2p serves as a molecular chaperone during carboxypeptidase Y folding in yeast. *J Cell Biol*. 1995; **130**: 41-9.

142. Cox JS, Shamu CE, Walter P. Transcriptional induction of genes encoding endoplasmic reticulum resident proteins requires a transmembrane protein kinase. *Cell*. 1993; **73**: 1197-206.

143. Krysan DJ. The cell wall and endoplasmic reticulum stress responses are coordinately regulated in Saccharomyces cerevisiae. *Commun Integr Biol*. 2009; **2**: 233-5.

144. Dupres V, Heinisch JJ, Dufrêne YF. Atomic force microscopy demonstrates that disulfide bridges are required for clustering of the yeast cell wall integrity sensor Wsc1. *Langmuir*. 2011; **27**: 15129-34.

145. Nakayama K, Nagasu T, Shimma Y, Kuromitsu J, Jigami Y. OCH1 encodes a novel membrane bound mannosyltransferase: outer chain elongation of asparagine-linked oligosaccharides. *EMBO J*. 1992; **11**: 2511-9.

146. Bates S, Hughes HB, Munro CA, Thomas WP, MacCallum DM, Bertram G, Atrih A, Ferguson MA, Brown AJ, Odds FC, Gow NA. Outer chain N-glycans are required for cell wall integrity and virulence of Candida albicans. *J Biol Chem*. 2006; **281**: 90-8.

147. Prinz WA, Grzyb L, Veenhuis M, Kahana JA, Silver PA, Rapoport TA. Mutants Affecting the Structure of the Cortical Endoplasmic Reticulum in Saccharomyces cerevisiae. *J Cell Biol* 2000; **150**: 461-464.

148. Cyert MS. Calcineurin signaling in Saccharomyces cerevisiae: how yeast go crazy in response to stress. *Biochem Biophys Res Commun* 2003; **311**: 1143-1150.

149. Qi M, Elion EA. MAP kinase pathways. *J Cell Sci* 2005; **118**: 3569-3572.

150. Uccelletti D, Farina F, Pinton P, Goffrini P, Mancini P, Talora C, Rizzuto R, Palleschi C. The Golgi $Ca^{2+}$-ATPase KlPmr1p Function Is Required for Oxidative Stress Response by Controlling the Expression of the Heat Shock Element HSP60 in *Kluyveromyces lactis*. *Mol Biol Cell* 2005; **16**: 4636-4647.

151. Sekiya-Kawasaki M, Botstein D, Ohya Y. Identification of functional connections between calmodulin and the yeast actin cytoskeleton. *Genetics* 1998; **150**: 43-58.

152. Boldogh I, Vojtov N, Karmon S, Pon LA. Interaction between mitochondria and the actin cytoskeleton in budding yeast requires two integral mitochondrial outer membrane proteins, Mmm1p and Mdm10p. *J Cell Biol* 1998; **141**:1371-81.

153. Kuznetsov AV, Hermann M, Saks V, Hengster P, Margreiter R. The cell-type specificity of mitochondrial dynamics. *Int J Biochem Cell Biol* 2009; **41**: 1928-39.

154. Frederick RL, McCaffery JM, Cunningham KW, Okamoto K, Shaw JM: Yeast Miro GTPase, Gem1p, regulates mitochondrial morphology via a novel pathway. J Cell Biol 2004, 167:87-98.

155. Han XJ, Li SA, Kaitsuka T, Sato Y, Tomizawa K, Nairn AC, Takei K, Matsui H, Matsushita M. CaM kinase I alpha-induced phosphorylation of Drp1 regulates mitochondrial morphology. *J Cell Biol* 2008; **182**: 573-585.

156. Cereghetti GM, Stangherlin A, Martins de Brito O, Chang CR, Blackstone C, Bernardi P, Scorrano L. Dephosphorylation by calcineurin regulates translocation of Drp1 to mitochondria. *Proc Natl Acad Sci* 2008; **105**: 15803-15808.

157. Graf A, Gasser B, Dragosits M, Sauer M, Leparc GG, Tüchler T, Kreil DP, Mattanovich D. Novel insights into the unfolded protein response using Pichia pastoris specific DNA microarrays. *BMC Genomics*. 2008; **9**: 390.

158. Xu YX, Liu L, Caffaro CE, Hirschberg CB. Inhibition of Golgi apparatus glycosylation causes endoplasmic reticulum stress and decreased protein synthesis. *J Biol Chem.* 2010; **285**: 24600-8.

159. Hong MP, Vu K, Bautos J, Gelli A. Cch1 restores intracellular Ca2+ in fungal cells during endoplasmic reticulum stress. *J Biol Chem*. 2010; **285**: 10951-8.

160. Cui J, Kaandorp JA, Sloot PM, Lloyd CM, Filatov MV. Calcium homeostasis and signaling in yeast cells and cardiac myocytes. *FEMS Yeast Res*. 2009; **9**: 1137-47.

161. Groppi S, Belotti F, Brandão RL, Martegani E, Tisi R. Glucose-induced calcium influx in budding yeast involves a novel calcium transport system and can activate calcineurin. *Cell Calcium*. 2011; **49**: 376-86.

162. Yoshimura H, Tada T, Iida H. Subcellular localization and oligomeric structure of the yeast putative stretch-activated Ca2+ channel component Mid1. *Exp Cell Res.* 2004; **293**: 185-95.

163. Kornmann B, Currie E, Collins SR, Schuldiner M, Nunnari J, Weissman JS, Walter P. An ER-mitochondria tethering complex revealed by a synthetic biology screen. *Science*. 2009; **325**: 477-81.

164. Chen XJ. Low- and high-copy-number shuttle vectors for replication in the budding yeast Kluyveromyces lactis. *Gene* 1996; **172:**131-136.

165. Sambrook J, Fritsch EF, Maniatis T. Molecular Cloning: a Laboratory Manual. New York: Cold Spring Harbor Laboratory Press; 2001.